Dissertation

submitted to the
Combined Faculties for the Natural Sciences and for Mathematics
of the Ruperto-Carola University of Heidelberg, Germany
for the degree of
Doctor of Natural Sciences

presented by

Matthew Lewis

Master of Science

born in London, United Kingdom

Dissertation

submitted to the
Combined Faculties for the Natural Sciences and for Mathematics
of the Ruperto-Carola University of Heidelberg, Germany
for the degree of
Doctor of Natural Sciences

presented by

Matthew Lewis

Master of Science

born in London, United Kingdom

Oral Examination: ……

An investigation into the pre-erythrocytic immune responses that modulate *Plasmodium berghei* immunopathology and protect against experimental cerebral malaria

Referees: Prof. Dr. Michael Lanzer

Dr. Ann-Kristin Mueller

Hiermit erkläre ich, dass ich die vorliegende Arbeit von Januar 2009 bis April 2013 unter Anleitung von Dr. Ann-Kristin Mueller selbst durchgeführt habe und schriftlich ausgearbeitet habe. Ich habe mich keiner anderen Hilfmittel und Quellen bedient als den hier ausdrücklich erwähnten.

....

Datum Matthew Lewis

Over the course of this thesis, the following papers were submitted or published:

Published:

Continuous oral chloroquine as a novel route for Plasmodium prophylaxis and cure in experimental murine models. Lewis MD, Pfeil J, Mueller A-K. BMC Research Notes 2011, 4:262

To go, or not to go, that is the question – six personal reflections on how geographic mobility may affect your career and life. Niopek D, Berrens R, Mockenhaupt S, Lewis MD, Mueller AK, Grimm D. Bioessays 2011 Oct; 33(10):728-31

Malaria: connecting reality with research. Lewis M. Eur J Immunol, 2011, 41(4):882-4

Submitted:

Chemical attenuation of Plasmodium in the liver modulates severe malaria disease progression. Lewis MD, Behrends J, Sandholdt-Paulsen E, Diegel M, Lasitschka F, Heiss K, Bringmann G, Frischknecht F and Mueller A-K. Under revision for PLOS Pathogens, February 2013

A primaquine-chloroquine hybrid with dual activity against Plasmodium liver and blood stages. Lewis MD*, Diegel M*, Paulsen E, Pradel G, Brun G, Bringmann G, Mueller A-K. Under revision for International Journal of Medical Microbiology, January 2013

$CD8^+$ T cells mediate robust stage-specific immunity to *P. berghei* following immunization under drug cover; blood-stage infection does not downregulate protective immunity. Lewis MD*, Pfeil J*, Heiss K, Mueller A-K. Submitted to PLOS One, May 2013

Contents

Summary

Cerebral malaria is caused by a complicated series of immune reactions in the host, marked by inflammatory immune responses, margination of leukocytes and parasitized erythrocytes in cerebral vessels leading to breakdown of the blood-brain-barrier. Studies of the immune responses that lead to human cerebral malaria are limited since patients typically present once symptoms have commenced. Along with ethical considerations, this has led to the immunopathogenesis of cerebral malaria being studied in the rodent model. Such studies have generally overlooked the very early stage of infection, during which the malaria parasite invades the liver, despite some evidence that early immune responses and intrahepatic attenuated infections, such as caused by the RTS, S vaccine, play a role in preventing cerebral pathology.

This thesis describes the development of a model that attenuates infection at a very early stage prior to the onset of blood infection by the subtherapeutic administration of isopentaquine, an 8-aminoquinoline. Such *chemical attenuation* of the parasite at the very early, clinically silent liver stage suppresses parasite development, delays the time until parasites establish blood-stage infection and provokes an altered host immune response, altering immunopathogenesis and protecting from cerebral disease. This early response is a pro-inflammatory, cell-mediated one with increased T-cell activation in liver and spleen, elevated numbers of effector T cells, cytokine-secreting T cells and proliferating, multifunctional T cells producing pro-inflammatory cytokines. The response destabilizes the usual series of events that leads to cerebral pathology, by downregulating inflammatory responses and T-cell activation at late infection. Dendritic cell numbers, T-cell activation and infiltration of $CD8^+$ T cells to the brain are decreased in later infection, mediated by the anti-inflammatory cytokine IL-10.

These data indicate that liver-stage-directed early immune responses can moderate the overall downstream host immune response and modulate severe malaria outcome. Strikingly, $CD8^+$ T cells isolated from the spleen as early as day 2 post infection are responsible for protection. Protection can be transferred to naïve animals by adoptive transfer of lymphocytes from the spleen at very early infection, but not when $CD8^+$ T cells are depleted.

The reliance of this phenotype on $CD8^+$ T cells and the transferability of protection are of particular interest, especially since these cells are isolated so early on in infection. Neither attenuated infections or early T cell responses have been studied in relation to cerebral pathology

before and this is the first evidence that they can influence the course of the downstream systemic immune response and alter cerebral pathology. This draws parallels with the RTS, S vaccine, which is designed to elicit strong $CD8^+$ T cell responses against the parasite in the liver, and produces similar protection exclusively against severe malaria, including cerebral malaria.

This work has larger implications in dissecting the complex sequence of inter-related events that form the immunological basis of human cerebral (malaria) pathology and uncovers a relationship in both localization and timing of anti-parasitic T-cell responses involved in the immunopathogenesis of cerebral malaria, presenting an insight into the potential role of the pre-erythrocytic response in tempering downstream cerebral immunopathogenesis. These data support the notion that Th1 cellular responses represent a *kill or cure* response to *Plasmodium* that must be tightly controlled in both a spatially and temporally specific manner.

Zusammenfassung

Die zerebrale Malaria wird durch eine komplexe Abfolge von Immunreaktionen im Wirt verursacht. Kennzeichnend sind dabei pro-inflammatorische Immunantworten und die Margination von Leukozyten sowie infizierter Erythrozyten an die Hirngefäße, was schließlich zu einem Zusammenbruch der Blut-Hirn-Schranke führt. Genauere Untersuchungen der Immunantworten, die im Menschen zur zerebralen Malaria führen, werden jedoch dadurch erschwert, dass betroffene Personen in der Regel erst bei fortgeschrittener Symptomatik einen Arzt aufsuchen. Einhergehend mit ethischen Überlegungen hat dies dazu geführt, dass es sinnvoll ist, die Immunpathogenese der zerebralen Malaria im Tiermodell zu untersuchen. Einige solcher Tiermodellstudien haben Hinweise darauf gegeben, dass gerade relativ frühe Immunantworten oder auch abgeschwächte intrahepatische Infektionen wie z.B. durch den RTS, S Impfstoff hervorgerufen eine zentrale Rolle bei der Prävention einer zerebralen Pathologie spielen. Dennoch wurde bei bisherigen Studien in der Regel das sehr frühe Stadium der Infektion, nämlich der Befall der Leber, vernachlässigt und nicht als Interventions-Zeitpunkt in Betracht gezogen.

Diese Arbeit beschreibt die Entwicklung eines Modells, in welchem die Malaria-Infektion in einem sehr frühen Stadium, noch vor dem Übertritt der Parasiten in das Blut, durch die subtherapeutische Verabreichung von Isopentaquin, einem 8-Aminochinolin, abgeschwächt wird. Durch diese *chemische Attenuation* des Parasiten während eines sehr frühen, klinisch asymptomatischen Leberstadiums kann die Entwicklung der Parasiten unterdrückt und die Zeitspanne bis zur Etablierung einer Blutstadieninfektion verlängert werden. Ferner wird eine veränderte Immunantwort ausgelöst, die wiederum zu einer Änderung der Immunpathogenese und zum Schutz vor zerebraler Malaria führt. Diese frühe Immunreaktion ist pro-inflammatorischer Natur sowie zellvermittelt. Besondere Charakteristika sind hierbei eine erhöhte T-Zell-Aktivierung in der Leber und der Milz, eine erhöhte Anzahl von Effektor-T-Zellen, Zytokin-produzierenden T-Zellen und proliferierenden, multi-funktionalen T-Zellen, die pro-inflammatorische Zytokine produzieren.

Eine wie hier beschrieben ausgelöste Immunantwort bringt die übliche Kette von Ereignissen, die zur Ausprägung der zerebralen Malaria führen, aus dem Gleichgewicht. Insbesondere wird dies durch die Herunterregulierung von Entzündungsreaktionen und verzögerte T-Zell-Aktivierung während der Infektion erreicht. In der späteren Phase der Infektion ist die Anzahl dendritischer Zellen, T-Zell-Aktivierung und die Infiltration von $CD8^+$ T-Zellen in das Gehirn verringert. Dieser Effekt wird durch das anti-inflammatorische Zytokin IL-10 vermittelt.

Die hier präsentierten Daten belegen, dass frühe Immunantworten, die sich gegen das Leberstadium richten, die gesamte nachgeschaltete Immunantwort moderieren und die Folgen der schwerwiegenden Form der Malaria modulieren können. Hervorzuheben ist, dass $CD8^+$ T-Zellen, die zwei Tage nach der Infektion aus der Milz isoliert wurden, für den Schutz vor zerebraler Malaria verantwortlich sind. Der Schutz kann auf naive Tiere durch den adoptiven Transfer von während der frühen Phase der Infektion aus der Milz isolierten Lymphozyten übertragen werden. Dieser schützende Effekt wird durch die Depletion von $CD8^+$ T-Zellen aufgehoben.

Die Abhängigkeit dieses Phänotyps von $CD8^+$ T-Zellen und die Übertragbarkeit des Schutzes sind von besonderem Interesse, insbesondere deshalb, weil diese Zellen in einer solch frühen Infektionsphase isoliert wurden. Bislang wurden weder attenuierte Infektionen noch frühe T-Zell-Antworten in Bezug auf die Pathologie der zerebralen Malaria untersucht. Diese Arbeit liefert somit den ersten Beweis, dass diese den Verlauf der nachfolgenden systemischen Immunantwort beeinflussen können und die zerebrale Pathologie verändern. Diese Resultate weisen Parallelen mit der Wirkweise des RTS, S-Impfstoffes auf, der konstruiert wurde, um vor allem starke $CD8^+$ T-Zell-Reaktionen gegen den Parasiten in der Leber hervorzurufen, und einen ähnlichen Schutz ausschließlich gegen zerebrale Malaria zeigt.

Die vorliegende Arbeit hat größere Auswirkungen bezüglich einer detaillierten Aufklärung der komplexen Abfolge von miteinander verbundenen Ereignissen, die die immunologische Grundlage der zerebralen Malaria Pathologie bilden und deckt eine Beziehung zwischen der Lokalisation und dem Zeitpunkt der anti-parasitären T-Zell-Reaktionen auf, die in der Immunpathogenese der zerebralen Malaria beteiligt sind. Die Ergebnisse dieser Arbeit gewähren einen ersten Einblick in die potenzielle Rolle der prä-erythrozytären Immunantwort, die nachfolgende zerebrale Immunpathogenese zu mildern. Diese Daten unterstützen die Vorstellung, dass Th1-Antworten eine *töten oder heilen* Reaktion auf *Plasmodium* repräsentieren, die sowohl räumlich als auch zeitlich gezielt kontrolliert werden muss.

Abbreviations

AMA-1	Apical membrane antigen 1
An	Anopheles
APC	Antigen-presenting cell
α	Anti-
BBB	Blood–brain barrier
BFA	Brefeldin A
BSA	Bovine serum albumin
°C	Degrees centigrade
CCL2	Chemokine (C-C motif) ligand 2
CCL5	Chemokine (C-C motif) ligand 5
CXCL10	C-X-C motif chemokine 10
CD	Cluster of differentiation
CDC	Center for Disease Control
CpG	C-phosphate-G
CSP	Circumsporozoite protein
CM	Cerebral malaria
CTLA-4	Cytotoxic T-lymphocyte antigen 4
CO_2	Carbon dioxide
CQ	Chloroquine
DTT	Dichlorodiphenyltrichloroethane
DC	Dendritic cell
ddH_2O	Double distilled water
dpi	Day(s) post infection
DTT	Dithiothreitol
ECM	Experimental cerebral malaria
EBL	Erythrocyte binding ligand
EEFs	Exo-erythrocytic forms
EDTA	Ethylene-diamine-tetra-acetic acid
ELISA	Enzyme linked immunosorbent assay
FACS	Fluorescence activated cell sorting
FCS	Fetal calf serum
FITC	Fluorescein isothiocyanate
g	Gram
GPI	Glycosylphosphatidylinositol
h	Hour
HBSS	Hanks Buffered Salt Solution
HCM	Human cerebral malaria
HEPES	2-(4-(2-Hydroxyethyl)- 1-piperazinyl) sulphanoic acid
HSPGs	Highly sulphated heparan sulfate proteoglycans
IFN	Interferon
IL	Interleukin
iNOS	Nitric oxide synthase
i.p.	Intraperitoneal
iRBCs	Infected red blood cells
i.v.	Intravenous
kg	Kilogram
KC	Kupffer cells
$KHCO_3$	Potassium bicarbonate

l	Litre
LSEC	Liver sinusoidal endothelial cell
MHC	Major histocompatibility complex
min	Minute
µg	Microgram
µl	Microliter
M	Molar
MCP-1	Monocyte chemoattractant protein-1
$MgCl_2$	Magnesium chloride
mg	Milligram
ml	Milliliter
mM	Millimolar
MSP-1	Merozoite Surface Protein 1
MYD88	Myeloid differentiation primary response gene (88)
NCM	Negated Cerebral Malaria
NH_4Cl	Ammonium chloride
NFκB	Nuclear factor kappa B
NK	Natural killer cell
NKT	Natural killer T cell
N_2	Liquid nitrogen
NaCl	Sodium chloride
nm	Nanometer
NO	Nitric oxide
O_2	Oxygen
OD	Optical density
Pb, P. berghei	*Plasmodium berghei*
PBS	Phosphate buffered saline
PE	R-phycoerythrine
Pf, P. falciparum	*Plasmodium falciparum*
Py, P. yoelii	*Plasmodium yoelii*
pH	Potential hydrogenii
PMA	Phorbol 12-myristate 13-acetate
P/S	Penicillin and streptomycin
PV	Parasitophorous vacuole
RAS	Radiation attenuated sporozoites
RMCBS	Rapid murine coma and behavior scale
rpm	Revolutions per minute
RT	Room temperature
sec	Second
spz	Sporozoites
T cell	T lymphocytes
TCR	T cell receptor
TGF-β	Transforming growth factor beta
Th1	T-helper cell type 1
Th2	T-helper cell type 2
TIR	Toll-IL-1 receptor
TLR	Toll-like receptor
TNF	Tumor necrosis factor
TRAP	Thrombospondin-related anonymous protein
Tregs	Regulatory T cells
U	Unit
UV	Ultra violet

VCAM-1	Vascular cell adhesion molecule 1
v/v	Volume to volume
Vol	Volume
w/v	Weight to volume
WHO	World Health Organization

Chapter 1

Introduction

1.1 A Brief History of Malaria

The term malaria originates from the mid-18th century Italian *mala aria*, meaning "bad air" [1]. Although intermittent fever is described in numerous historical texts of ancient Chinese, Indian and Greek origin dating from the third millennium BCE, [2] the first reliable historical account of malaria is attributed to Celsus in the first century CE [3]. Nonetheless, modern techniques in molecular biology and genetic anthropology have revealed that *P. falciparum* diverged from *P. reichenowi* some five to ten million years ago, parallel to the divergence of *Homo* from chimpanzees (fig 1.1) [2]. The most recent common ancestor of *P. falciparum* existed in tropical Africa some 100,000 years ago [4] and the species underwent significant expansion 10,000 years ago upon the adoption and expansion of agriculture [5]. In contrast to *P. falciparum*, the strains *P. ovale*, *P. vivax* and *P. malariae* transferred laterally from primates to humans [2]. Malaria has had a significant influence on humanity, changing settlement patterns, agricultural systems and the age structures of early societies [6]. Malaria represents one of the strongest selective pressures on the history of the human genome [7] and is responsible for several diseases, including thalassemia, sickle-cell disease and glucose-6-phosphatase deficiency [8].

It was not until the end of the nineteenth century that significant advances were made in elucidating the true nature of malaria transmission. Within a relatively short period of time, parasites were discovered within the blood of a malaria patient by French army surgeon Charles Louis Alphonse Laveran [9] and shortly afterwards British medical officer Ronald Ross discovered that malaria is transmitted by mosquito bite [10].

Treatment of malaria in the ancient world ranged from herbal preparations in China and Europe [11] to the administration of garlic in Ancient Egypt [12]. By far the most historically significant antimalarial is quinine, which was brought to Europe in the 17th century in the form of bark of the cinchona tree. By 1820 quinine was routinely extracted from the bark directly and is still administered today to treat cases of severe malaria [13-15], although a recent review of healthcare practises suggested that this should be stopped in favour of artesunate administration [16]. Chloroquine was synthesized *en masse* after world war two and displayed far greater potency than other synthetic antimalarials of its time [17]. For this reason, despite the emergence of chloroquine-resistant strains in the late 1950s, chloroquine remained the pre-eminent antimalarial compound for over 40 years. Indeed, the 20th century was marked by a decrease in malaria mortality due to drug and other public health interventions (fig 1.2). In the wake of chloroquine resistance, other antimalarials such as mefloquine, artemisinin derivatives, sulphadoxine-pyrimethamine and atovquone-proguanil (Malarone®) were developed [13, 14]. Resistance commonly develops to antimalarials after 10-15 years and there are resistant strains to sulphadoxine-pyrimethamine, mefloquine and atavoquone, amongst others, although no clinically relevant artemisinin-resistant strain is reported to date [18].

1.2 The Global Health Burden of Malaria

Over a century after the discovery of the causative agent of malaria, it still wreaks a devastating global health burden [19]. The number of deaths from malaria has increased by approximately 20% since 1980 [20]. Today, there are approximately 250 million clinical cases of malaria annually with a mortality of 1.2 million individuals [20]. A recent study found that the number of malaria deaths has previously been underestimated, although control measures are steadily reducing the burden of disease, with a 34% reduction in mortality since 2004 [20]. The vast majority of deaths occur in sub-Saharan Africa, especially in children under the age of 5 (fig 1.3). The sheer numbers of deaths in this region dictate the rise and fall in global malaria statistics. Approximately 430,000

children younger than 5 in sub-Saharan Africa died of malaria in 2010, down from 1,000,000 in 2004 but up from 377,000 in 1980 [20].

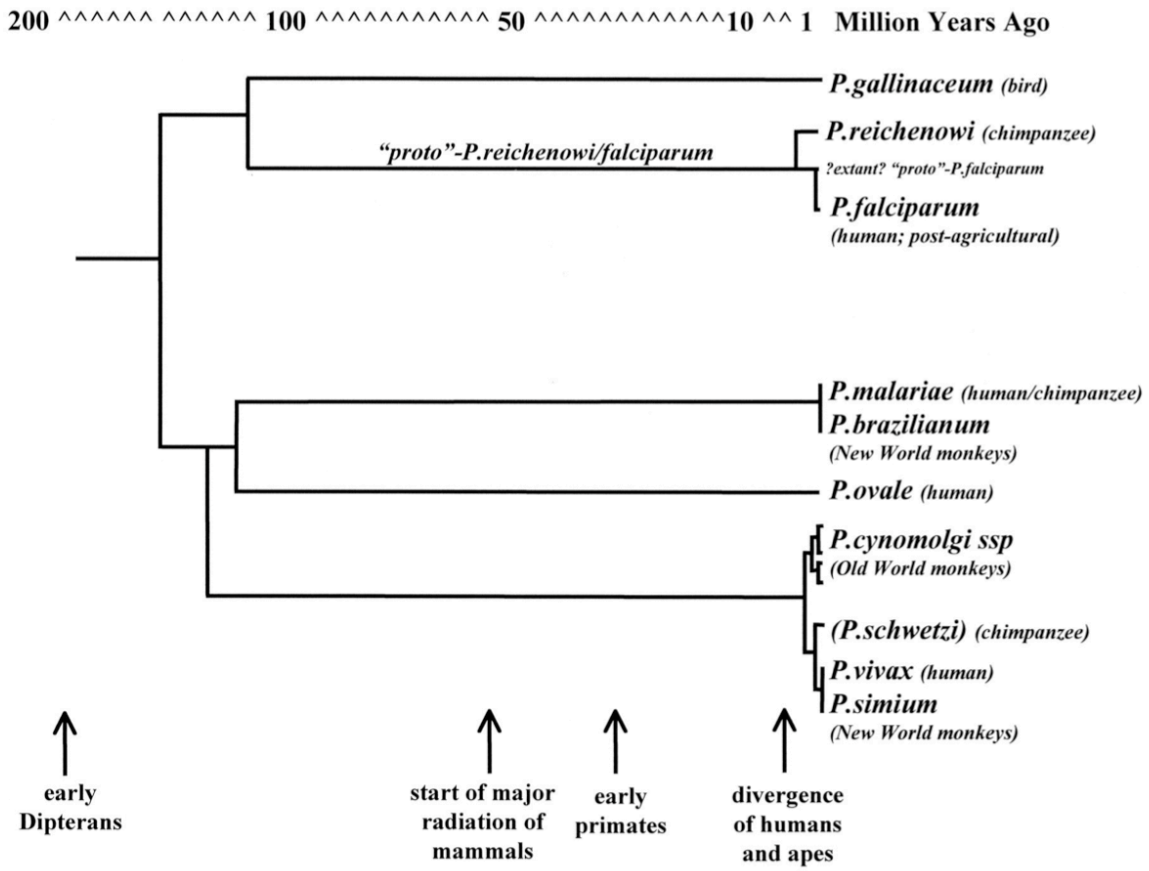

Figure 1.1 Phylogenetic tree for human *Plasmodium* (Carter and Mendis, 2002) [21]
Deaths amongst individuals over the age of 5 show a similar trend. Outside of Africa, there has been a general decrease in malarial mortality from 199,000 in 1980 to 15,000 in 2010, amongst under-fives [20]. The substantial public health burden of malaria generates significant damage to the economy and productivity of affected regions. Malaria deaths are thought to account for 3% of the total world's Disability Adjusted Life Years (DALYs) [22]. The impact on Africa is the most substantial, with malaria accounting for 10% of DALYs [22, 23] generating an annual cost of 12 billion USD (W.H.O. 2009).

Public health efforts to combat malaria take the three-pronged approach of insecticide-treated bed nets, case management of malaria illness and preventative treatment. Despite a proven track record in reducing malarial transmission and pathology, they are not adequately controlling infection in sub-Saharan Africa [24, 25]. This is partially due to the emergence of drug-resistant strains but also the economic instability of affected countries and the lack of infrastructure required to instigate these public health measures *en masse*.

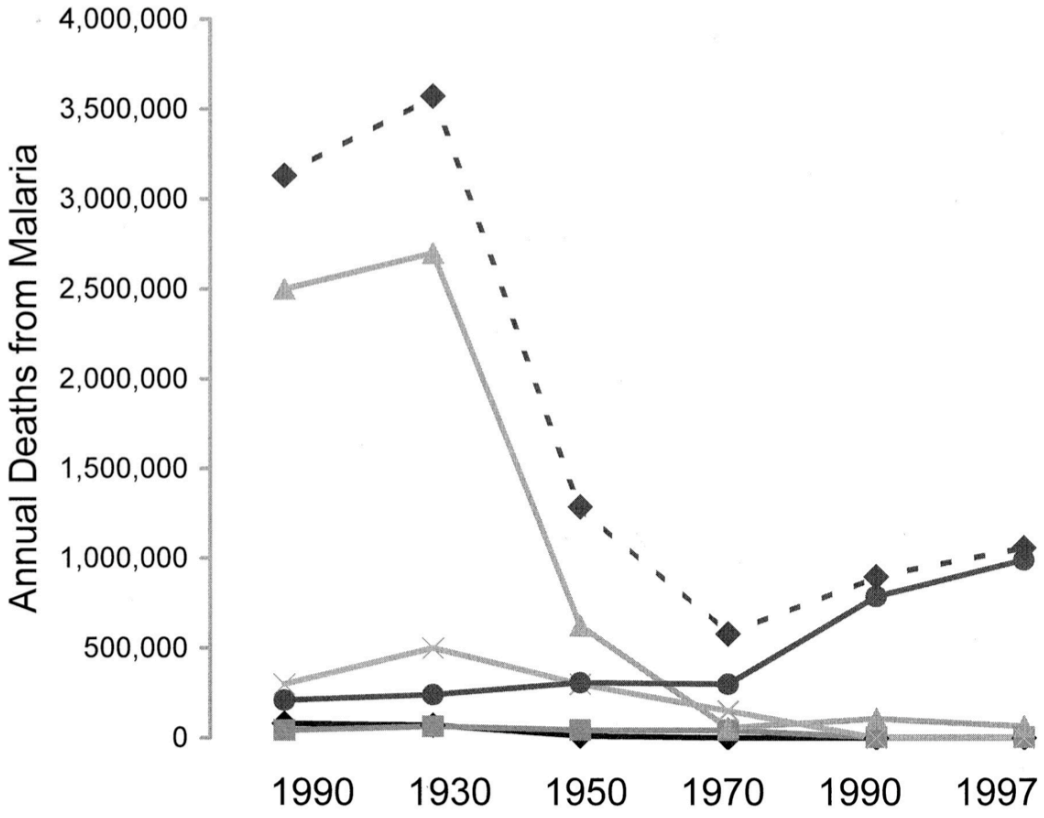

Figure 1.2 Historical perspective of malaria mortality in the last 100 years (Carter and Mendis 2002) [21] Europe and North America (□—□); the Caribbean and Central and South America (▪——▪); sub-Saharan Africa (•——•); China and Northeast Asia (X—X); the Middle East, South Asia, and the Western Pacific (□——□); and worldwide (□---□) (Legend from Carter and Mendis, 2002).

Artemisinin-based combination therapy, which results in rapid clearance of both asexual and sexual blood stages, in combination with a compound with a longer half-life, is partially reducing the effect of parasite resistant strains [26]. Intensive DDT treatment of bed nets and homesteads in the 1950s and 60s, although largely effective in eliminating malaria from the west, were discontinued amid resistance development in *Anopheles* mosquitoes and public health concerns [27-29]. To further combat the disease, investment in a combination of both traditional and new public health interventions is required. This may take the form of new drugs and larvicides, along with novel approaches such as transgenic "malaria-resistant" mosquitoes and vaccine design [24, 29].

1.3 *Plasmodium* and its life cycle

Malaria is caused by protozoan parasites of the *Plasmodium* genus. *P. vivax*, *P. ovale*, *P. malariae*, *P. knowlesi* and *P. falciparum* species specifically infect humans. The latter, *P. falciparum*, causes a severe form of malaria infection and is accountable for approximately 90% of deaths and 80% of human infections, with symptoms arising after approximately 6 to 14 days, including fever, vomiting, arthalgia, shivering, convulsions, haemoglobinuria and anaemia caused by haemolysis [30]. Symptoms peak approximately every 48 hours, marked by each successive release of merozoites from infected red blood cells [31].

1.3.1 The pre-erythrocytic stage

Plasmodium has a complex life cycle (fig 1.4) that utilizes the female *Anopheles* mosquito as a vector for transmission into the human bloodstream as the *Anopheles* mosquito takes a blood meal. An infected *Anopheles* mosquito will pierces an individual's skin to take a blood meal and release sporozoites from the saliva into the injection site. Upon injection of sporozoites into the skin, a significant proportion remain in the dermis while the rest enter the lymphatic circulation and are caught in the proximal lymph node where they present antigen to $CD11c^+$ dendritic cells [32, 33]. Sporozoites cross the liver sinusoid by gliding along its surface and traverse kupffer cells [34-37]. Sporozoites migrate through several hepatocytes within the liver parenchyma before establishing a parasitophorous vacuole [38-40] derived from the host-cell membrane which is rapidly remodelled by parasite proteins [41]. The parasitophorous vacuole forms as the parasite migrates forward from an invagination in the cell plasma membrane [33], mediated via the hepatocyte

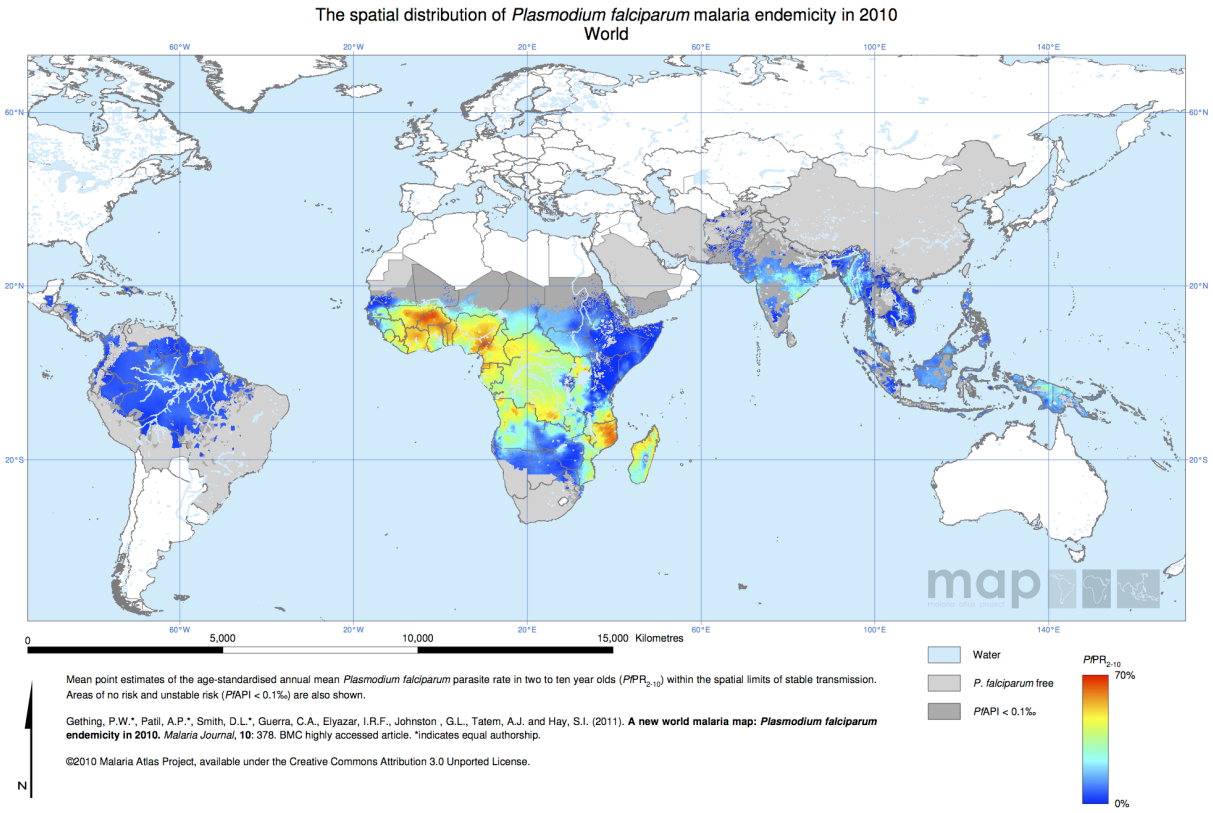

Figure 1.3 The distribution of malaria across the world in 2010. Colour scale represents "age standardized annual mean *Plasmodium falciparum* parasite rate in two to ten year olds" (Malaria Atlas Project) [42].

surface molecules, scavenger receptor BI and tetraspanin CD81 [43-46] and the parasite ligand TRAP [47, 48], although in the latter case, direct host-parasite interaction has not been biochemically demonstrated [33]. Once the parasitophorous vacuole is established, the parasite undergoes multiple nuclear divisions asexually and asymptomatically, then schizogony [49], which leads to the budding of merosomes from the infected hepatocyte [50, 51]. Merosomes are vesicles consisting of hundreds or thousands of merozoites [33]. They cross the sinusoidal barrier via an unknown mechanism and become trapped in the lung microvasculature, where they release their payload of merozoites directly into the lung capillaries [33, 52]. Merozoites are capable of invading erythrocytes and initiate the blood stage of the infection (fig 1.4).

1.3.2 The erythrocytic stage

Following merosome disintegration, individual *P. falciparum* merozoites invade erythrocytes via a very efficient mechanism that involves the erythrocyte surface molecules glycophorins A/B/C and sialic acid as receptors [53-56]. Erythrocyte binding ligands (EBLs) are a family of *Plasmodium* type I transmembrane proteins that interact with reticulocyte binding proteins [57]. The existence of five paralogues of each in *P. falciparum* reflects the redundant pathways utilised by the parasite and the versatility it possesses in invading both normocytes and reticulocytes [33, 57]. Generally, rodent malaria strains are able to invade both normocytes and reticulocytes whereas human strains exhibit preference for normocytes [58]. Merozoite surface protein 1 (MSP-1) is inserted into the merozoite plasma membrane via a GPI anchor and is processed into five fragments from release to entry [33, 59]. The merozoite re-orients its apical end to face the erythrocyte surface via apical membrane antigen 1 (AMA-1) [60] and upon penetration the parasitophorous vacuole forms [61]. Each merozoite undergoes asexual reproduction leading to schizogony. 16-32 merozoites are released upon rupture of the erythrocytic schizont and the asexual cycle is re-initiated. Differentiation into male and female gametocytes eventually occurs, which are subsequently ingested by the female *Anopheles* mosquito as it takes a blood meal. Gametocytes differentiate into gametes within the mosquito midgut that fuse forming a zygote. This zygote multiplies and transforms into ookinetes with motile function. These traverse the midgut and encyst between the basal lamina and the midgut epithelia [62]. Ookinetes differentiate into oocysts consisting of mid-gut sporozoites, which migrate to the salivary gland and the infected mosquito re-initiates the infection-replication cycle [13] (fig 1.4).

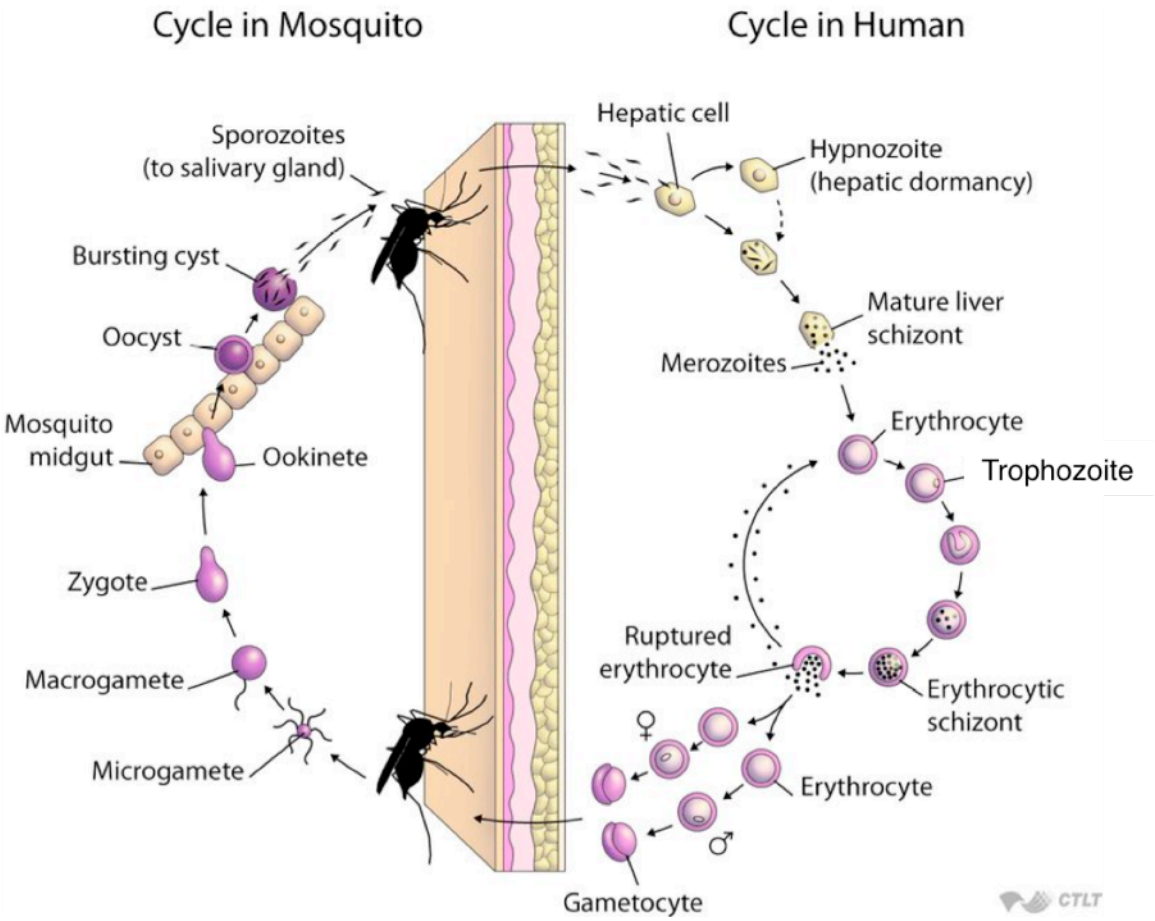

Figure 1.4 Life cycle of the malaria parasite (from Epidemiology of Infectious Diseases, Johns Hopkins Bloomberg School of Public Health, OpenCourseWare)

1.4 Malaria Immunopathogenesis

1.4.1 The pre-erythrocytic stage

Some sporozoites, once injected into the skin, present antigen to $CD11c^+$ dendritic cells in the proximal lymph node after draining into the lymphatic circulation, while others remain in the skin [32]. However, the precise interaction of sporozoites with specialized DCs in the skin, such as Langerhans cells, and the role of innate immune signalling mechanisms (such as MyD88/Toll-like receptor signalling) remain unelucidated [33].

The liver is capable of autonomously priming $CD8^+$ T cell responses in the absence of infiltrating APCs [63]. KCs, LSECs, Hepatic DCs, stellate cells and hepatocytes themselves are able to

present antigen [64], although with limited effector outcome as the liver feature a unique tolerogenic environment [65, 66]. Although it is unknown if parasite molecules retrotranslocate from the PV into the host cell cytoplasm to present antigen via MHCI [67, 68], as per DCs infected with *Toxoplasma* [41], DCs are capable of processing *P. berghei* circumsporozoite protein (CSP) *in vitro* and inducing *P. berghei* CSP-specific $CD8^+$ T cell clones that produce IFN-γ [69]. CSP is the major sporozoite surface protein shed by the sporozoite during its motile behaviour and has been extensively utilized to study antigen-specific cellular immune responses [33].

Upon merosome budding, the infected hepatocyte disintegrates and releases remnant parasite material [52] which leads to the formation of small granulomas as macrophages and neutrophils perform phagocytosis [33]. Granulomas, bundles of accumulated cells consisting primarily of macrophages, associated with severe inflammation [70], also form upon premature rupture of exoerythrocytic forms (EEFs) and host cell necrosis [33]. This inflammatory response varies according to the host and the parasite strain. Merosomes avoid KC phagocytosis in the liver sinusoid by not expressing phosphatidyl serine on their cell membrane [50].

Since the pre-erythrocytic stage is pathologically silent and somewhat a bottleneck in the parasite life cycle, it is an excellent target for vaccines and therapies because successful elimination of the parasite would lead to protection from malarial disease. Indeed, proteins expressed during this phase, such as the UIS gene family, when knocked out, confer sterile protection against re-infection [49] (discussed in 1.5.2). The pre-erythrocytic phase is the only stage of the parasite life cycle that can be eliminated by the induction of sterilizing immunity.

1.4.2 The erythrocytic stage

The erythrocytic stage of infection marks the onset of pathology in the afflicted individual. In malaria-endemic countries, adults and older children develop non-sterilizing immunity against the

malaria erythrocytic stage [71, 72]. Parasites retain a reservoir in such semi-immune individuals, which contributes significantly to the spread of infection. In non-immune individuals, erythrocytic rupture and the release of soluble parasitic products induces macrophages to produce IL-1 and TNF-α [73] and paroxysms of malarial fever are concurrent with the rapid production of pro-inflammatory cytokines such as TNF-α and IFN-γ [33, 74]. Macrophages, activated by TNF-α, secrete NO which upregulates intracellular cell adhesion molecule-1 (ICAM-1) in leukocytes and endothelial cells. Infected erythrocytes activate DCs through toll-like receptors, ancient components of the innate immune system: pattern-recognition receptors that recognise both extracellular and intracellular "molecular patterns" [75]. Indeed, DCs are activated through TLR 9 and MyD88 [33, 76] and malarial GPI toxin activates TLR2 [77] and haemozoin acts as a ligand for TLR9 [78].

Infected erythrocytes cytoadhere to the vascular endothelium to avoid clearance by the spleen [74]. In doing so, they cause damage to organs and, via binding to ICAM-1 and other receptors, cause cerebral malaria, described in further detail below (1.6). This binding generates a large inflammatory cascade marked by an overriding Th1 response involving TNF-α and IFN-γ, which in turn upregulates ICAM-1 on the endothelium and CD36 on platelets, which are primarily bound by the parasitic ligand *Pf*EMP-1 [74]. IFN-γ plays a key role in malaria immunopathogenesis. It is first produced by NK cells [79] and it is assumed this cell subset bridges the gap between the innate and adaptive response [33].

The pro-inflammatory response, primarily consisting of IFN-γ and TNF-α, is tempered by a responding increase in TGF-β and IL-10 [80] produced in part by activated regulatory T cells that suppresses the pro-inflammatory response [81]. $CD4^+CD25^+FOXP3^+$ regulatory T cells achieve this by producing a rapid burst of TGF-β during blood-stage infection [82]. IL-10- and IFN-γ-producing $CD4^+CD45RO^+FOXP3^-$ regulatory T cells have been associated with regulation of the

immune response during acute infection in uncomplicated malaria, rather than severe disease [83].

Naturally acquired non-sterile protection against malaria is predominantly maintained by antibody-mediated immune responses [71, 72, 84, 85]. Antibodies play a key role in enhancing monocyte/macrophage activity, inhibiting the sequestration of parasitized erythrocytes and inhibiting erythrocyte invasion. Children who have not yet developed protection to malaria typically exhibit non-cryophilic antibodies (such as IgM, IgG2 and IgG4) whereas older individuals who have acquired resistance to malaria show marked increases in parasite-specific cryophilic antibodies (IgG1 and IgG) [86-88]. The events that lead to antigen-specific B cell activation at the blood-stage are currently unelucidated [33]. Despite some studies indicating that merozoite surface protein 1 (MSP-1)-specific antibody responses feature a seropositivity half-life of decades [89], protective parasite-specific antibody responses are apparently short-lived since titres decline following acute infection [71, 72] and are re-acquired upon subsequent infection, indicating inadequate generation of memory responses. Although studies into specific B cells are limited, expansion of FCRL4-expressing B cells [90], $CD38^{+}IgD$ and $CD10^{+}CD19^{+}$ cells in acute malaria [91] have been reported in exposed individuals, albeit antigen specificity and memory establishment and maintenance were not analysed.

1.5 Parasite Attenuation and its Protective Effects

Attenuation of the *Plasmodium* liver stage by radiation, gene knockout and drug treatment has been previously shown to cause vaccine-like sterilizing protection to subsequent wild-type challenge, mediated predominantly by $CD8^{+}$ T cells [92-98]. These studies in attenuated strains have informed the majority of data pertaining to adaptive immune responses to *Plasmodium*.

1.5.1 Radiation Attenuated Sporozoites (RAS)

Multiple immunizations with gamma-irradiation attenuated sporozoites render both humans and rodents completely protected against subsequent challenge with wild type sporozoites [94, 95]. This protective immunity is mediated by numerous mechanisms, including αβ $CD8^+$ T cells and sporozoite-specific antibodies [98, 99] with a central role for IFN-γ [98, 100, 101] and can be transferred to naïve mice via adoptive transfer of both polyclonal antibodies and T cells [100, 102, 103]. Interestingly, protection can also be established in an entirely class II restricted manner, in β2-microglobulin deficient mice, implicating $CD4^+$ T cells and IFN-γ in protection [104]. Specifically, peptide-MHC recognized by $CD8^+$ T cells activates them to produce IFN-γ, which in turn provokes the secretion of IL-12, itself stimulating NK cells to produce more IFN-γ in a positive feedback loop [105]. This causes the activation of the NO pathway, which induces the killing of the infected hepatocyte [33, 106, 107].

1.5.2 Genetically Attenuated Parasites (GAP)

Murine parasites lacking genes that are critical for liver stage development [93, 108, 109] are a fairly recent development. These transgenic parasites are viable at the sporozoite stage and are able to successfully invade the liver but arrest prior to liver stage maturity, generating complete protective immunity against wild type sporozoite challenge in a manner comparable to radiation attenuated sporozoites [93, 108-113] mediated by MHC class I-dependent IFN-γ producing $CD8^+$ T cells [97, 110]. Similar transgenic parasites have been produced in *P. falciparum*, indicating a potential translational approach to human vaccinology [114, 115].

1.5.3 Chemical Attenuation and Chemoprophylaxis (CPS)

An alternative option is to inoculate mice with wild type sporozoites under prophylactic drug cover, using an anti-erythrocytic antimalarial compound. Several drugs have been tested in this approach, although most studies have utilized chloroquine. Chloroquine is an antimalarial that

kills parasites within erythrocytes, accumulating at high concentrations within the blood-stage digestive vacuole [116]. This form of immunization, termed chloroquine chemoprophylaxis (CPS), permits complete pre-erythrocytic development of the parasite prior to its destruction by the compound upon egress from the liver into the blood [96]. Infection and the acquisition of immunity are thereby the result of natural wild type infection, as opposed to the attenuated infection induced by genetically modified or radiation exposed parasites.

Immunization of whole sporozoites under prophylactic drug cover in this manner with chloroquine or primaquine generates protection against subsequent wild type challenge in a manner comparable to radiation and genetically attenuated parasites in both rodents [92, 117] and humans [118]. Protection is specific to the mediated by both $CD8^+$ and $CD4^+$ T cells, NO and IFN-γ [92] and a recent study found long-term responses are mediated by $CD8^+$ IFN-γ producing hepatic memory T cells [96]. This protection is specific to the liver stage, rather than the blood stage, in both humans [119] and rodents (Lewis *et al* unpublished). In the case of primaquine drug attenuation, the long-term persistence of the metabolically-active parasite within the liver was shown to be vital in ensuring long-term immune responses [117], although the requirement for persistance has been questioned [120]. CPS with antibiotics that inhibit apicoplast biogenesis similarly provoke sterile protection in a comparable manner, provoking liver stage specfic responses that depend on $CD8^+$ T cells and IFN-γ [121].

In a phase 1-2b trial of a recombinant blood-stage malaria vaccine in which sulphadoxine-pyrimethamine was administered to clear prior infections [122], it was found that drug administration correlated with reduced incidence of severe malaria, including cerebral malaria. The authors speculate that this may be due to the drug causing low-dose blood stage inocula resulting in an attenuated infection [122-125].

1.6 Human Cerebral Malaria

In the late 19th century, parasites were discovered in the brains of patients infected with malaria [126]. Today, human cerebral malaria (HCM) affects approximately 1% of all *P. falciparum* infections causing up to 500,000 deaths per year and long-term cognitive and physical dysfunction in those who survive the condition [127-129].

The early symptoms of HCM occur after 2-3 days of fever and include malaise, fits, vomiting, headache and diarrhoea. These are not pathognomonic of HCM, rendering early diagnosis uncommon and treatment is often delayed until the rapid progression to late symptoms occur, including haemiparesis, ataxia and coma. Late presentation of disease results in relatively low survival rates of 85% and 80% to first-line antimalarial drugs artemisinin and quinine, respectively [130]. Immunomodulatory therapies that abrograte or alter the immunopathogenesis of HCM are lacking, largely due to lack of understanding of the complicated series of events by which HCM occurs.

The brain pathology that leads to HCM has been partially revealed by post-mortem histological analysis of cerebral tissues. Histopathological analyses have lead to the description of "classical" HCM as the plugging of cerebral capillaries with parasitized erythrocytes and margination of monocytes and macrophages within cerebral vessels [131-133]. This coincides with both swelling and haemorrhaging within the corpus callosum and subcortical rim. Haemorrhages within the cerebella and cerebral cortices are also evident [131].

However, the classical presentation of HCM is not always consistent amongst patients. The absence of a detailed comparative analysis of cerebral pathology has led to numerous clinical descriptions of atypical HCM, not necessarily featuring the classical triad of leukocyte infiltration, perivascular haemorrhage and parasite sequestration. The reasons for atypical presentation are

unknown, although may be due to environmental factors, host immune responses or genetic variation between *Plasmodium* strains and hosts [133]. Indeed, two further non-classical histopathological presentations of HCM are reported in African children alone: Firstly, parasite sequestration in the absence of other typical signs and secondly, an "HCM-like" syndrome clinically defined as HCM but with no evidence of parasite sequestration in the cerebral tissues [133-135]. Furthermore, numerous differences exist between paediatric and adult HCM and it is unknown, although generally suspected, that pathology is not consistent between non-immune adults and children [136].

This is supported by epidemiological data relating to severe malaria, including HCM. Adults in endemic areas acquire non-sterilizing immunity to malarial infection and severe malaria is a complication almost exclusively associated with infancy [137]. However, HCM does not occur in children upon first infection, but after exposure to at least one prior infection [133, 137]. This is in contrast to non-immune adults who travel to endemic regions and develop HCM upon first infection with a higher mortality rate than non-immune children. Artavanis-Tsakonas and colleagues suggest that this may be because first infection of an infant living in an endemic area induces only low levels of both IFN-γ and TNF-α by the innate immune response since T cells are not yet primed to parasite-specific antigen. The authors suggest that clinical symptoms are minimal due to maternal antibody, cytokine-mediated killing or physiological barriers, such as dietry deficiencies. However, upon subsequent infection, the authors hypothesize that primed T cells produce increased IFN-γ leading to HCM and systemic shock. Over time, if the child survives repeated infections, the immune response becomes more efficient at reducing parasitemia an the level of antigenic stimulation is in turn reduced, thereby decreasing the inflammatory response and incidence of HCM. This is correlated with a switch in lymphocyte subsets from Th1 to Treg, producing IL-10 and TGF-β rather than IFN-γ In contrast, the authors suggest that non-immune adults develop overriding inflammatory responses upon first

infection due to cross-reactivite priming of T cells. Non-immune children, however, have fewer cross-reactively primed lymphocytes due to exposure to fewer cross-reacting pathogens, therefore experience less incidence of HCM [137] (fig 1.5).

1.7 Experimental Cerebral Malaria

Since HCM studies are largely restricted due to late presentation of symptoms and obvious ethical considerations, little work has been done to uncover the immunological processes in HCM immunopathogenesis beyond descriptive studies. *In vivo* imaging techniques including magnetic resonance spectroscopy, computational topography and magnetic resonance imaging are reversing this trend, but are hampered by ethical and financial constraints [133, 138-142]. Hence experimental models have been relied upon to uncover the pre-clinical features and immunopathogenesis of disease.

Some studies have been conducted in squirrel [143] and rhesus [144, 145] monkeys but such studies are restricted due to ethical and financial considerations. Infection of inbred mouse strains with lethal *P. yoelii* [146] and *P. berghei* [147, 148] has been shown to mimic human cerebral symptoms but by far the infection of C57BL/6 mice with *Plasmodium berghei* ANKA (*Pb*ANKA) is the best animal model for the disease [133] termed Experimental Cerebral Malaria (ECM).

The onset and progression of ECM occurs rapidly between days 5 and 10 post-infection and includes fitting, ataxia, respiratory distress and coma leading to death within 5 hours [149]. Symptoms can be scored against the Rapid Murine Coma and Behavior Scale (RMCBS) [150] (Appendix 1) to aid diagnosis and quantitative description of disease pathology. Scoring typically progress from < 5 to 20 within one day.

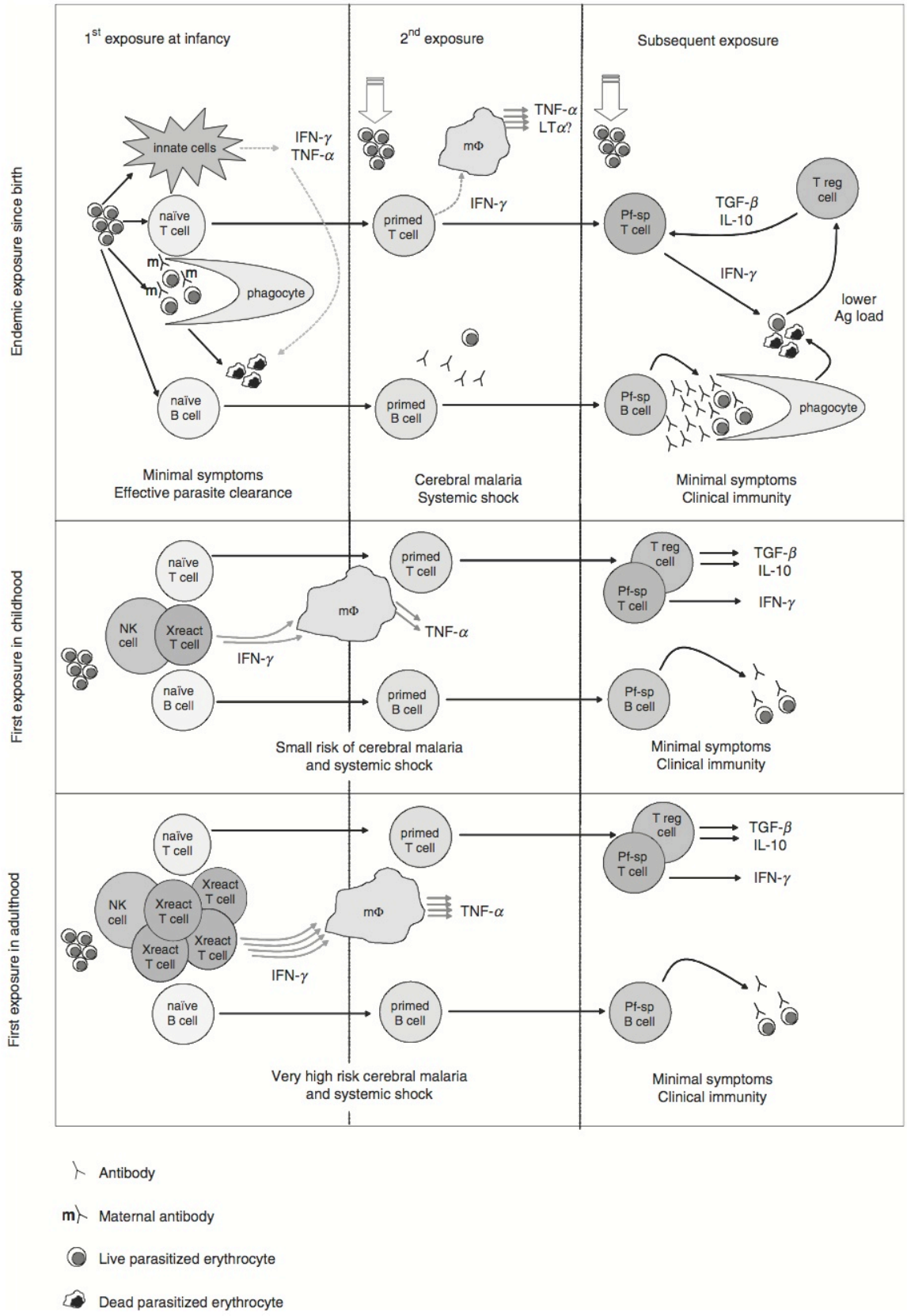

Figure 1.5 Hypothetical model for the clinical immunity to *P. falciparum* dependent upon age at first exposure (Artavanis-Tsakonas, 2003)[137].

ECM causes blood-brain barrier damage and vascular leakage associated with the olfactory bulb, cortex and cerebellum [141, 151], destruction of neuronal populations in the striatum and cortex [152], inflammation in the perivascular region [153] and accumulation of parasitized erythrocytes [147, 154] and platelets [155, 156] within the brain microvasculature, the latter of which cause damage to endothelial cells [133, 157]. In addition to the pathological symptoms, these factors cause cognitive dysfunction and impaired visual memory [158]. A recent study employing intravital microscopy indicated that ECM is associated with platelet marginalization, CD14 expression, fibrin deposition and vascular leakage in the postcapillary venules, rather than the capillaries or arterioles. Microhaemorrhaging was rarely reported and it was concluded that ECM pathology is caused by the opening of the transcellular-vesicular fluid transport and paracellular-junctional pathways at the blood-brain barrier (BBB) [159].

Susceptibility of C57BL/6 mice to ECM is dependent upon environmental exposure and age; animals older than 16 weeks are generally resistant [154]. Genetic factors are also involved in ECM susceptibility, with (as-yet-unknown) genes encoded within chromosomes 1, 9, 11, 17 and 18 identified as responsible via crossing of resistant and susceptible mouse strains [133, 160-163]. Furthermore, distinct gene expression profiles involved in apoptosis, immune-activation, neurotoxicity and neuroprotection have been identified in the brain [133, 164-166].

Controversy exists about the accuracy and relevance of ECM as a model to study HCM [167-169]. The majority of concerns have focused on the role of parasite sequestration, an apparently integral component of HCM immunopathogenesis, and its relevance in the ECM model [170, 171] and the translational relevance of interventions in the murine model to human therapy [168]. Since mouse brains are often perfused before histopathological investigation, a practice that is rarely employed in the preparation of materials from human subjects, the extent of parasite sequestration in ECM may be underestimated [133]. Indeed, a recent study demonstrated that

treatment with an antimalarial 15-20h prior to the onset of ECM symptoms delays pathology until parasitemia returns to the same level at pre-treatment. This does not alter the number of $CD8^+$ T cells in the brain, and the authors conclude that parasite sequestration is an integral component of ECM immunopathogenesis [172]. Nonetheless, blocked cerebral vessels in ECM-symptomatic animals contain a mixture of leukocytes and parasitized erythrocytes [154, 173]. Sequestration alone is likely not adequate for ECM pathology. Sequestration remains a largely uninvestigated aspect of ECM pathology, although brain-localized parasite biomass has been correlated with ECM [174, 175], albeit not by binding to CD36 [133, 171].

1.8 Immunopathogenesis of Experimental Cerebral Malaria

The immunopathogenesis of cerebral pathology in both HCM and ECM is a complicated series of inter-related events involving multiple organs, parasite and host immune factors over a period of some 5-10 days. The precise events that lead to BBB breakdown and cerebral pathology are not entirely elucidated although the literature has enabled postulation of a hypothetical scheme of events that results in the definitive endpoint: alteration of the BBB and the onset of ECM symptoms [176-181]. *In toto* the literature indicates that ECM immunopathogenesis involves a multifaceted Th1 host response with an essential requirement for IFN-γ [182] and lymphotoxin-β [153, 183] and that the balance between pro-inflammatory and regulatory T cell responses [184-186], rather than Th2 responses [187] ultimately determines susceptibility [133]. Despite it being partly suppositional, the literature yields a comprehensive dataset that allows a corresponding series of events to be presented as a hypothetical schema for ECM immunopathogenesis (fig 1.5). As per the literature, schematic descriptions of the events that lead to both HCM and ECM typically commence at the rupture of infected erythrocytes, rather than the pre-erythrocytic stage (the steps involved in ECM immunopathogenesis described below are mostly adapted from Renia *et al* 2006 and de Souza *et al* 2010) [181] [133]:

STEP ONE: Parasitized erythrocytes adhere to endothelial cells in the brain and other peripheral tissues, inducing chemokine secretion and activation of the endothelium. At the same time, parasitized erythrocytes rupture and induce monocyte, neutrophil and DC activation. A state of systemic inflammation is established.

Malaria infection commonly features the sequestration of mature parasites within peripheral tissues to avoid immune clearance in the spleen via binding to the vascular endothelium [188]. Pro-inflammatory cytokine levels, mostly IFN-γ, TNF-α and lymphotoxin, are significantly increased [182, 189], activate the endothelium and upregulate adhesion receptor expression. Parasites adhere to liver, lung and brain tissue and induce chemokine secretion. Chemokine production and expression of chemokine-receptors on leukocytes is upregulated [190-192]. Indeed, *Pb*ANKA infection causes upregulation of CCL2 (MCP-1), CXCL10 (glP-10) and CCL5 (RANTES) expression, the latter of which is specifically associated with ECM [193].

A proportion of infected erythrocytes that do not sequester undergo clearance in the spleen [194], the secondary lymphoid organ that filters the blood and filters blood-borne organisms from the blood circulation [195]. Within the spleen, antigen uptake and processing is performed by $CD11c^{high}CD8^{+}$ DCs, which are responsible for ECM immunopathogenesis [196]. Parasites associate with $CD11c^{hi}CD8^{+}$ DCs, which capture dying cells and exogenously process antigen for cross-presentation via MHCI [197]. Activation of the innate branch of the cellular immune system is a key feature of the early immune response in ECM, monocytes and macrophages in particular, and is believed to be an essential component of ECM immunopathogenesis at this early time point [198-200].

STEP TWO: Neutrophils and monocytes migrate to the brain via chemotaxis

During fulminant infection, brain-sequestered leukocytes express CCR2 and CCR5. While the former has been shown to be non-essential [201], the latter is required for full ECM

development, with CCR5-deficient animals exhibiting reduced leukocyte brain infiltration [202, 203]. Neutrophils and monocytes express these receptors and, via chemotaxis, migrate to the brain where they remain intravascular, a classic and unique indicator of cerebral pathology [132, 204]. The blood-brain-barrier is made up largely of endothelial cells [205]. Neutrophils and monocytes bind to the brain endothelium via ICAM-1 and LFA-1, which is upregulated on activated brain endothelial cells [178] in addition to P selectin and VCAM-1 [190, 192] and, in the case of ICAM-1, this upregulation is essential for the development of ECM [206]. This early migration of innate leukocytes to the cerebral tissues causes initial damage to the BBB and stimulates more chemokine and cytokine production [181].

STEP THREE: Naïve T cells are primed in an antigen-specific manner by CD11c$^+$ DCs and activated T cells migrate to the brain in response to chemokines

Several days post-infection, naïve T cells are fully primed by CD11c^{high}CD8$^+$ DCs [196] and these cells migrate to the brain in a full assault of the blood-brain-barrier. This phase represents the central component of ECM immunopathogenesis and is responsible for severe symptoms and mortality. DCs present antigen to CD4$^+$ and CD8$^+$ T cells and CD4$^+$ T cells assist CD8$^+$ T cell activation and proliferation, possibly via the CD40/CD40L system [207].

Following cross-presentation by DCs, IFN-γ derived from NK cells upregulates chemokine-receptor CXCR3 on CD8+ T cells [208] and they migrate to the brain in an antigen-specific manner via chemotaxis [209-211] to IFN-γ induced chemokines as described in step two.

STEP FOUR: CD8$^+$ T cells accumulate within the cerebral vessels, recognise and kill endothelial cells presenting parasite antigen by MHCI on their surface

In addition to CD8$^+$ T cell chemotaxis, CXCR3 upregulation by IFN-γ derived from NK cells mediates CD8$^+$ T cell accumulation within the cerebral tissues [208] and IFN-γ signalling mediates their sequestration within the brain [212]. Antigen-specificity is mostly unknown,

although 50% of brain-sequestered $CD8^+$ T cells bear the same Vβ 8 segment in their T-cell receptor as a dominant and expanding subset of $CD8^+$ T cells in the periphery, indicative of a dominant parasite epitope [213].

Activated endothelial cells efficiently present antigen [214] and it has been suggested that Th1-cytokine-activated endothelial cells resident in both brain and other tissues phagocytose parasite-derived material from sequestered parasites and present antigen to $CD8^+$ T cells [181]. *Pb*ANKA infection induces the upregulation of both MHCI and II on cerebral endothelial cells [215] and studies in MHC-impaired transgenic mice suggest a crucial role for MHC presentation in ECM immunopathogeneis [213].

Studies into the cytotoxic mechanism of $CD8^+$ T cells sequestered within the brain microvasculature have yielded assorted results. The perforin pathway is one potential candidate for targeted killing since perforin-deficient mice do not develop ECM [203, 216]. Fas-deficient mice did not develop ECM in one study [216] but did in others [203, 217] and the TNF factor pathway can be excluded on the basis that TNF-α deficient animals succumb to ECM [153].

STEP FIVE: The blood-brain barrier ruptures and haemorrhages

The migration of $CD8^+$ T cells to the cerebral vessels and their cytotoxic activity on the endothelium is directly responsible for the damage to the blood-brain-barrier that is the hallmark of ECM pathology. $CD8^+$ T cell depletion at both early and late infection prevents ECM pathology [217-219]. Ultrastructural changes to the blood-brain-barrier occur and severe perturbation causes perivascular oedema and haemmorhaging [178, 220] and, as a result, ECM symptoms and death occur within hours [176-180].

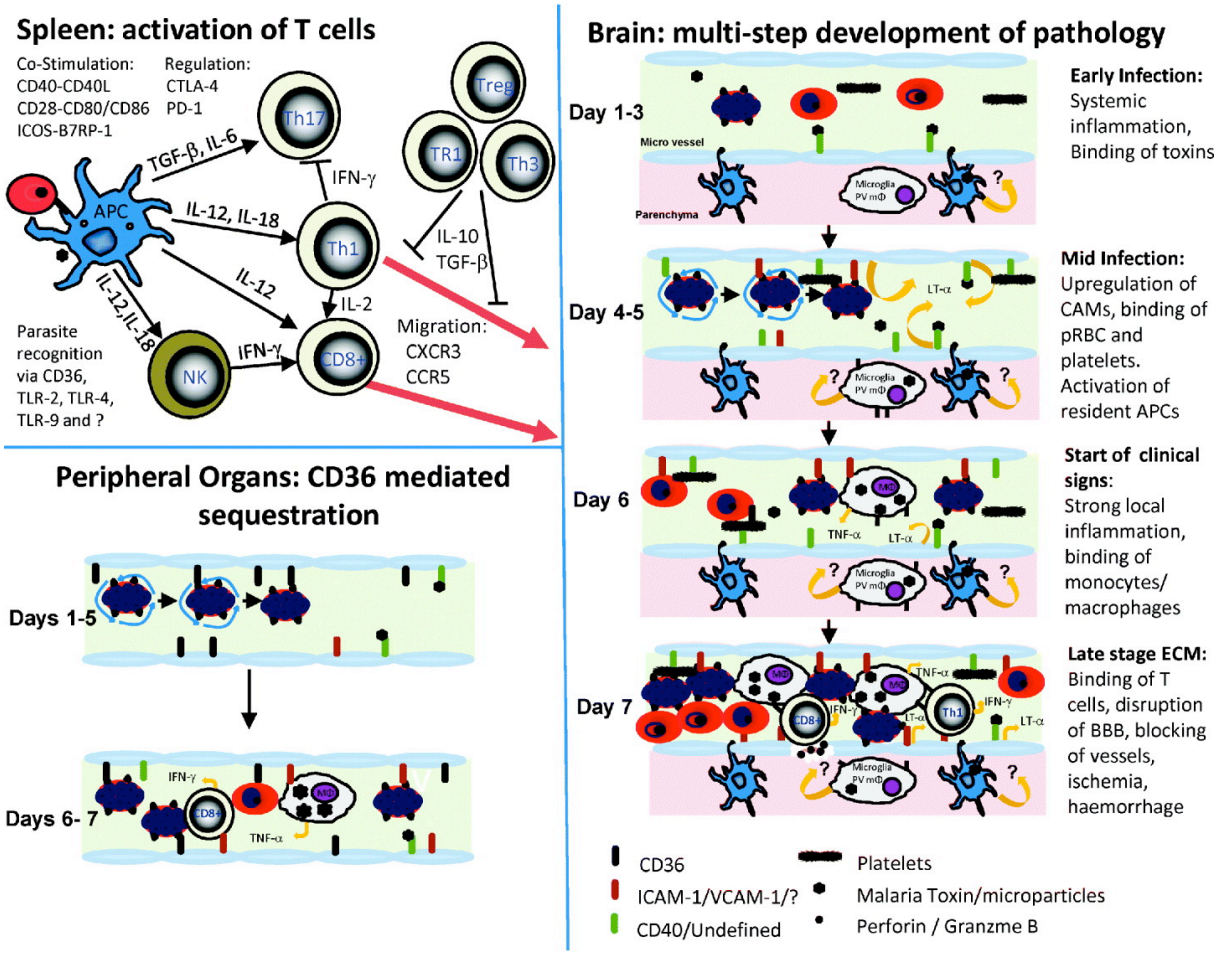

Figure 1.6 The immunopathogenesis of cerebral malaria (de Souza *et al*, 2010) [133] Parasitized erythrocytes rupture and the resultant Th1 response and released molecules cause the activation of endothelial cells and parasite-specific receptors. Phagocytosis of parasite moieties causes the priming of lymphocytes within the spleen, in turn promoting systemic inflammation and further activating endothelial cells, microglia, perivascular macrophages and astrocytes within the brain. Endothelial receptors and bound platelets bind parasitized erythrocytes. Lymphocytes and myeloid cells chemotax to the brain guided by chemokines produced by glial cells and the activated endothelium. Leukocytes and parasitized erythrocytes bound to the endothelium interefere with the circulation and produce cytotoxic molecules. This damages the blood-brain-barrier and causes haemorrhages and oedema. (Legend adapted from de Souza et al [133]).

1.9 T cells in ECM Immunopathogeneis and Immunopathology

The crucial role of T cells in ECM immunopathology cannot be overstated (fig 1.6 and 1.7). ECM mice feature a thirty-fold increase in brain-sequestered $CD8^+$ $CD3^+$ T cells compared to naïve animals and fifteen-fold compared to infected but non-cerebral animals [202]. $CD8^+$ T cell-depleted mice do not succumb to ECM [217] and splenic $CD8^+$ T cells adoptively transferred from ECM-suffering mice to RAG-2-deficient donors, normally resistant to ECM [203, 217, 218, 221-223], migrate to the brain and cause ECM pathology [181, 203]. Studies into the specific

surface marker expression of sequestered $CD8^+$ T cells in ECM yield contrasting data: $CD44^+$ $CD62L^-$ LFA-1^+ ICAM-1^+ $CD8^+$ T cells were isolated from homogenized brain tissue purified by percoll gradient [203, 213] whereas $CD44^{low}$ $CD62L^{low}$ LFA-1^{low} ICAM-1^{low} $CD8^+$ T cells were isolated from collagenase-treated brain tissue isolated from intracardially-perfused animals [181]. Renia *et al* speculate that these apparently contradictory data may represent two distinct populations of $CD8^+$ T cells: a *recently-arrived* activated subtype and an earlier subset that have downregulated their expression markers following interaction with monocytes and platelets or endothelial cells [181].

The precise role of $CD4^+$ T cells has not been elucidated, and though they undoubtedly represent a central component in ECM immunopathogenesis [217, 218, 223], their role is either restricted to the innate or induction phase of ECM depending upon the *Pb*ANKA clone and mouse strain utilised [217, 218, 224, 225]. There is a 9-fold increase in their sequestration in the brains of ECM animals as compared to non-cerebral [202] but their precise role in the induction versus effector mechanisms of ECM pathology is not clear. In C57BL/6 mice infected with *Pb*ANKA clone BdS, late (days 5-6) $CD4^+$ T cell depletion had no effect on ECM outcome, but early (days 0-3) depletion did have an effect, suggesting that in the classic ECM model, $CD4^+$ T cells play an essential role in the induction of ECM and activation of $CD8^+$ T cells [217]. In one study, in which $CD4^+$ T cells were purified from brain tissue homogenates, they were of the $CD44^+$ $CD62L^-$ effector memory subset [203].

In addition to $\alpha\beta$ T cells, there is an increase in $\gamma\delta$ T cells sequestered in the brain microvasculature in ECM mice [217]. Although they do not have an effector function in ECM immunopathogenesis [225], they may play a role in ECM induction, since depletion of $\gamma\delta$ T cells at very early blood-stage infection has been shown to prevent ECM [181, 223, 225].

1.10 Disrupting the immunopathogenesis of Experimental Cerebral Malaria

Numerous studies have interrupted the finely tuned balance of interrelated events that lead to cerebral pathology in mice. The overall host inflammatory response is of paramount importance to cerebral immunopathogenesis and it is unsurprising that the C57BL/6 mouse strain, which has a strong Th1 bias [226], produces the model reaction of overriding pro-inflammatory responses that cause pathology. This is comparable to the human situation, in which polymorphisms in genes associated with the innate immune response, such as the IL-10 promoter, cause IL-10

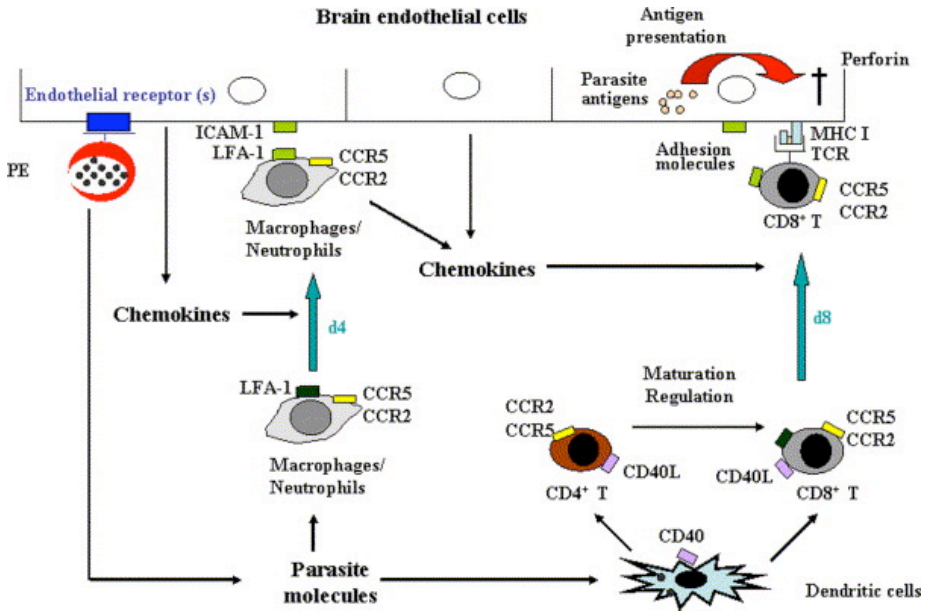

Figure 1.7 The role of T cells in Experimental Cerebral Malaria (Renia *et al*, 2006) [181] At blood stage infection, increasing blood stage parasitemia and rupture of infected erythrocytes is associated with phagocytosis of parasite moieties by splenic $CD8^{+}CD11c^{+}$ dendritic cells, which exogenously process antigen via MHCI, prime and activate lymphocytes and cause systemic inflammation, associated with pro-inflammatory cytokines such as IFN-γ. Systemic inflammation and parasitized erythrocytes activate neutrophils and monocytes, which migrate to the brain from day 4 by chemotaxis through receptors CCR2 and CCR5, amongst others, and bind to the endothelium through adhesion molecules LFA-1, ICAM-1 and others. Systemic inflammation increases endothelial activation in the brain, increased binding of infected erythrocytes to endothelial receptors and increased migration of lymphocytes from the spleen to the brain microvasculature in response to chemokines. Primed lymphocytes migrate to the brain in a similar manner. Leukocyte and parasite sequestration damages the blood-brain barrier and leads to cerebral pathology, possibly through antigen-specific T cell cytotoxicity, via MHCI restricted presentation of parasite-derived antigen on endothelial cells; haemorrhaging, coma and death results. (Legend adapted from Renia et al [181]).

promoter haplotypes that confer a high IL-10 : IL-12 ratio. Individuals with these haplotypes feature decreased IFN-γ production, correlated with increased incidence of malarial anaemia

[227] and presumably reduced incidence of HCM. The inflammatory response that leads to ECM in susceptible mice can be downregulated by various means to prevent the development of cerebral pathology. For example, neutralization of TNF-α was historically thought to prevent the development of ECM [200, 228-230] until later studies found that related cytokine lymphotoxin-α is responsible [153] via signalling through LT-beta and TNF receptor 2 [181, 183]. Similarly, neutralization of IFN-γ [182] and depletion of macrophages [229] has been shown to prevent ECM development. Additionally, neutralization of IL-10 causes ECM-like cerebral symptoms and brain pathology in C57BL/6 mice infected with non-ECM inducing parasite strains [231] (A Joschko MSc Thesis 2012). Conversely, studies in Th2-biased mouse strains have found that ECM symptoms can be provoked in non-ECM-susceptible mice by modulating the immune system to produce an inflammatory response. This has been demonstrated by administration of endotoxin (concomitant with increased TNF-α production) [232], inhibition of CTLA-4 signalling [233], administration of CpG [234], neutralisation of haeme oxygenase 1 [235] and neutralisation of the anti-inflammatory cytokine IL-10 [184] in non-susceptible mouse strains. Despite its crucial importance, the exact role of IL-10 in the suppression of ECM immunopathogenesis has not been fully elucidated, since IL-10 is produced in abundance in both the plasma [174] and spleen [236] of ECM-symptomatic mice, possibly as the result of a cytokine storm.

Co-infection of ECM-susceptible mice with *Pb*ANKA and other parasite strains or infections is associated with protection from ECM. This may be due to modulation of key factors in the innate immune response and/or the activation of dendritic cells and it has been suggested that non-ECM parasite strains may activate a different subset of dendritic cells that leads to a reduction and/or failure in the priming and expansion of lymphocytes [237]. Indeed, co-infection of *Pb*ANKA with murine AIDS [238], Filaria [239], nonlethal *Pb*XAT [240] and *Py* 17XNL [241] protects against ECM by downregulation of the Th1 response. In the former

three, protection is mediated via the upregulation of IL-10, with protection abolished in the absence of this cytokine [238-240] but in the latter case protection is independent of IL-10, $CD4^+CTLA\text{-}4^+$ and $CD4^+CD25^+$ cells [238, 240, 241]. In contrast, ECM induced by normal *Pb*ANKA infection can be ablated independently of IL-10 by the expansion of regulatory T cells, via IL-2/anti-IL2 complexes. This protection is dependent on CTLA-4 and features a marked reduction in the recruitment of $CD8^+$ and $CD4^+$ lymphocytes to the cerebral microvasculature [242]. Interestingly, the oral administration of activated charcoal, which is highly effective at adsorbing cytokines such as IL-6, TNF-α and IL-1 [243] has been demonstrated to protect against both ECM and HCM [244] and is being expanded into clinical trials. Few studies have examined the effect of antimalarial treatment on malaria immunopathogenesis. It has been demonstrated that treatment of infected mice with an antimalarial prior to the onset of ECM symtoms – the usual endpoint of infection – attenuates infection by decreasing parasitemia and causing a delay in the onset of cerebral pathology. [172]. Another study of antimalarials indicated that attenuation of early blood-stage infection may show similar effects. [245].

Very few studies have examined *early* cellular immune responses associated with parasite attenuation in terms of its role in protection from cerebral pathology. This is in contrast to studies of vaccine-like sterilizing immunity, such as those produced by GAP and RAS, which have been extensively studied at the pre-erythrocytic stage. Co-infection of ECM-susceptible mice with *Pb*ANKA and *Pb*K173, which results in protection from ECM, was found to be associated with increased IFN-γ at 24 hours post-infection and an increase in transcriptional abundance of IFN-γ, IL-10 and IL-12 [236]. Interestingly, an early Th1 peak was also apparent in *Pb*K173 infection alone and was credited as the protective agent against cerebral pathology, by altering downstream ECM immunopathogenesis. The source of IFN-γ was identified as β2-microglobulin specific, a component of MHC-I [246], and not NK, γδ T cell or NKT cell-specific. From these data the authors hypothesized that the source of IFN-γ is $CD8^+$ T cells,

which, despite being classically defined as a component of the adaptive immune response, are able to rapidly produce the cytokine non-clonally via bystander activation under numerous conditions, such as LPS [247] and bacterial [248-250] challenge. In another study, the vaccination of susceptible animals with irradiated blood stages was found to prevent the development of ECM in susceptible animals upon challenge with non-irradiated parasites [251]. Vaccinated animals produced splenic IFN-γ when challenged with parasite antigen and, while the source of the cytokine is not addressed, the authors speculate that early IFN-γ produced by splenic lymphocytes is responsible for protection.

Very few studies have examined the pre-erythrocytic stage or the interaction between liver and blood that occurs in early infection on the immunopathogenesis of ECM. Some initial work has indicated a potential role for the liver stage in modulation of disease severity. A recent study reported that a transgenic parasite line lacking a *Plasmodium*-specific apicoplast protein resulted in attenuated merozoite formation and impaired liver-stage development. This is turn correlated with a reduced incidence of cerebral pathology [252].

1.11 Hypothesis

ECM is caused by a complicated series of interrelated events that involves both host and parasite, systemic and organ-specific pathology and immune responses (fig 1.8). Hypothetical descriptions of ECM immunopathogenesis have classically started at the onset of blood stage infection, which is coincident with systemic pathology, the induction of innate immunity and the priming of the adaptive immune response. The pre-erythrocytic and very early stages of the disease have been largely overlooked in the literature, despite some evidence to suggest that early immune responses, specifically inflammatory responses, are capable of altering downstream immunopathogenesis in a manner that involves $CD8^+$ T cells and IFN-γ [236, 251]. As described above, the attenuation of *Plasmodium* at the pre-erythrocytic stage via various means, such as

GAP, RAS and CPS can provoke the host immune response to generate protective immunity against subsequent infection.

1. I propose that it is possible to attenuate *Plasmodium* liver stage development as a means of manipulating the host immune response to alter the clinical outcome of ECM via sub-therapeutic chemoprophylaxis in a manner similar to GAP, RAS and CPS. Chemoprophylaxis must necessarily be administered at a sub-therapeutic dosage to permit the development of the parasite successfully through the liver stage.

2. Since all forms of pre-erythrocytic parasite attenuation (RAS, GAP and CPS) have been demonstrated to manipulate the host immune response via induction of $CD8^+$ T cells and IFN-γ, I hypothesize that sub-therapeutic chemoprophylaxis of the parasite at the pre-erythrocytic stage will induce $CD8^+$ T cells earlier and in greater abundance than would occur in natural infection. I further hypothesize that induced $CD8^+$ T cells will modulate the outcome and severity of cerebral pathology in C57BL/6 mice infected with *Pb*ANKA sporozoites by the induction of a cell-mediated Th1 response that occurs earlier than in natural infection. This response will deregulate downstream systemic Th1 responses and reduce $CD8^+$ T cell priming that normally occurs much later in infection.

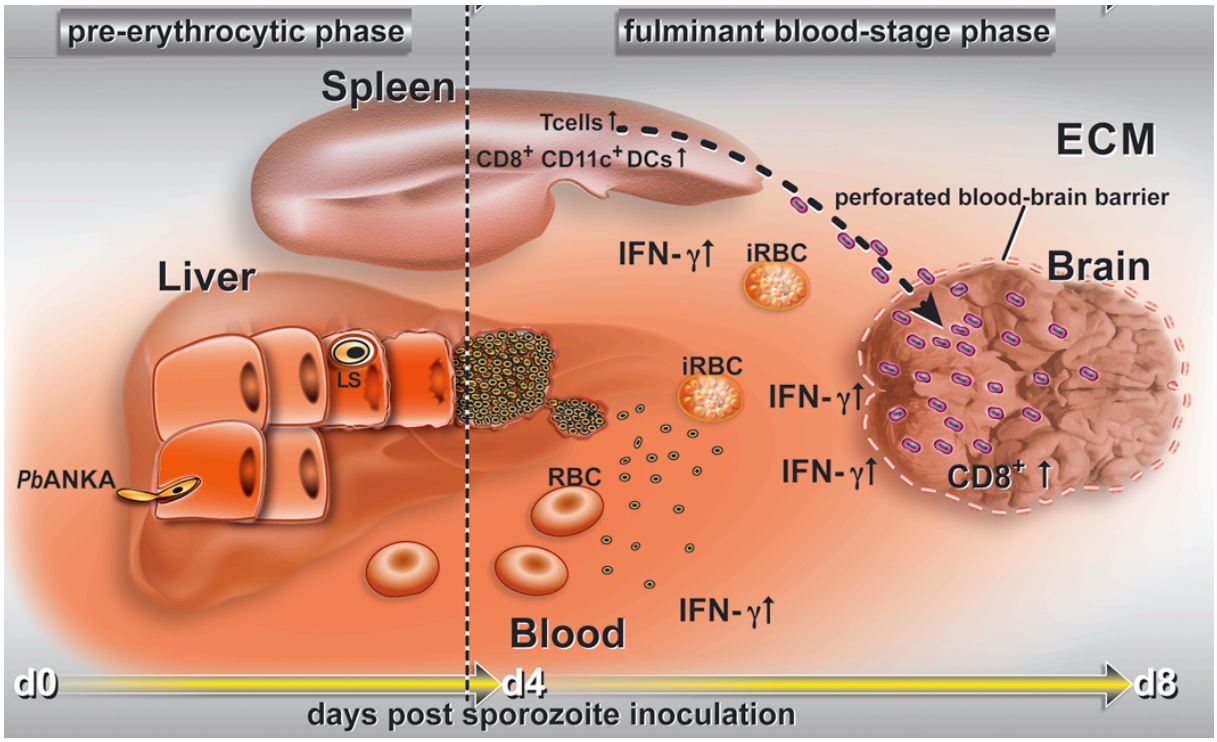

Figure 1.8 The pre-erythrocytic / erythrocytic immunopathogenesis of Experimental Cerebral Malaria . Following sporozoite invasion, parasites undergo pre-erythrocytic development in the liver prior to the onset of blood stage infection. No significant protective pro-inflammatory response occurs at either liver or spleen at the pre-erythrocytic stage. At blood stage infection, increasing blood stage parasitemia and rupture of infected erythrocytes is associated with phagocytosis of parasite moieties by splenic $CD8^{+}CD11c^{+}$ dendritic cells, which exogenously process antigen via MHCI, prime and activate lymphocytes and cause systemic inflammation, associated with pro-inflammatory cytokines such as IFN-γ. Systemic inflammation increases endothelial activation in the brain, increased binding of infected erythrocytes to endothelial receptors and increased migration of lymphocytes from the spleen to the brain microvasculature in response to chemokines. This leukocyte and parasite sequestration damages the blood-brain barrier and leads to cerebral pathology, possibly through antigen-specific T cell cytotoxicity, via MHCI restricted presentation of parasite-derived antigen on endothelial cells; haemorrhaging, coma and death result.

Chapter 2

Materials and Methods

2.1.1 Materials

Computer software:

7500 Software v2.0.5	Applied Biosystems, USA
CellQuestPro	BD Biosciences, Germany
Endnote X4	Thomson Reuters, USA
FCAPArray software	BD Biosciences, Germany
Magellan V 5.0 software	Tecan, Austria
Microsoft Excel for Mac 2008	Microsoft Corporation, USA
Microsoft Powerpoint for Mac 2008	Microsoft Corporation, USA
Microsoft Word for Mac 2008	Microsoft Corporation, USA

Laboratory equipment:

ABI 7500	Applied Biosystems, USA
BD FACSCanto	BD Biosciences, Germany
BD FACSCalibur	BD Biosciences, Germany
Centrifuge 5415 R	Eppendorf, Germany
Cryotome	Leica Microsystems, Austria
Freezer -20°C	Liebherr, Germany
Freezer -80°C HeraFreeze Top	Thermo Scientific, Germany
Fridges	Liebherr, Germany
Hemocytometer, Neubauer	Labotec, Labor-Technik, Germany
Hera Cell Incubator	Heraeus Instruments, Germany
Ice machine ZIEGRA	Isernhagen, Germany

Light optical microscope, Axiostar plus	Zeiss, Germany
Light optical microscope, Axioskop	Zeiss, Germany
Light optical microscope, Axiovert 25	Zeiss, Germany
Liquid nitrogen tank	CBS, USA
Magnetic stirrer	Heidolph MR3001 NeoLab, Germany
Megafuge 1.0R	Heraeus Instruments, Germany
Microwave oven	MDA, Germany
Mosquito cages	BioQuip Products Inc, USA
NanoDrop ND-1000	Thermo Fischer Scientific, USA
pH-meter	Inolab, Germany
Photometer Eppendorf	Eppendorf, Germany
Pipetman Gilson (P2, P20, P200, P1000)	Abimed, Germany
Scales	Sartorius, Germany
Sterile work bench	Gelaire, BSB4A Flow Laboratories, Germany
SUNRISE Absorbance Reader	Tecan, Austria
Superfrost/Plus slides	Microm International, Germany
Vacuum membrane pump	KNF Neuberger Laboport,Germany
Vortex Genie 2	Scientific Industries Roth,Germany
Water Bath	GFL, Germany

2.1.2 Disposables

96-well cell culture plate	Sarstedt, Germany
Aluminum foil	Roth, Germany
Cell strainer	BD Bioscience, (70µm Nylon)
Centrifuge tubes (15 ml, 50 ml)	Sarstedt, Germany

Falcon tubes (15ml, 50ml)	Sarstedt, Germany
Gloves, Peha soft satin	Hartman, Germany
Immersion oil	Waldeck, Germany
Microfuge tubes (0.5 ml, 1.5 ml, 2.0 ml)	Sarstedt, Germany
Microscope cover slips	Marienfeld, Germany
Needles	BD DiscarditII (0.4mm x 19 mm; 0.6 mm x 30 mm; 0.9 mm x 40 mm) Becton Dickinson, Germany
Nunc Lab-Tek II Chamber Slide System	Thermo Scientific, Germany
Object slides	Marienfeld, Germany
Parafilm	Pechiney Plastic Packaging, USA
Petri dishes (145 x 20 mm; 94 x 16 mm)	Sarstedt, Germany
Pipettes (1 ml, 5 ml, 10 ml, 25 ml),	Sarstedt, Germany
Pipette tips	Sarstedt, Germany
Syringe	BD Discardit II (U-100 Insulin, 1 ml, 5 ml, 20 ml) Becton Dickinson, Germany
Sterile filter millipore bottle	Sarstedt, Germany
Thermo Fast 96 PCR detection plate	Thermo Scientific, Gemany
UV-micro cuvettes	Micro Brand, Germany

2.1.3 Chemicals

Bovine Serum Albumin (BSA)	Roth, Germany
Brefeldin A	Sigma, Germany
Collagenase (Clostridium histolytica)	Sigma, Germany
Complete protease inhibitors	Roche, Germany

Cremaphor RH 40	BASF, Germany
DMSO	Sigma Aldrich, Germany
Easycoll Density 1.124 g/ml	Biochrom AG
Eosin	Thermo Fisher Scientific, US
Ethylenediaminetetraacetic acid (EDTA)	AppliChem, Germany
Evans blue	Sigma, Germany
Fetal calf serum (FCS)	Gibco Invitrogen, Germany
Formamide	Merck, Germany
Giemsa (0,4%, w/v)	Roth, Germany (for rodent parasitemia analysis) and Thermo Fischer Scientific, USA (for histological anaylsis)
Haemotoxylin	Thermo Fisher Scientific, US
Hanks Balanced Salt Solution (HBSS)	Gibco Invitrogen, Germany
Heparin	Rathiopharm, Germany
$KHCO_3$	AppliChem, Germany
Ionomycin	Sigma-Aldrich, Germany
Formaldehyde (4%)	AppliChem, Germany
NH_4Cl	AppliChem, Germany
Non-essential amino acids	Gibco Invitrogen, , Germany
Methanol	Applichem, Germany
1 x PBS	Gibco Invitrogen, Germany
Penicillin (10000 U/ml)	GibcoBRL, Germany
Streptomycin (10000µg/ml)	GibcoBRL, Germany
Phosphate Buffered Saline (PBS)-pellets	Gibco Invitrogen, Germany
PMA	Sigma-Aldrich, Germany
RPMI 1640 (+25 mM HEPES,	

+ L Glutamine) w/ and w/o phenol red	Gibco, Germany
Saponin	Sigma, Germany
Sodium pyruvate	Gibco Invitrogen, Germany
Trypan blue	Sigma-Aldrich, Germany

2.1.4 Buffers

10 x PBS (pH 7)	50 PBS-pellets dissolved in 1l ddH_20
CBA Buffer	100 ml 1 x PBS 2 tablets of complete protease inhibitor cocktail (Roche, Mannheim), 0.05 % Tween 20
MACS Buffer	1 x PBS 0.5 % BSA 2 mM EDTA
Red cell lysis Buffer	1 liter ddH2O 8.26 g NH_4Cl 1 g $KHCO_3$ 0.037 g EDTA
Saponin Buffer	1 x PBS 0.1% BSA 0.3% Saponin

2.1.5 Media

Growth Media	RPMI (Life Technologies, Germany)
	10 % FCS
	5 ml Non-essential amino acids
	5 ml Sodium pyruvate
	5 ml 1 M HEPES, pH 7,5
	5 ml penicillin / streptomycin
	10 µl heparin
Hepatocyte culture media	1 x Dulbecco's Modified Eagle Medium
	10% FCS
	1% penicillin / streptomycin

2.1.6 Parasite media

Freezing solution	Glycerin : Alsever´s solution (1:9)
Sporozoite-isolation medium (*P. berghei*)	3% BSA in RPMI 1640

2.1.7 Antibodies

Table 1: Fluorescent antibodies

Antibody	Concentration	Clone	Working Dilution	Manufacturer
APC Rat α-Mouse CD25	0.2 mg/ml	PC61.5	1:150 [0.6 µg/ml]	BD Bioscience
APC Rat α-Mouse CD3	0.2 mg/ml	17A2	1:150 [0.6 µg/ml]	eBioscience
APC Rat α-Mouse CD44	0.2 mg/ml	IM7	1:150 [0.6 µg/ml]	eBioscience
APC Rat α-Mouse TNFα	0.2 mg/ml	MP6-XT22	1:150 [0.6 µg/ml]	eBioscience
FITC Rat α-Mouse CD4	0.5 mg/ml	GK1.5	1:150 [1.5 µg/ml]	eBioscience
FITC Rat α-Mouse IFNγ	0.5 mg/ml	XMG1,2	1:150 [1.5 µg/ml]	eBioscience

PE Rat α-Mouse CD4	0.2 mg/ml	L3T4	1:150 [0.6 µg/ml]	BD Bioscience
PE Rat α-Mouse CD62L	0.2 mg/ml	MEL-14	1:150 [0.6 µg/ml]	BD Bioscience
PE Rat α-Mouse IL-2	0.2 mg/ml	JES6-5H4	1:150 [0.6 µg/ml]	BD Bioscience
PE-Cy7 Rat α-Mouse CD69	0.2 mg/ml	H1.2F3	1:150 [0.6 µg/ml]	BD Bioscience
PerCP Rat α-Mouse CD4	0.2 mg/ml	RM4-5	1:150 [0.6 µg/ml]	BD Bioscience
PerCP Rat α-Mouse CD8a	0.2 mg/ml	53-6.7	1:150 [0.6 µg/ml]	BD Bioscience
Rat α-Mouse CD16/CD32	0.5 mg/ml	2.4G2	1:200 [1.3 µg/ml]	BD Bioscience

Table 2: Immunofluorescence antibodies

Antibody	Concentration	Manufacturer / Source
α-*Pb* HSP70 (Mouse)	Undiluted	Hybridoma supernatant [253]
ALEXA Fluor 488 (Goat α-Mouse)	1:1000	Invitrogen, Germany
Hoechst	1:1000	Invitrogen, Germany

Table 3: Depleting antibodies

Antibody	Concentration	Clone	Manufacturer
LEAF Purified α-mouse CD8	250 µg/ml	53-6.7	Biolegend,
LEAF Purified α-mouse CD25	200 µg/ml	PC61	Biolegend
LEAF Purified α-mouse CD210 (IL-10R)	200 µg/ml/ 250 µg/ml	1B1.3A	Biolegend

2.1.8 Kits

BD Cytometric Bead Array (CBA) Mouse Th1/Th2/Th17 Cytokine Kit

Containing:	Assay Diluent 1 bottle, 30 mL
	Mouse IFN-γ capture beads
	Mouse IL-2 capture beads
	Mouse IL-4 capture beads
	Mouse IL-6 capture beads
	Mouse IL-10 capture beads
	Mouse IL-17 capture beads
	Mouse Th1/Th2/Th17 cytokine standards
	Mouse Th1/Th2/Th17 PE detection reagent
	Mouse TNF capture beads
	Wash buffer 1 bottle, 130 ml

Green DYE Master Mix (P.J.K., Germany)

Containing	2 x master mix

RETROscript kit (Ambion, Germany)

Containing:	Control Template RNA
	10 x RT Buffer
	10 x PCR Buffer
	dNTP mix (2.5mM)
	Random Decamers (50μM)
	Oligo(dT) Primers (50μM)
	MMLV-RT (100 units/μl)
	RNAse Inhibitor (10 units /μl)

	Control PCR primers (5µM)
	High resolution gel loading solution (5x)
	Nuclease-free water

RNeasy Mini Kit (Qiagen, Germany)

Containing:	RNeasy mini spin columns
	Collection tubes (1.5ml and 2ml)
	Buffer RLT
	Buffer RW1
	Buffer RPE (concentrate)
	RNase-free water

2.1.9 Anaesthetic

Ketamine/ Xylazine (K/X)	Ketamine 100 mg/ml
	Xylazine 3 mg/ml

2.1.10 Parasite strains

Plasmodium berghei ANKA cl15cy1	Hall *et al* 2005 [254]

2.1.11 Cell lines

Human hepatocarcinoma (HuH-7) cells	Nakabayashi *et al* 1982 [255]

2.1.12 Mouse strains

NMRI Rjttan, outbred mice	Janvier, France
	Charles River, Germany
C57BL/6 JRi, inbred mice	Janvier, France

	Charles River, Germany
IL-$10^{-/-}$ /IL-10^{tm1Cgn} mice	gift from the University of Bonn;
	[256] (129/Ola x C57BL/6 genetic background)

2.1.13 Mosquito strain

Anopheles stephensi	Nijmegen, Netherlands/Berlin, Germany

2.1.14 Oligonucelotides

Invitrogen, Germany

(as reported by Friesen *et al* 2010) [121]

Primers were ordered from Invitrogen as custom DNA oligonucleotides, dissolved in H_2O to 100μM and stored at -20°C.

***P. berghei* 18S rRNA** GenInfo Identifier 160641:

Forward 5' AAGCATTAAATAAAGCGAATACATCCTTAC – 3'

Reverse 5' – GGAGATTGGTTTTGACGTTTATGTG – 3'

Mouse GAPDH GenInfo Identifier 281199965:

Forward 5' – CGTCCCGTAGACAAAATGGT – 3'

Reverse 5' – TTGATGGCAACAATCTCCAC – 3'

2.2 Methods

2.2.1 *Anopheles* methods

2.2.1.1 Breeding of *Anopheles stephensi*

Four days following blood-meal, eggs were collected from filter paper placed within a petri dish containing 0.1% salt solution. Eggs were washed 1x in 70% ethanol and 2x in 0.1% salt solution. Eggs were transferred to trays containing 0.1% salt solution until hatching into larvael forms

occured. Larvae were fed with pieces of commercially available dry cat food and relocated into fresh salt solution every third day. Nine days post blood-meal larvae transform into pupae and hatch into mosquitoes. Mosquitoes were collected and transferred to cages. Mosquitoes were infected with *P. berghei* by being permitted to feed on an infected mouse with blood-resident exflagellating gametocytes (described below). *P. berghei* infected mosquitoes were maintained at 80% humidity and 21°C with a 12 hour light/dark cycle. Three cotton wool pads saturated with 10% sucrose soution supplemented with 20 μg / ml para-aminobenzoic acid and 0.1% salt solution were placed on top of mosquito cages as mosquito food. Pads were refreshed every three days.

2.2.1.2 *Anopheles* infection

Anopheles stephensi mosquitoes were infected with *P. berghei* clone cl15cy1 [257] by feeding for 15 minutes on an infected mouse with exflagellating gametocytes at 2 x 24 hour intervals. Infected mosquitoes were kept under defined conditions of 80% humidity and 21-24°C. Sporozoites were dissected from mosquito salivary glands at day 17 post infection.

2.2.1.3 Examination of infection rate (prevalence)

Oocysts develop on the midgut basal lamina 10 days post-blood meal. Ten *Anopheles* mosquitoes were anaesthetized on ice and and midguts isolated in RPMI supplemented with 3% BSA via a binocular microscope. Midguts were prepared for examination on glass slides under glass cover slips and examined by light microscopy at 40x magnification with phase contrast. Oocyst number was calculated per mosquito to indicate the number of infected mosquitoes and yield the infectivity rate per mosquito.

2.2.1.4 Isolation and determination of the number of salivary gland sporozoites

Seventeen to twenty four days post-blood meal, *Anopheles* mosquitoes were anaesthetized on ice and salivary glands were isolated in PBS. Salivary glands were homogenized by grinding action with a pestle in a 1.5 ml microfuge tube. The homogenate was subjected to centrifugation at 1000rpm for 3 minutes at 4°C, the supernatant was transferred into a new tube and the pellet re-suspended in PBS and subject to further homogenization and centrifugation at 1000rpm. The second supernatant was pooled with the first and isolated sporozoites counted in a Neubauer haemocytometer. Sporozoite number is calculated by the formula 10000(x/y) to give number of sporozoites per mililitre where x is the number of sporozoites per quadrate and y is the number of quadrats counted. For accuracy, four quadrats were counted in total.

2.2.2 Rodent Methods

2.2.2.1 General

All animal experiments were performed according to European regulations and approved by the state authorities (Regierungspräsidium Karlsruhe). For all experiments, C57BL/6 mice were purchased from Janvier, France and kept under specified pathogen-free (SPF) conditions within the animal facility at Heidelberg University (IBF). Animals were matched for sex and age (female, 6-8 weeks old). For *in vivo* experiments compounds were administered to groups of C57BL/6 mice by either intraperitoneal (IP) or subcutaneous (SC) injection at stated concentrations at days -2, -1, and 0. 10,000 infectious salivary gland sporozoites were inoculated at day 0 by intravenous injection into the tail vein 1h after the final compound injection (Appendix 2). Parasitemia was monitored by daily blood smear and Giemsa stain.

2.2.2.2 Anaesthesia of malaria-infected mice

Experimental animals were anaesthetized by intraperitoneal injection of 80 µl Ketamine/Xylazine. Animals were placed on mosquito cages for 15 minutes and 4 day-old mosquitoes permitted to feed.

2.2.2.3 Rapid Murine Coma and Behavior Scale (RMCBS)

To determine ECM pathology in C57BL/6 mice, animals were assessed for ten parameters of cerebral symptoms as described previously [150], such as coordination and motor performance, and scored 0 to 2, where a 0 score correlates with lowest function and 2 the highest. Animals were assessed daily and scored from 0 to 20 according to this scale (Appendix 2).

2.2.2.4 Evans Blue Quantification

Quantification of vascular leakage was performed as described previously [234]. Briefly, mice were injected intravenously with 150 µl of 1.5 % Evans Blue (Sigma-Aldrich) and sacrificed 2 h later with brains isolated in formamide at 48 h to assess vascular leakage. Absorbance was measured at 620 nm in an ELISA reader with Evans blue concentration assessed automatically by Magellan V 5.0 software via standard curve starting at 400mg/ml and expressed as mg dye per gram of brain tissue.

2.2.2.5 Histology

(conducted by Dr. Felix Lasitschka, Institute of Pathology, Heidelberg University Hospital)

Histological analysis was performed as described previously [258]: Brains were removed after death and snap-frozen in liquid nitrogen. 10-µm thick coronal sections were cut on a cryotome (Leica Microsystems, Austria) and mounted on SuperFrost/Plus slides (Microm International, Germany). Serial sections were stained with eosin and haematoxylin (Thermo Fisher Scientific, Waltham, MA, USA) and Giemsa (Thermo Fisher Scientific). Slides were blinded and three

randomly selected sections per coronal plane were subjected to histological analysis. Examinations were done on an Olympus BX45 research microscope (Olympus, Japan). Visualization by haematoxylin/eosin was achieved by immersing slides in haematoxylin for 60 seconds to stain the nucelus, followed by a quick washing step with distilled water to remove excess dye, a quick immersion in 2% acetic acid to differentiate nuclear staining, 60 seconds immersion in distilled water to produce blue nuclear staining, counterstaining by 5 second immersion in alcoholic eosin (15g eosin, 2000ml 70% ethanol, 10ml acetic acid), colour differentiation by sequential immersion in 2 x 70% ethanol, 2 x 96% ethanol and 2 x 100% ethanol until the sections appeared transparent, immersion in xylol for 5 minutes before sections were mounted with Consul Mount.

2.2.3 *P. berghei* Methods

2.2.3.1 *In vitro* parasite inhibition assays

Exoerythrocytic stages were cultivated in a standard experimental system as previously described [259]. One day prior to sporozoite infection, 8-well chamber slides (Nunc) were plated with 3 x 10^4 HuH-7 cells and cultured to confluency at 37°C. Purified sporozoites suspended in complete medium were added to the chambers and permitted to invade for 90 min. Medium was refreshed and supplemented with 1μM-10 nM of the 8-aminoquinolines indicated. Thereafter, medium was refreshed daily.

2.2.3.2 Microscopical demonstration of *P. berghei* infection using Giemsa staining

The tail vein was pricked with a needle and a drop of blood smeared onto a glass slide. After the smear had dried, it was fixed in 100% methanol for 30 seconds, dried, and then stained in fresh 10% Giemsa solution for 30 minutes. Slides were washed in water, permitted to air dry and then analysed by light microscopy at 100x magnification with oil immersion. Parasitemia was

quantified by counting the number of infected red blood cells relative to the number of uninfected. A minimum of 5 fields were counted for accuracy.

2.2.4 Cell Biological Methods

After 24 or 48 h liver-stage development, parasites were fixed with 100% ice cold methanol for 10 minutes, washed with PBS / 1 % FCS followed by a 15 min blocking step with PBS / 10 % FCS at 37°C. Liver stages were visualized using hybridoma culture supernatant anti-HSP70 antibody [253] and 1:1000 Alexa Fluor 488 goat anti-mouse (Invitrogen). Wells were mounted with 10 % glycerol in PBS and embedded with nail varnish. Experiments were conducted in triplicate and all liver stages counted per well. Statistical significance was assessed by one-way ANOVA with bonferonni post-hoc adjustment.

2.2.5 Cell Culture

2.2.5.1 Maintenance of human hepatocarcinoma (HuH-7) cells

Cells were stored in liquid nitrogen in 20% DMSO, 80% FCS. To bring cells into culture from frozen stocks, cell stocks were placed in a 37°C water bath and, once thawed, cell suspensions were transferred to 15ml DMEM culture media supplemented with 10% FCS and 1% penicilin/streptomycin. Cells were subject to centrifugation at 200 x g and resuspended in DMEM culture media supplemented with 10% FCS and 1% penicilin/streptomycin within a 25cm^2 gas-permeable culture flask. Cells were maintained at 37°C and 5% CO_2 until confluence. Cells were "split" for cell culture maintenance by removing the media, washing with HBSS, and incubating cells in 0.25% Trypsin/EDTA (Gibco) for 5 minutes to cause detachment. Cells were transferred to a 50ml tube and subject to centrifugation at 200 x g for 5 minutes, the pellet washed with HBSS and resuspended in 15ml DMEM culture media supplemented with 10% FCS and 1% penicilin/streptomycin. A 1ml aliquot from this suspension was then transferred to a

new 25cm^2 culture flask with culture media to maintain the cell culture. Cells were prepared for frozen stocks by resuspending cells in freezing solution (20% DMSO 80% FCS) and transferring them to -80°C for 24 hours, followed by storage in liquid nitrogen.

2.2.5.2 Calculation of cell number

Following trypsinization of cells, a small aliquot (2µl) was diluted in trypan blue to permit determination of live and dead cells. Live cells were counted within four large fields and calculated by the formula 10000 (x/y) to give number of viable cells per mililitre where x is the number of sporozoites per quadrat and y is the number of quadrats counted. For accuracy, four quadrats are counted.

2.2.7 Chemistry Methods

2.2.7.1 General

All solvents were distilled before use. Commercially available material was used without further purification. NMR spectra were recorded on a DMX 600 instruments. Assignments of the NMR signals were performed using Dept, COSY, HSQC and HMBC. IR spectra were recorded on a Jasco-FT-410-spectrometer with wavelength ($\tilde{\nu}$) reported in cm-1. High resolution MS (HRESIMS) was performed on a Bruker Daltonik microTOF spectrometer. Reactions were routinely monitored by thin-layer chromatography (TLC) using pre-coated plates (Silica Gel 60, F254, Merck) and visualized by UV light. Detection of the compounds was achieved using the ninhydrin stain. Flash column chromatography was carried out using deactivated (7.5 % of ammonia) Silica Gel 60 (0.032-0.063 mm particle size, Merck). Primaquine was obtained from commercially available primaquine bisphosphate by extraction of the compound as a free base from an aqueous solution of sodium hydrocarbonate by dichloromethane.

2.2.7.2 N1-isopropyl-N4-(6-methoxyquinolin-8-yl)-pentane-1,4-diamine (isopentaquine) synthesis

(Conducted by Eleonora Paulsen, Department of Organic Chemistry, University of Copenhagen)

The free base of primaquine (846 mg, 3.262 mmol, 1 equiv) in dry methanol (15 mL) was added to acetone (960 μL, 13.048 mmol, 4 equiv). The mixture was stirred at room temperature overnight before sodium borohydride (370 mg, 9.782 mmol, 3 equiv) was added in small portions and the mixture was stirred for additional 15 hours. The crude was filtered and concentrated under reduced pressure. Purification by column chromatography with dichloromethane/methanol 50:1 as an eluent yielded the desire product as a yellow oil.

2.2.7.3 Compound preparation

For all *in vitro* studies, compounds were dissolved in dimethyl sulfoxide (DMSO) to a stock concentration of 0.02 M and further diluted where required by serial dilution in complete cell culture medium (DMEM, 10% heat inactivated FCS, 1 % pen/strep). Final DMSO concentration was always <0.01%. For all *in vivo* studies, compounds were dissolved in DMSO to produce a stock concentration of 0.2 mg/μL. The stock concentration was further diluted in sterile PBS with 4 % Cremophor RH 40 (BASF) to the final concentrations stated.

2.2.8 Molecular Biological Methods

2.2.8.1 Isolation of RNA with RNeasy Mini Kit

Cells were disrupted by the addition of 350μl RLT lysis buffer with 1% β-mercaptoethanol (14.3M). The mixture was vortexed for 60 seconds and total RNA isolated from the cell lysate as per the manufacturer's instructions. The cell lysate was homogenized in buffer to ensure inactivation of RNAses and applied to a RNA-binding membrane spin column in the presence of ethanol. Isolated RNA was eluted in distilled water and stored at -80°C.

2.2.8.2 DNase treatment of RNA

Following RNA isolation with the RNeasy Mini Kit, contaminating DNA was digested by the addition of DNase. Isolated RNA was mixed with 1µl TURBO DNase and 1/10 volume 10 x TURBO DNase buffer and incubated at 30°C for 30 minutes. The reaction was stopped by the addition of 1/10 DNase Inactivation Reagent and incubation at room temperature for 2 minutes. The mixture was subject to centriguation for 1 minute at 10,000 x g and the supernatant (containing the RNA) transferred to a fresh tube.

2.2.8.3 RNA Integrity

Concentration and contamination of isolated RNA was assessed via a NanoDrop spectrophotometer. Only those RNA samples with a 260/280 ratio >1.8 were utilized.

2.2.8.4 First strand cDNA synthesis with Fermantas "First Strand cDNA Synthesis Kit"

cDNA reverse-transcription from RNA was achieved according to the manufacturer's manual. 5µl of isolated RNA was mixed with 0.5µl random decamer primers, 0.5µl oligo dT primers. After mixing, the mixture was subjected to incubation at 72°C for 3 minutes, cooled on ice and 1µl RT buffer, 2µl dNTP, 0.5µl RNAse inhibitor and 0.5µl reverse transcriptase was added. This mixture was then homogenized, briefly centrifuged and subject to incubation at 42°C for 1 hour and 92°C for 10 minutes.

2.2.8.5 Quantitive RealTime PCR (QRT-PCR)

Quantification of parasite liver loads by quantitative real-time PCR was conducted as previously described [121, 260]. Briefly, mice were killed 42 h after sporozoite infection and livers were removed, homogenized and subjected to RNA isolation via the RNeasy kit (Qiagen) with complementary DNA (cDNA) synthesized by the First strand cDNA Synthesis kit (Fermentas)

as per manufacturer's instructions. qRT-PCR was conducted with the ABI 7500 (Applied Biosystems) and Green DYE Master Mix (P.J.K.) using gene-specific primers for the *P. berghei* 18S rRNA and the mouse GAPDH gene. Samples were analysed in triplicate on 96-well plates. Samples were incubated with an activation step of 95°C for 10 minutes, followed by 15 seconds denaturation at 95°C, 15 seconds annealing at 55°C and 45 seconds extension at 60°C. The three latter steps were repeated for 40 cycles. Fluorescence data was collected during the extension phase. Following amplification, a melting curve to test for false positive signals caused by primer dimers was performed, consisting of a gradient from 55°C to 95°C increasing by 1°C steps. Relative copy numbers were determined via the ΔCt method where housekeeper GAPDH values were substracted from 18srRNA values and the mean calculated [260]. Statistical significance was determined on ΔC_t values by student's *t* test. Asterisks signify degrees of significance where *** indicates $P < 0.001$, ** indicates $P = < 0.01$, * indicates $P < 0.05$ and "ns" indicates $P > 0.05$.

2.2.9 Immunological methods

2.2.9.1 Cytokine Bead Array Analysis

Cytokine Bead array analysis was performed according to the manufacturer's protocol using a Th1/Th2/Th17 CBA kit (BD Biosciences). For analysis of cytokine concentration, organ homogenates were isolated at the designated timepoint post-infection. Briefly, the liver was gently pressed through an iron mesh sieve, washed with 1x PBS containing 2 mM EDTA and 1% FCS and subject to centrifugation at room temperature at 1500rpm for 10 min. Supernatants were stored at -20°C in protease inhibitor cocktail (1 x protease inhibitor (Roche), 0.05 % Tween 20 in PBS) for cytokine analysis. Organ homogenates and serial dilutions of cytokine standards were incubated with 50 µl of beads diluted in dilution buffer. PE-detection reagent mix was added and samples were incubated for 2 h in the dark. Samples were subsequently washed in wash buffer, 300 events/cytokine were acquired on a FACSCalibur, gating on the total bead population

identified by FSC-SSC profile. Cytokine concentrations were analysed by FCAPArray software version 2.0 (BD Biosciences).

2.2.9.2 Flow Cytometry

For flow cytometry analysis of intracellular cytokines, T, DC and NK cells, mice were anaesthetized and perfused intracardially with 20ml 1xPBS. Organs were prepared as single cell suspensions via homogenization through a 70 μm cell strainer in PBS. Liver lymphocytes were isolated by resuspension in 70 % percoll and collected in the cell pellet after centrifugation at 2000 rpm. Cells were then subjected to erythrocyte lysis in erythrocyte lysis buffer for 15 minutes at room temperature. Cells were then washed and counted in a hemocytometer. For multifunctional T-cell analysis, cells were stimulated *ex vivo* with 1 μM ionomycin (Sigma-Aldrich) and 50 ng/ml PMA (Sigma-Aldrich) with 10 μg/ml Brefeldin A to inhibit Golgi function for 5 h at 37°C. Afterwards, and where cells were not stimulated, cells were stained and analysed for expression of CD8a, CD4, CD44, CD62L, CD25, CD69, CD3, CD11c and NK1.1 markers. For intracellular staining, after surface staining cells were fixed in 2 % PFA, washed, permeablized with 0.2 % saponin lysis buffer and stained for intracellular cytokines TNF-α (clone: MP6-XT22/APC, eBioscience), IFN-γ (clone: XMG1.2/FITC, eBioscience) and IL-2 (clone: JES6-5H4/PE, eBioscience). Data was collected on a FACSCanto and analysed by CellquestPro software (BD Biosciences). Brain leukocyte isolation was conducted by cutting brains into pieces and digesting in 0.5 mg/ml Collagenase A (Sigma-Aldrich) at 37°C for 30 min. Organs were subsequently passed through an iron mesh sieve to obtain a single cell suspension. Cells were pelleted and resuspended in 3 ml 30 % Percoll underlayed by 3 ml 37 % and 3 ml 70 % Percoll. Cells were centrifuged at 2000 rpm for 20 min at room temperature and cells were collected from the interphase.

2.2.9.3 Depletion experiments

IL-10-receptor depleting antibody, clone 1B1.3A was purchased from Biolegend, USA and administered intraperitoneally at 250 μg at either day -1 or 5 as indicated in the results (-1 to deplete IL-10 during liver stage development, 5 to deplete IL-10 at fulminant infection) and 200 μg daily thereafter until the endpoint of the experiment. $CD8^+$ T cell depleting antibody clone 53-6.7 was purchased from Biolegend, USA and administered 150 μg 3 days prior to the experiment commencement and every 3 days thereafter until the endpoint of the experiment. Anti-CD25 depleting antibody clone PC61 was purchased from Biolegend, USA and 250 μg administered intraperitoneally 8 days prior to sporozoite inoculation to deplete those cells expressing CD25, expressed on activated T and B cells, thymocyte subsets, pre-B cells and regulatory T cells (Biolegend: www.biolegend.com) [261, 262].

2.2.9.4 Isolation of splenocytes

Sacrificed animals were dissected and spleens isolated in 2 ml PBS. The organ was homogenized through a cell strainer with the plunger from a 5 ml syringe and the suspension centrifuged at 1500 rpm for 5 minutes at 4°C. The cells were then resuspended in 2 ml erythrocyte lysis buffer for 15 minutes at room temperature. 2 ml PBS was then added to stop osmotic lysis and the cells resuspended in 2 ml PBS. Cells were then diluted 1:200 in trypan blue to differentiate between live and dead cells and live cells were quantified using a hemocytometer. $2x10^6$ cells were seeded into 1.5ml reaction tubes in 200 μl PBS, stained immediately with fluorescent antibodies and analysed by flow cytometry or resuspended in growth medium and cultured at 95% humidity, 37°C and 5% CO_2 overnight.

2.2.9.5 Isolation of liver-infiltrating lymphocytes

Sacrificed animals were dissected and livers isolated in 2 ml PBS. Similarly as for the spleen, the liver was homogenized with the plunger from a 5 ml syringe and the suspension centrifuged at

1500 rpm for 5 minutes at 4°C. The cells were resuspended in 14 ml percoll mixture consisting 29.1ml HBSS, 14.2ml percoll, 1.6ml 10x PBS and subjected to 2000rpm centrifugation without brake. Liver infiltrating lymphocytes are located in the pellet, with fatty tissue and debris suspended above. The cells were then resuspended in 2-5 ml erythrocyte lysis buffer for 15 minutes at room temperature. 2ml PBS was then added to stop osmotic lysis and the cells resuspended in 2ml PBS. Cells were then diluted 1:200 in trypan blue to differentiate between live and dead cells and live cells were quantified using a hemocytometer. As with splenic lymphocyte isolation above, 1- $2x10^6$ cells were seeded in 200 µl PBS, stained immediately with fluorescent antibodies and analysed by flow cytometry or resuspended in growth medium and cultured at 95% humidity, 37°C and 5% CO_2 overnight.

2.2.9.6 Isolation of brain-infiltrating lymphocytes

The brain was isolated from sacrificed mice, cut into pieces, suspended in 0.05% collagenase and incubated at 37°C, 5% CO_2 and 95% humidity for 45 minutes. The cells were homogenized by passing the solution through a syringe multiple times and by being passed through an iron mesh sieve. Cells were centrifuged for 8 minutes at 1500rpm and resuspended in 7ml 70% percoll, layered with 6ml 30% percoll on top. This two-gradient percoll step was subjected to centrifugation for 25 minutes at 2000rpm and the cells isolated from between the two percoll layers (fig 2.1). After centrifugation for 8 minutes at 1500 rpm, cells were resupended in 0.3 ml PBS and a 1:100 dilution made in 1:10 trypan blue (diluted in distilled water) and counted in a hemocytometer.

2.2.10 Statistical Analysis

Statistics calculated by one-way ANOVA with Bonferonni post-hoc adjustment and student's T test. Asterisks signify degrees of significance where *** indicates P < 0.001, ** indicates P = < 0.01, * indicates P < 0.05 and "ns" indicates P >0.05.

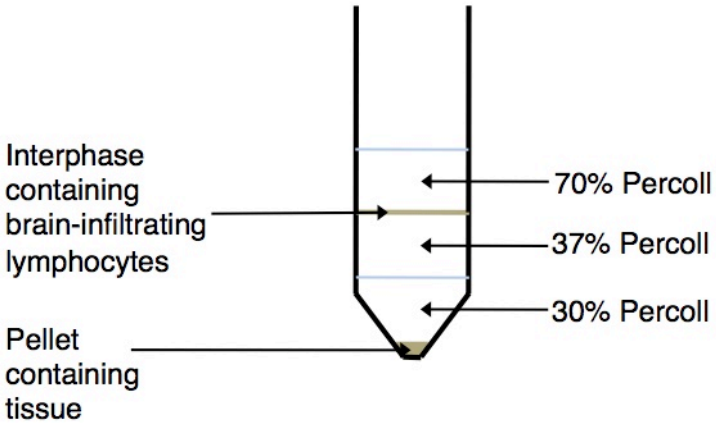

Figure 2.1 Brain-infiltrating lymphocyte isolation from the interphase following percoll gradient centrifugation.

Chapter 3

Results

3.1 Isopentaquine and primaquine administration causes inhibition of *P. berghei* liver stage development *in vitro*

To test for a potential inhibitory effect on parasite liver stage development by 8-aminoquinolines, isopentaquine, pamaquine, primaquine and a hybrid of chloroquine-primaquine (synthesized by Melanie Diegel, University of Wuerzburg) were administered to *in vitro* cultures of immortalized human hepatoma cell lines infected with *P. berghei* sporozoites. Compounds were administered to the culture media some two hours after the addition of sporozoites, so that any parasite inhibition due to the compound would specifically effect the liver stage development, rather than sporozoite motility or liver cell invasion. Liver stage development was stopped after 24 and 48 hours and numbers of liver stage parasites were counted by immunofluorescence microscopy as a measurement of the inhibition of liver stage development. Although not statistically significant, there was a notable decrease in numbers of liver stages at 48 hours in cultures containing both isopentaquine and primaquine (fig 3.1). In addition, liver stages cultured in the presence of these compounds showed an altered morphology to those cultured in the absence of compound. This indicates that these compounds had an effect on attenuating liver-stage development

3.2 Isopentaquine and primaquine administration causes inhibition of *P. berghei* ANKA-induced cerebral malaria development *in vivo*

In light of this finding, isopentaquine and primaqine were selected based on their liver-stage attenuating effect and were administered *in vivo* at sub-therapeutic concentrations by different

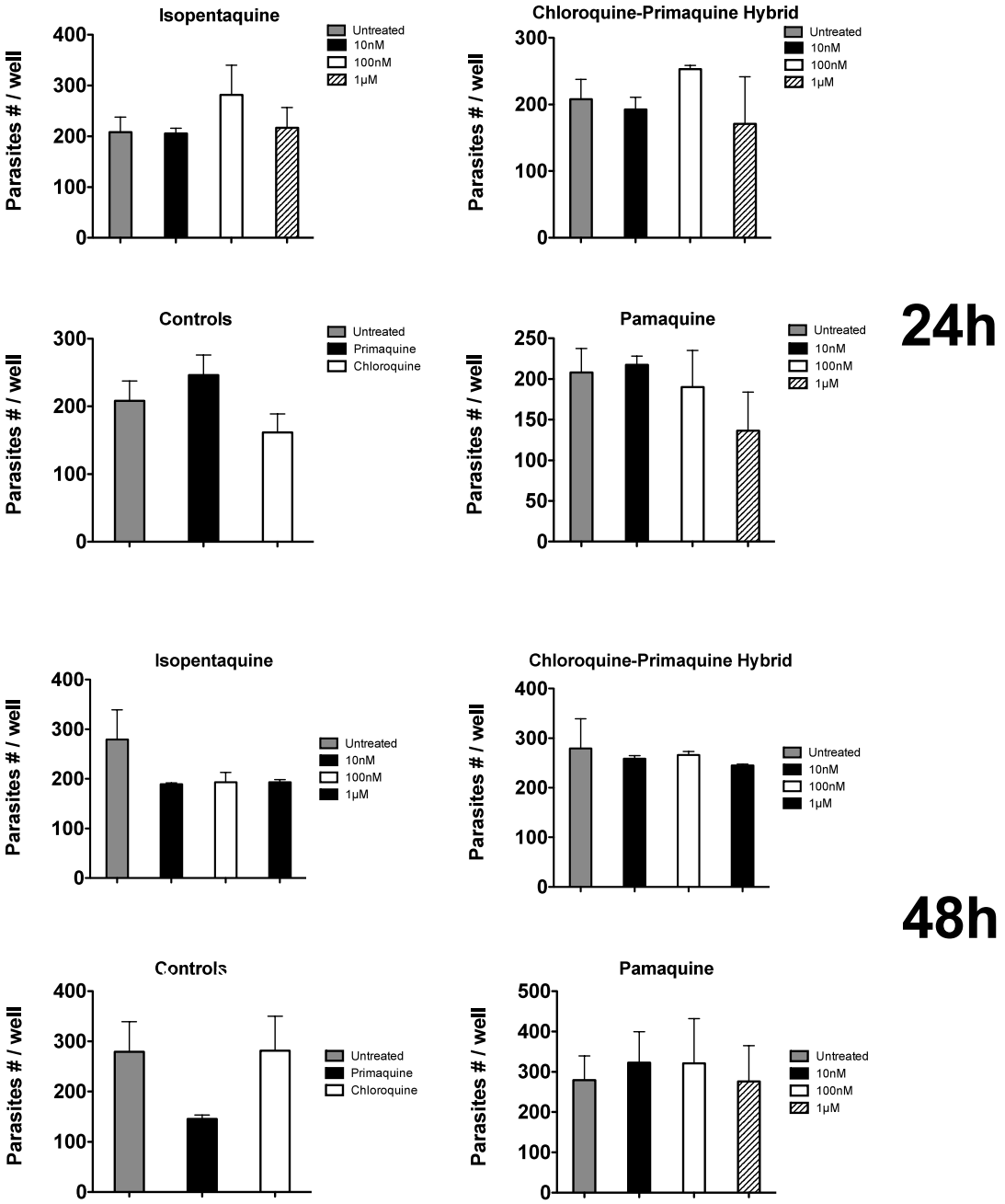

Figure 3.1. Isopentaquine and primaquine administration causes inhibition of *P. berghei* liver stage development *in vitro* Confluent HuH-7 cell cultures were infected with 30,000 *P. berghei* ANKA sporozoites. After two hours, cultures were incubated with 8-aminoquinoline compounds as indicated at 1µM, 100nM or 10nM. Control substances were administered at 10µM final concentration (standard inhibitory concentration). Untreated wells were given culture medium alone. After either 24 or 48hrs, cells were stained with anti-HSP70 antibody and parasite numbers per well measured by microscopy. Statistical significance was calculated by one-way ANOVA with Bonferonni post-hoc adjustment. In all cases p = >0.05

routes (intraperitoneal and subcutaneous injection) to determine their tolerance by experimental animals and the effect of infection on cerebral pathology. I hypothesized that chemical attenuation during liver stage development may lead to a change in disease outcome. Primaquine was well-tolerated by mice at 60mg/kg and no cytotoxic effects were observed (defined as abnormal motor and grooming behaviour, weight loss, change in diet or sleeping habits) and intriguingly, by the intraperitoneal route of administration, mice did not develop cerebral symptoms as measured by the rapid murine coma and behaviour scale [150] (Appendix 1).

Isopentaquine proved to be cytotoxic at 60mg/kg by both intraperitoneal and subcutaneous administration and experiments were discontinued (table 3.1). At 30mg/kg, isopentaquine caused mild and limited cytotoxic symptoms by intraperitoneal administration (altered motor and grooming behaviour lasting several hours) and experiments were similarly discontinued, although these mice did not develop cerebral symptoms. No cytotoxic effect was apparent, however, by subcutaneous administration of isopentaquine, and animals were protected against cerebral symptoms (Table 3.1).

Table 3.1. Primaquine and isopentaquine administration by different routes and their cytotoxic effect and influence on the development of cerebral pathology.

Compound	Administration Route	Concentration	Cytotoxic Behaviour	Cerebral Symptoms (# animals)
Isopentaquine	IP	60mg/kg	Y	2/10
Isopentaquine	SC	60mg/kg	Y	0/10
Isopentaquine	IP	30mg/kg	Y	0/10
Isopentaquine	SC	30mg/kg	N	0/10
Primaquine	IP	60mg/kg	N	0/10
Primaquine	SC	60mg/kg	N	8/10
None	-	-	N	9/10

Animals were administered isopentaquine or primaquine at varying concentrations administration routes as indicated at days -2, -1 and 0. Treated animals and control mice were injected intravenously with 10,000 *Pb*ANKA salivary gland sporozoites at day 0. Cytotoxicity was determined qualitatively (abnormal motor and grooming behaviour, weight loss, change in diet or sleeping habits) and cerebral malaria was determined as either positive or negative by quantitative analysis via the RMCBS scale.

It is important to note that while all experimental mice treated with primaquine and isopentaquine did not develop cerebral symptoms, they developed patent blood-stage parasitemia. In a head-to head comparison between the different administration routes that did not cause cytotoxic effects, animals administered both isopentaquine by the subcutaneous route and primaquine by the intraperitoneal route developed hyperparasitemia-associated anaemia and died after day 15 post-infection. However, those animals treated with isopentaquine developed higher parasitemias and died at later time points than those treated with primaquine (fig 3.2).

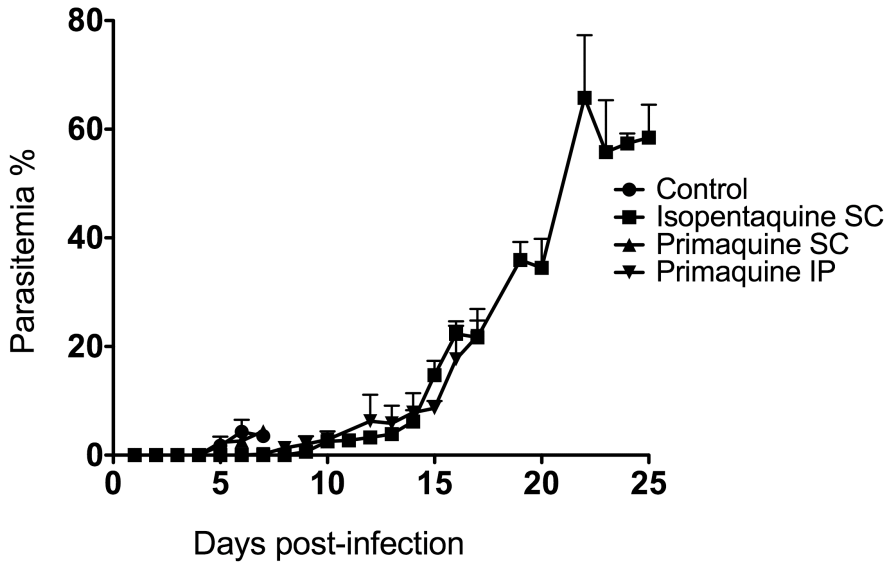

Figure 3.2. Outcome of isopentaquine and primaquine treatment on blood-stage parasitemia *in vivo*. Animals were administered isopentaquine at 30mg/kg or primaquine at 60mg/kg by either subcutaneous or intraperitoneal injection at days -2, -1 and 0. Treated animals and control mice were injected intravenously with 10,000 *Pb*ANKA salivary gland sporozoites at day 0. Parasitemia was determined by giemsa-stained blood smears.

3.3 Experimental animals subjected to chemical attenuation with isopentaquine sustain high parasitemias, die from hyperparasitemia-associated anaemia and do not develop experimental cerebral malaria. This model of attenuation is hereafter termed "Negated Cerebral Malaria" (NCM).

Due to it causing a favourable outcome of infection (absence of cerebral pathology, prolonged period until death of approximately 16 days), the subcutaneous administration of isopentaquine at 30mg/kg was selected as the best means by which to alter the outcome of ECM by chemical attenuation. This model consists of three sub-therapeutic doses of isopentaquine prior to intravenous infection of 10,000 *Plasmodium berghei* ANKA (*Pb*ANKA) salivary gland sporozoites (appendix 2). All mice became patent but did not show any typical cerebral symptoms, as measured by the RMCBS scale described previously [150] but the onset of patency was delayed by 3-4 days (fig 3.3). Furthermore these mice did not show any typical cerebral symptoms. This negated-cerebral-malaria (NCM) outcome was characterized by death from hyperparasitemia-associated anaemia at day 25-30 post-infection.

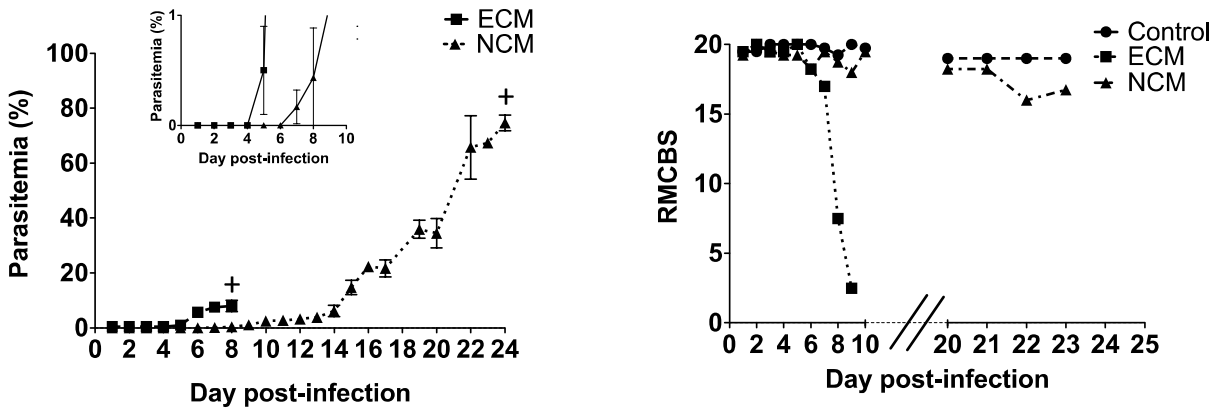

Figure 3.3. Outcome of chemical attenuation on blood-stage parasitemia and cerebral pathology. Animals were subjected to chemical attenuation (NCM) and uninfected control mice (Control) were subcutaneously injected with 30 mg / kg isopentaquine at days -2, -1 and 0. Animals subjected to chemical attenuation and positive control (ECM) mice were injected intravenously with 10,000 *Pb*ANKA salivary gland sporozoites at day 0 and chemically attenuated mice (n = 5) were infected with 10,000 *Pb*ANKA sporozoites. Parasitemia was determined by blood smear and Giemsa staining (left panel, with inset figure zoomed into days 0-10) and their behaviour scored from 0 - 20 according to the Rapid Murine Coma and Behaviour Scale (RMCBS) (right panel).

The brain is the centrepiece of ECM pathology. To determine if mice subjected to chemical attenuation were free of the clinical manifestations of ECM within the brain, and not only appearing outwardly healthy, we assessed the brain for indicators of pathology by evaluating the

integrity of the blood-brain barrier and by quantifying the number of infiltrating lymphocytes present in the organ. ECM pathology is associated with blood-brain barrier damage and haemorrhage, oedema and sequestration of parasitized erythrocytes and lymphocytes in the brain microvasculature. To ascertain whether mice subjected to chemical attenuation bear any of these hallmarks of ECM pathology, histological analysis was performed on cryosections of brain tissue isolated from chemically attenuated, positive and negative control mice at day 8 post-infection. Positive control mice that developed ECM featured clear signs of pathology, such as subarachnoidal bleeding, leukocyte infiltration and adherence of leukocytes to venule walls with associated accumulation of malaria pigment (fig 3.4) No such symptoms were evident in chemically attenuated mice, however, with the NCM phenotype consistent with an absence of leukocyte infiltration in cerebral blood vessels and intact epithelial walls (fig 3.4).

Since ECM is associated with leukocyte sequestration in the brain [147, 154, 173, 220, 263] I quantified $CD8^+$ and $CD4^+$ T cells from the brains in animals displaying ECM and NCM phenotypes. Interestingly, NCM mice showed dramatically fewer $CD8^+$ infiltrates, but a comparable number of $CD4^+$ infiltrates (Fig 3.5). This correlates with the observation that $CD8^+$ T cells in the brain-sequestered leukocytes are essential for the cerebral symptoms and mortality in ECM [217].

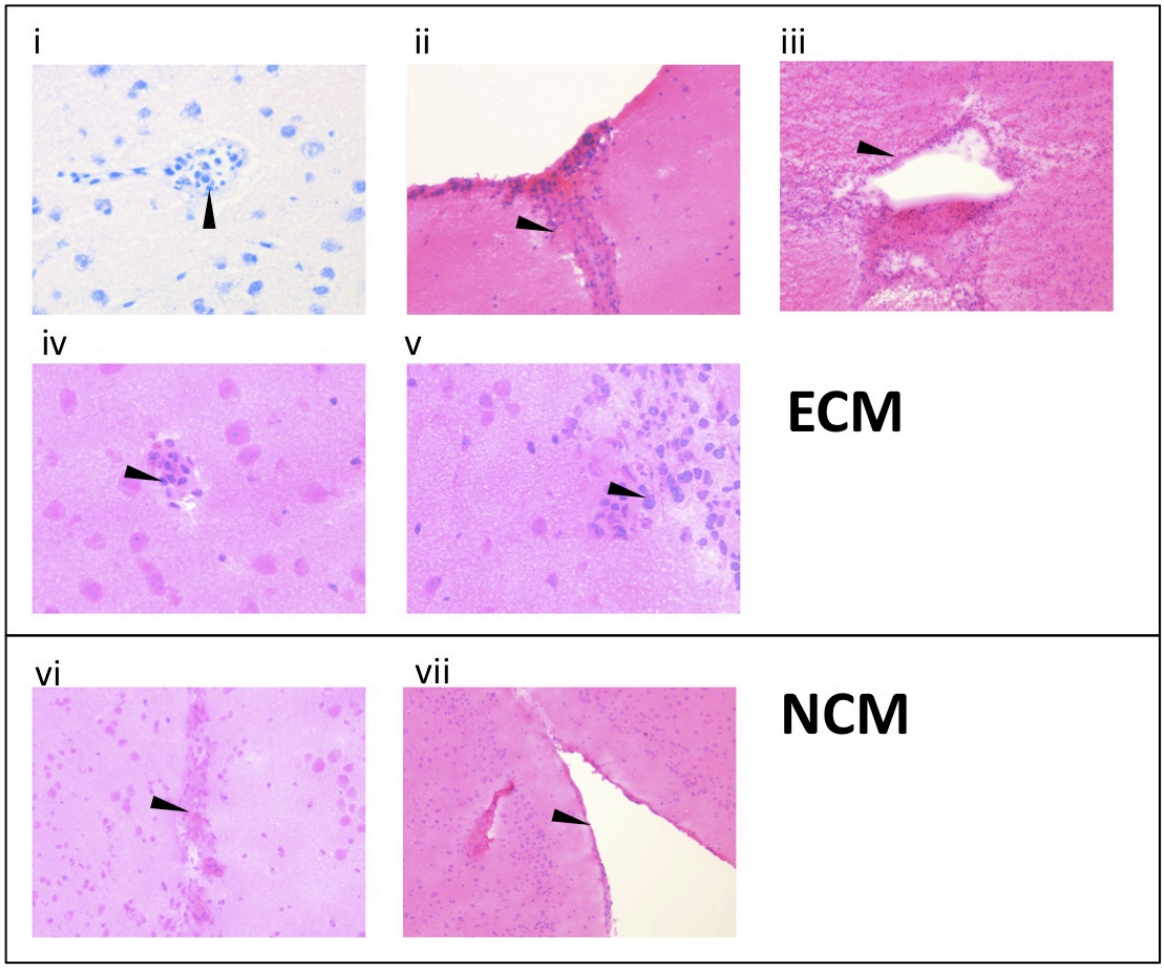

Figure 3.4. Animals subjected to chemical attenuation show absence of pathology by histological examination at the timepoint post-infection that control mice are in coma. Test animals (NCM) were subjected to chemical attenuation and both NCM and control animals (ECM) infected with 10,000 *Pb*ANKA sporozoites. Sections were isolated from brain tissue, stained with haematoxylin and eosin and analysed for indicators of cerebral pathology. Representative slides with arrowheads point to incidences of subarrachnoidal bleeding and haemorrhaging in the ECM panel, and a vessel absent from lymphocyte sequestration and an intact epithelium in the NCM panel. Analysis performed by Felix Lasitschka, Institute of Pathology, University Hospital Heidelberg.

To assess the integrity of the vascular endothelium in experimental animals, evans blue dye was injected into experimental animals at day 8 post-infection, the time point at which control mice succumbed to cerebral symptoms. Upon injection of Evans Blue, BBB disruption leads to extravasation of dye into the brain tissue, which can be visualized and assessed quantitatively and qualitatively. Control animals that developed ECM displayed evidence of cerebral pathology: a

dark, evenly distributed staining, compared to very faint staining in brains from chemically attenuated NCM animals (fig 3.6) that was not statistically significantly different to naïve brains

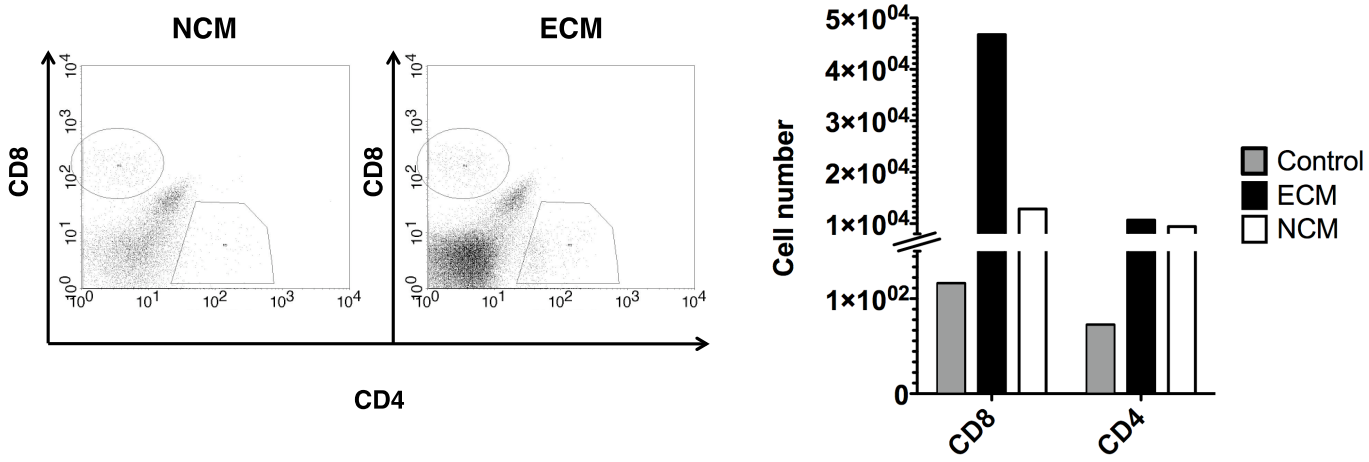

Figure 3.5. Animals subjected to chemical attenuation show absence of brain-infiltrating lymphocytes by flow cytometry analysis at coma Whole number cerebral $CD8^+$ and $CD4^+$ T cell infiltration at day 8 post-infection was analysed by flow cytometry in animals subjected to chemical attenuation and protected from ECM (NCM), untreated controls (ECM) and uninfected but chemically attenuated controls (Control). Representative dot blot indicates CD4 vs CD8 cell distribution in mice presenting ECM and NCM phenotypes.

from non-infected animals by colourimetric analysis (fig 3.6), indicating that the BBB and vascular endothelium remained intact in animals subjected to chemical attenuation.

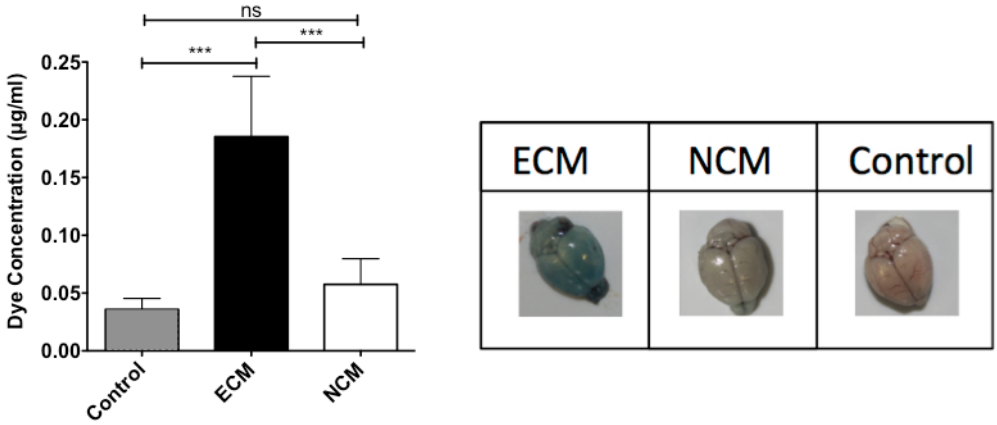

Figure 3.6. Animals subjected to chemical attenuation do not feature blood-brain barrier permeabilization. Animals (groups of 5) were assigned to ECM, NCM and control groups as described, and infected with 10,000 *Pb*ANKA sporozoites and sacrificed at day 8 post-infection. Evans Blue extravasation in formamide at day 8 post-infection was compared between chemically attenuated and ECM control mice by visual appearance. Statistics calculated by one-way ANOVA with Bonferonni post-hoc adjustment. Asterisks signify degrees of significance where *** indicates $P < 0.001$, ** indicates $P = < 0.01$, * indicates $P < 0.05$ and "ns" indicates $P > 0.05$.

Having established that animals subjected to chemical attenuation do not bear any of the hallmarks of ECM and that the NCM phenotype is indistinguishable from uninfected mice in terms of histology, BBB integrity and animal behaviour, I focussed on the delay in the onset of patency that is apparent in NCM. To investigate this delay qRT-PCR analysis of the *P. berghei* 18S rRNA transcript levels were performed. Liver stage development in NCM, characterized by multiple nuclear divisions [264], was decreased as shown by quantitative transcriptional analysis at 48h post-infection (fig 3.7). This is indicative that chemical attenuation causes attenuated growth of the parasite pre-erythrocytic development at the liver stage.

Having established that chemical attenuation with isopentaquine causes a delay in the onset of patent parasitemia, lower liver loads and absence of cerebral symptoms (the NCM phenotype) I next examined if the early host immune response, during which delayed, attenuated liver-stage development occurs, is responsible for the protective phenotype in NCM by parasite transfer experiments. To investigate whether the absence of cerebral pathology in NCM is due to a modification of the parasite at the blood stage I isolated 10^6 parasitized erythrocytes (pRBC) from NCM mice at day 2 post-patency and transferred them by intravenous injection into naïve, uninfected animals. All recipient mice suffered clinical symptoms and died of ECM (fig 3.8), thus indicating that intra-erythrocytic development after chemical attenuation remains unaffected and infected erythrocytes retain their ability to cause ECM.

Furthermore, to determine whether residual isopentaquine affects the parasite at the blood stage during patency, animals were subjected to chemical attenuation and challenged intravenously with 10^6 parasitized erythrocytes at day 5 post-infection. This protocol was chosen to mimic the onset of patency in NCM. However, animals were not protected and succumbed to cerebral pathology. Thus the NCM phenotype is only produced when parasites undergo liver stage development in

an animal subjected to chemical attenuation and is retained in that animal alone. It was therefore assumed that an immune response to the pre-erythrocytic stage is responsible for the protective

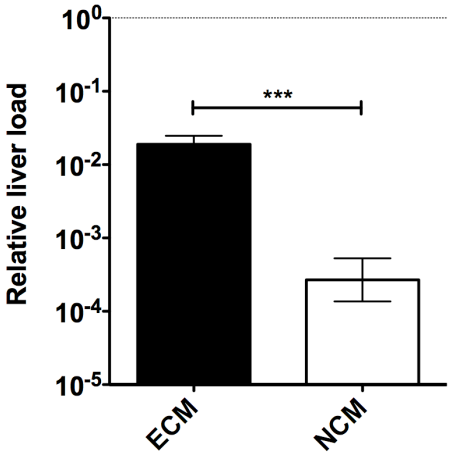

Figure 3.7. Animals subjected to chemical attenuation show decreased transcript abundance of parasite-specific 18S rRNA at 42 h post-infection. Animals (groups of 3), assigned to chemically attenuated (NCM) and positive control (ECM) mice, were infected with 10,000 *Pb*ANKA sporozoites and sacrificed at 42 h post-infection. Livers were extracted and RNA isolated and cDNA synthesized. Relative liver load calculated via ΔCt analysis based on parasite-specific 18S rRNA transcription. Statistics calculated by student's T test. Asterisks signify degrees of significance where *** indicates P < 0.001, ** indicates P = < 0.01, * indicates P < 0.05 and "ns" indicates P >0.05.

phenotype in NCM and that this pre-patent period, during which delayed, attenuated liver-stage development occurs, is crucial for the outcome of ECM.

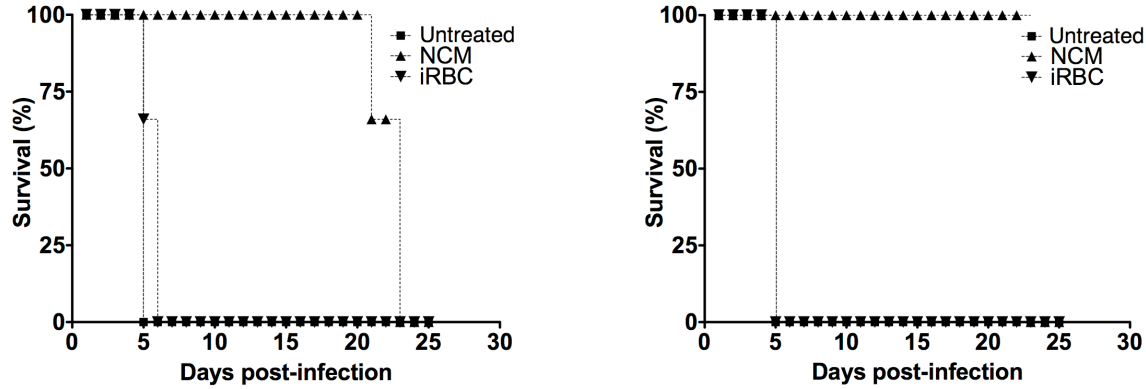

Figure 3.8. The host immune response from the liver induces protection from ECM. Parasitized erythrocytes from chemically attenuated mice remain able to induce ECM Left panel) Mice in group "iRBC" (groups of 5) were infected with pooled 1 x 10^6 infected erythrocytes from patent NCM mice (groups of 5). Right panel) Mice in group "iRBC" (groups of 5) were subjected to chemical attenuation and at day 5 post-attenuation were infected with 1 x 10^6 infected erythrocytes from pooled

infected but untreated mice.

3.4 Cytokine Bead Array analysis reveals an increase in IFN-γ in the liver tissue and serum in experimental animals subjected to chemical attenuation at day 4 post-infection

Since it was hypothesized that the immune system is responsible for the NCM phenotype and that the pre-patent period is a crucial requirement for protection, as described above, the immune response prior to patency was analysed. Since IFN-γ and IL-10 are the archetypal Th1 and Th2 cytokines associated with the two main branches of the cellular immune response, their protein concentrations were measured by cytokine bead array analysis in both the liver and serum. I observed a remarkable increase in total IFN-γ protein in both the liver and serum at day 4 in animals subjected to chemical attenuation compared to ECM control and uninfected control mice. This was particularly pronounced in the liver (fig 3.9).

Since IFN-γ is mainly produced by T lymphocytes and to a minor extent by NK and NKT cells, flow cytometry analysis was performed on cells isolated from liver and spleen tissue to determine T lymphocytes and NK cell numbers. This was followed by intracellular cytokine staining to determine their cytokine output. I observed only a minor difference in the NK cell populations in these organs and no difference in their IFN-γ cytokine staining (fig 3.10) and therefore concluded that these cells are not responsible for the high concentration of IFN-γ characteristic of the NCM phenotype.

3.5 Flow cytometry analysis reveals an increase in T effector cells, a decrease in CD25 and CD69 T cell marker expression and increased cytokine production and Th1 multifunctionality intrahepatic T cells from experimental animals subjected to chemical attenuation at day 4 post-infection *ex vivo*.

Having excluded NKs as the cell type responsible for the high levels of IFN-γ I subjected the other typical IFN-γ producing cell, the T lymphocyte, to flow cytometric analysis. I observed a higher number of both $CD8^+$ and $CD4^+CD44^{hi}CD62L^-$ effector memory T cells present in the

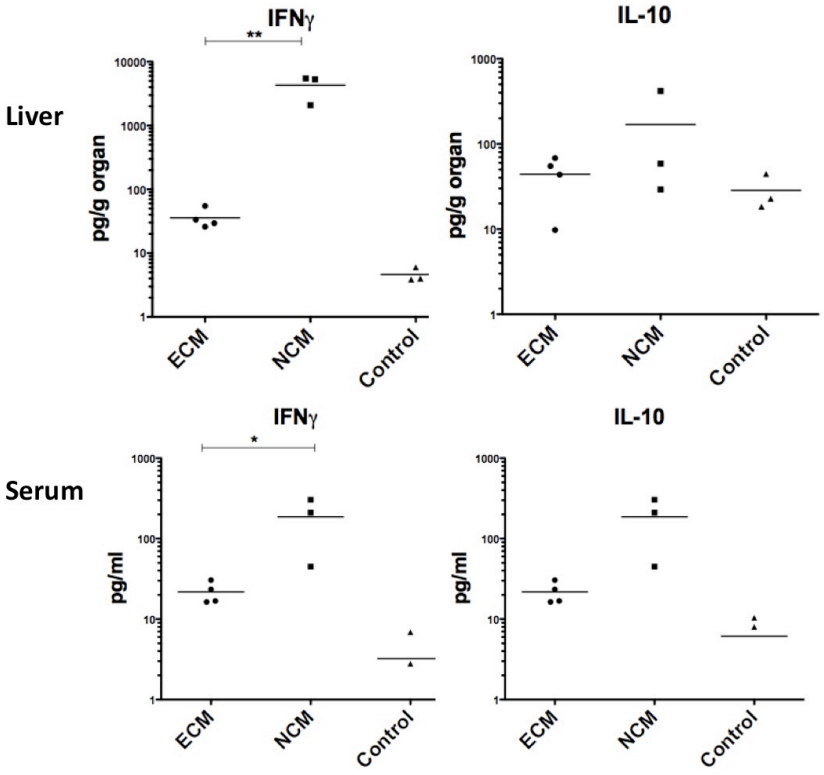

Figure 3.9. Mice subjected to chemical attenuation show elevated IFN-γ in both liver and serum at day 4 post-infection *ex vivo*. Animals were subjected to chemical attenuation, sacrificed at day 4 post-infection and their liver and blood serum were harvested and assessed for IFN-γ and IL-10 by cytokine bead array analysis. Statistics calculated by one-way ANOVA with Bonferonni post-hoc adjustment. Asterisks signify degrees of significance where *** indicates $P < 0.001$, ** indicates $P = < 0.01$, * indicates $P < 0.05$ and "ns" indicates $P > 0.05$.

spleen and a markedly higher number of $CD8^+CD44^{hi}CD62L$ T effector cells in the livers of animals subjected to chemical attenuation compared to ECM control mice. The increase in this subset of T cells corresponded with a pronounced increase in the expression of activation marker CD44 on both $CD8^+$ and CD4+ T cells in liver and spleen at day 4 post-infection (fig 3.11). Intracellular cytokine staining of the intrahepatic $CD8^+$ and $CD4^+$ T lymphocytes revealed an increased number of IFN-γ-positive cells, in addition to IL-2 and TNF-α (fig 3.12).

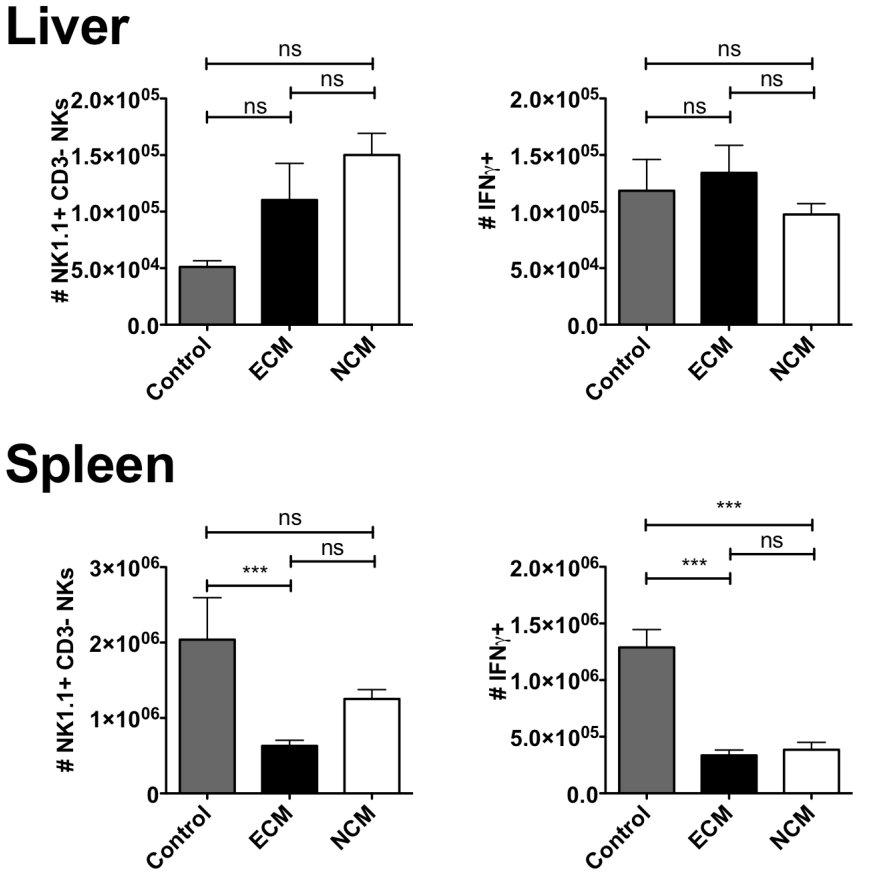

Figure 3.10. Mice subjected to chemical attenuation do not show elevated NK cells or NK-derived IFN-γ in both liver and serum compared to ECM controls at day 4 post-infection. Animals (groups of 5) were assigned to ECM, NCM and control groups as described, and infected with 10, 000 *Pb*ANKA sporozoites and sacrificed at day 4 post-infection. Additionally uninfected control mice were sacrificed. Organs were harvested and lymphocytes isolated and stained for NK1.1, CD3 and IFN-γ to determine whole number NK cells and whole number NK cells producing IFN-γ. Statistics calculated by one-way ANOVA with Bonferonni post-hoc adjustment. Asterisks signify degrees of significance where *** indicates $P < 0.001$, ** indicates $P = < 0.01$, * indicates $P < 0.05$ and "ns" indicates $P > 0.05$.

These liver-derived $CD8^+$ and $CD4^+$ T lymphocytes showed an increase in production of multiple pro-inflammatory cytokines and T cell multifunctionality, skewed towards a Th1 response in NCM (figure 3.10). It was therefore deemed highly likely that $CD8^+$ T cells are responsible for the IFN-γ observed in the liver of chemically attenuated mice (fig 3.9).

Multifunctional T cells are $CD4^+$ T cells that simultaneously secrete IFN-γ, IL-2 and TNF-α. These cells are associated with Th1 responses and protection from several infections [265]. Cell

"multifunctionality" can be measured by the number of cytokines they secrete. Cells can be categorized into single, double or triple cytokine producers. In addition, $CD8^+$ T cells can be analysed by the same criteria to ascertain Th1-like behaviours. Interestingly, at day 4 post-infection, spleen-derived $CD8^+$ and $CD4^+$ T lymphocytes in chemically attenuated mice showed an increase in production of multiple pro-inflammatory cytokines and T cell multifunctionality, skewed towards a Th1 response in NCM (fig 3.13). The NCM phenotype featured 15% triple-positive CD8+ T cells, compared to 8% in ECM control mice and 23% triple positive $CD4^+$ T cells, compared to 14% in ECM control mice.

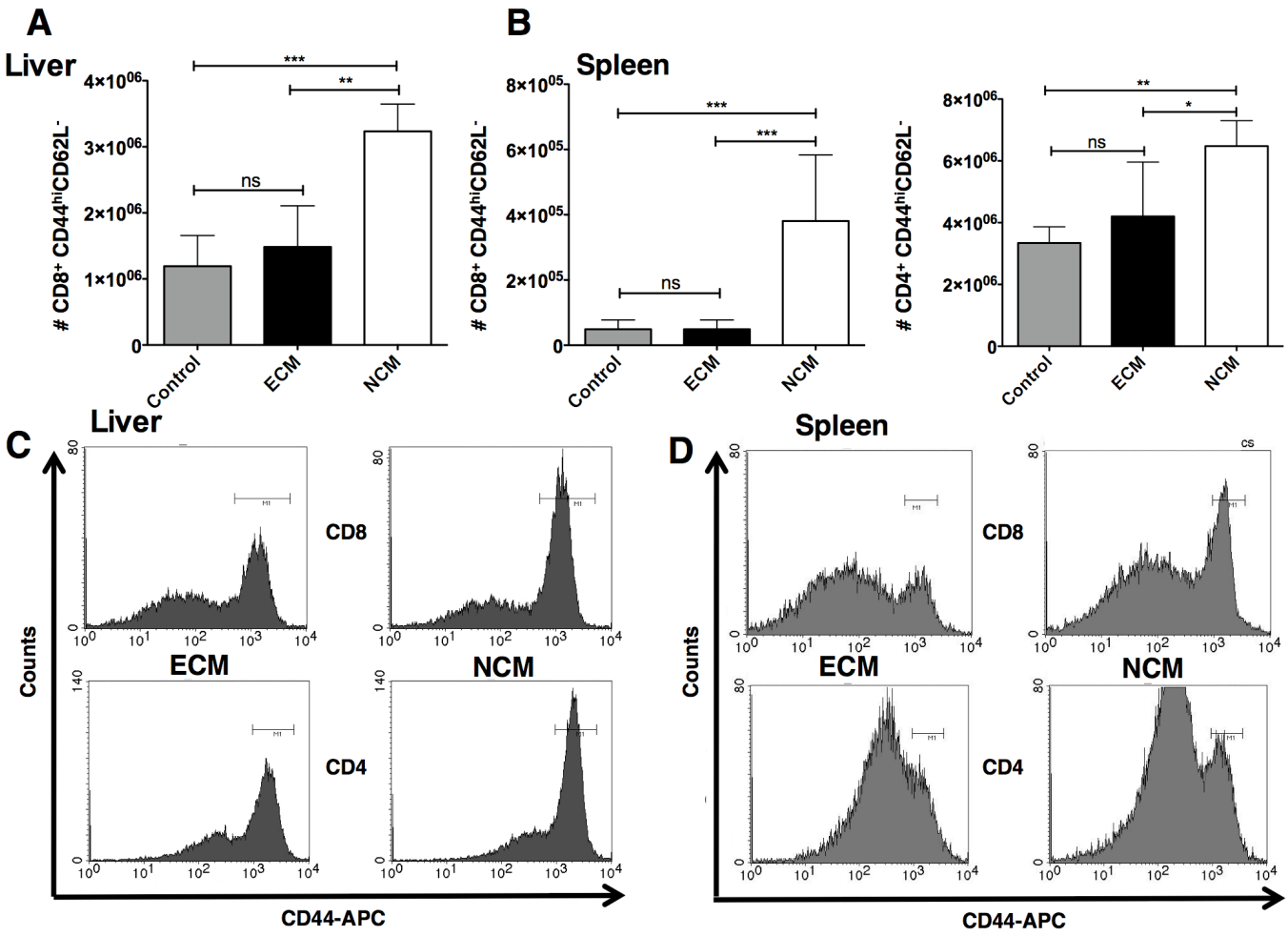

Figure 3.11. Animals subjected to chemical attenuation show increased accumulation of T effector cells at the liver and spleen, increased CD44 activation. Animals (groups of 5) were assigned to ECM, NCM and control groups as described, and infected with 10,000 *Pb*ANKA sporozoites and sacrificed at day 4 post-infection. Organs were harvested and lymphocytes isolated and stained for CD8, CD4 and CD44 and CD62L to determine A) whole number liver effector memory cells

($CD8^+CD44^{hi}CD62L^-$); B) whole number splenic effector memory cells ($CD8^+CD44^{hi}CD62L^-$ and $CD4^+CD44^{hi}CD62L^-$); C) percentage CD44 expression by $CD8^+$ and $CD4^+$ T cells in liver and D) spleen. Upper histograms represent $CD8^+$ T cells and lower histogram $CD4^+$ T cells and are single representative samples from whole experimental group. E) Representative dot-blot illustrating gating. Statistics calculated by one-way ANOVA with Bonferonni post-hoc adjustment. Asterisks signify degrees of significance where *** indicates $P < 0.001$, ** indicates $P = < 0.01$, * indicates $P < 0.05$ and "ns" indicates $P > 0.05$.

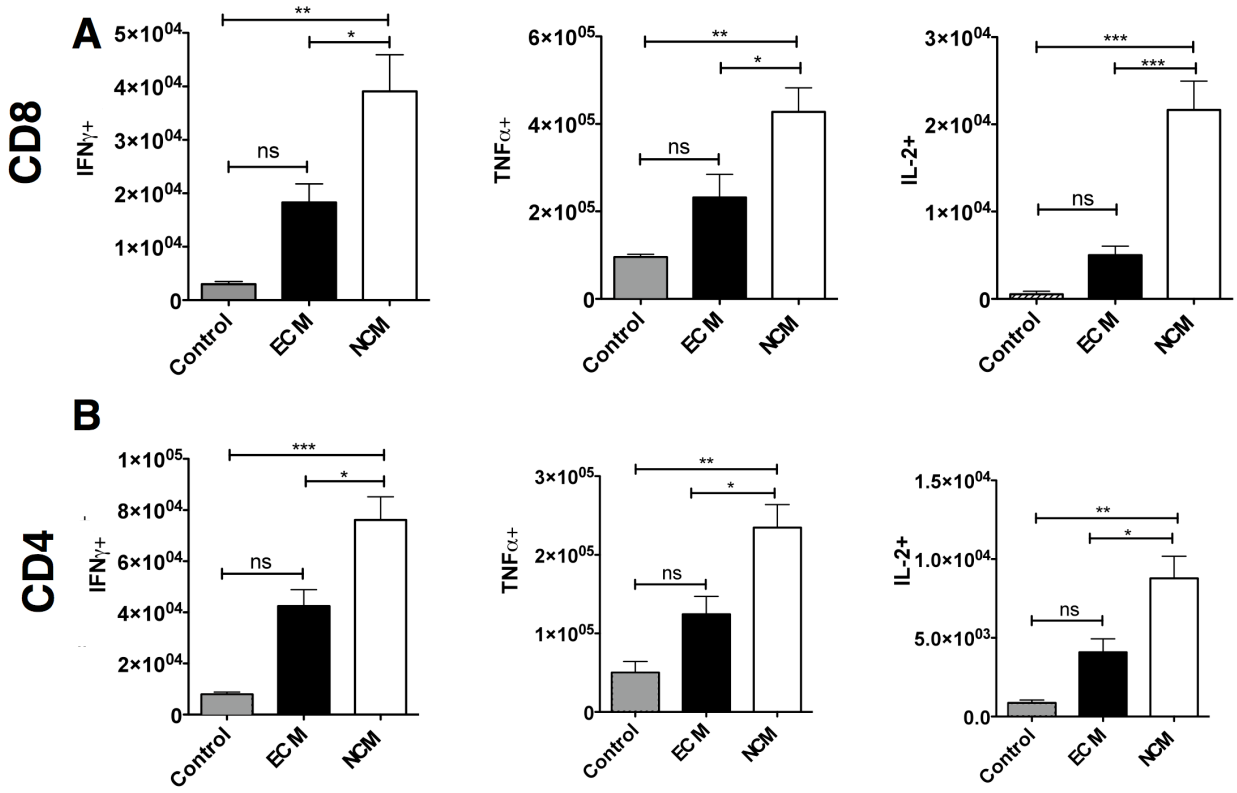

Figure 3.12. Liver-infiltrating lymphocytes expressing IL-2, TNF-α and IFN-γ are increased in animals subjected to chemical attenuation at day 4 post-infection *ex vivo*. Animals (groups of 5) were assigned to ECM, NCM and control groups as described, NCM and ECM mice were infected with 10,000 *Pb*ANKA sporozoites. Livers were harvested at day 4 post-infection and liverderived lymphocytes isolated. Cells were stained for CD8 (A) and CD4 (B), permeabilized and stained for intracellular cytokines IFN-γ TNF-α and IL-2. Statistics calculated by one-way ANOVA with Bonferonni post-hoc adjustment. Asterisks signify degrees of significance where *** indicates $P < 0.001$, ** indicates $P = < 0.01$, * indicates $P < 0.05$ and "ns" indicates $P > 0.05$.

Given this apparent T cell phenotype in NCM at day 4 post-infection - increased splenic and intrahepatic multifunctional effector T cells producing Th1 cytokines – T lymphocytes were subjected to further analysis. To assess early T-cell activation in NCM, I examined CD69 and CD25 at day 4 post-infection. CD69 is an early lymphocyte activation marker associated with active, tissue-invading cells [251] while CD25 forms part of the IL-2 receptor and has been

associated with several cell phenotypes, including early T cell activation [266] and regulatory T cells. I observed a decrease in CD25 and CD69 expression on $CD8^+$ and $CD4^+$ splenic T cells in NCM but not in the liver (fig 3.14). This may indicate decreased priming of splenic T-cells destined to migrate to the cerebral tissues in NCM at this stage of infection in contrast to ECM, where activation of T cells occurs later after the onset of blood infection. These data suggest that early NCM immunopathogenesis features increased accumulation of T-effector cells in both liver and spleen and a pronounced Th1-multifunctional environment.

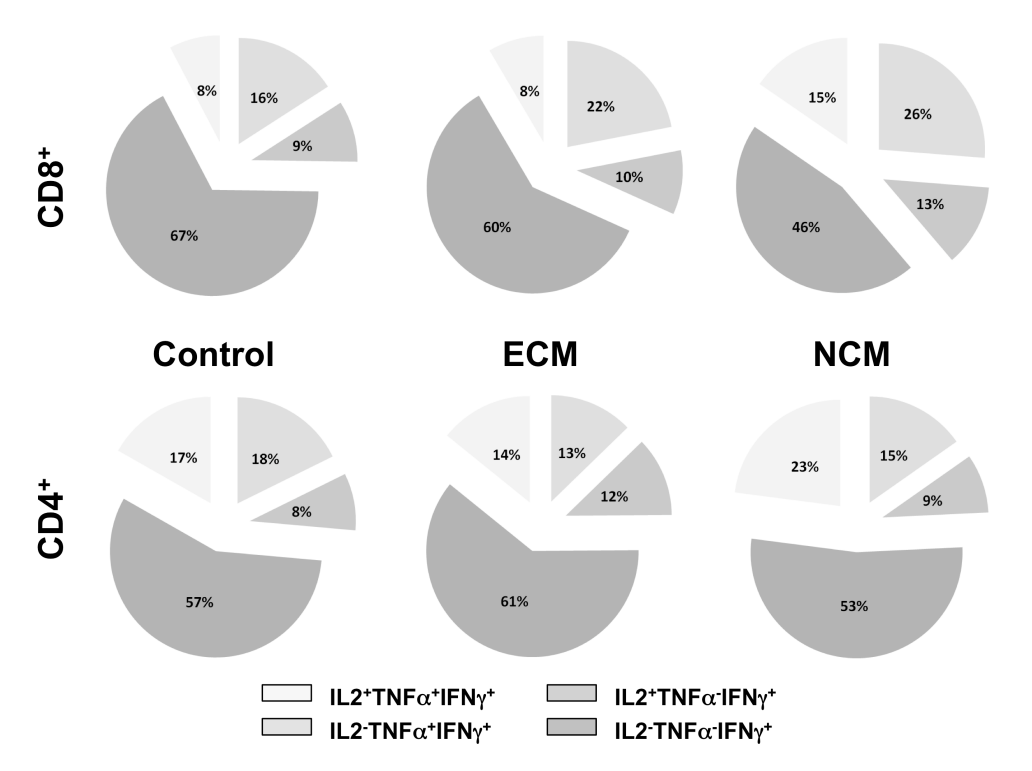

Figure 3.13. Animals subjected to chemical attenuation feature elevated T-cell multifunctionality at day 4 post-infection. Animals (groups of 5) were assigned to ECM, NCM and control groups as described, and infected with 10,000 *Pb*ANKA sporozoites and sacrificed at day 4 post-infection. Additionally uninfected control mice were sacrificed. Organs were harvested and lymphocytes isolated and cultured *ex vivo* with PMA/Ionomycin and Brefeldin A. Cells were stained for CD8, CD4 and IFN-γ, TNF-α and IL-2. IFN-γ positive cells were gated and assessed for their multifunctionality by co-expression of TNF-α and IL-2, represented by percentage according to whether they express one, two or three cytokines. Analysis performed by Jochen Behrends, Research Institute Borstel.

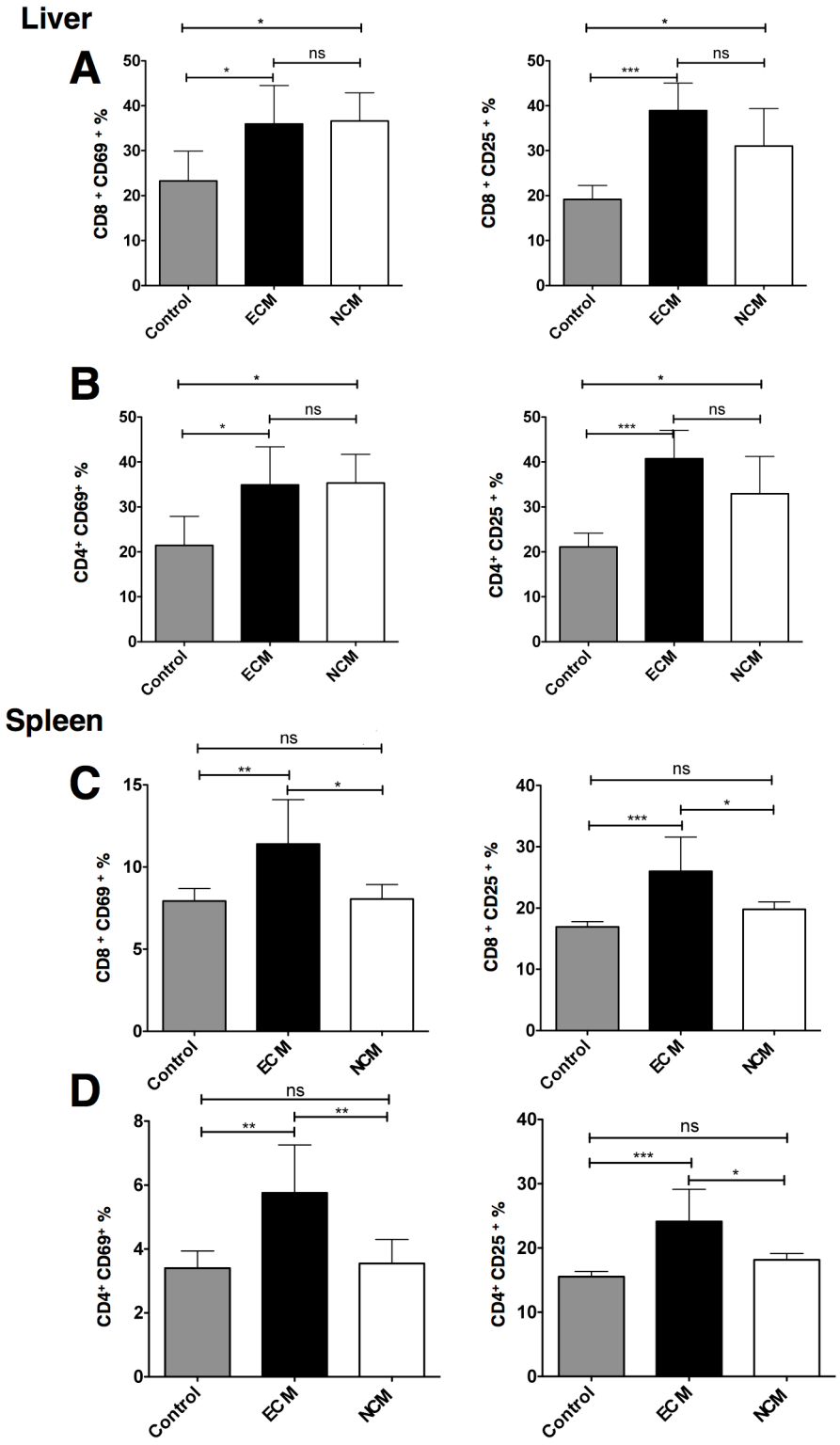

Figure 3.14. Animals subjected to chemical attenuation feature decreased expression of CD69 and CD25 on their splenic CD8⁺ T cells at day 4 post-infection. Animals (groups of 5) were assigned to ECM, NCM and control groups as described, infected with 10,000 *Pb*ANKA sporozoites and sacrificed at day 4 post-infection. Organs were harvested and splenic and liver-derived lymphocytes isolated and stained for CD8 (A, C), CD4 (B, D), CD69 and CD25. Expression was calculated as percentage activation. Statistics calculated by one-way ANOVA with Bonferonni post-hoc adjustment. Asterisks signify degrees of significance where *** indicates $P < 0.001$, ** indicates $P = < 0.01$, * indicates $P < 0.05$ and "ns" indicates $P > 0.05$.

3.6 Flow cytometry analysis reveals a decrease in T effector cells and CD25 and CD69 expression on intrahepatic and splenic T cells in experimental animals subjected to chemical attenuation at day 8 post-infection.

Having established a significant divergence in T cell behaviour at day 4 post-infection, splenic and intrahepatic T cells were analysed during fulminant disease at day 8 post-infection, at which timepoint host immunopathogenesis diverges significantly from control ECM mice. At day 8-9 post-infection, NCM mice show a decrease, albeit not statistically significant, in their splenic $CD8^{+}CD44^{hi}CD62L^{-}$ T effector subset (fig 3.15).

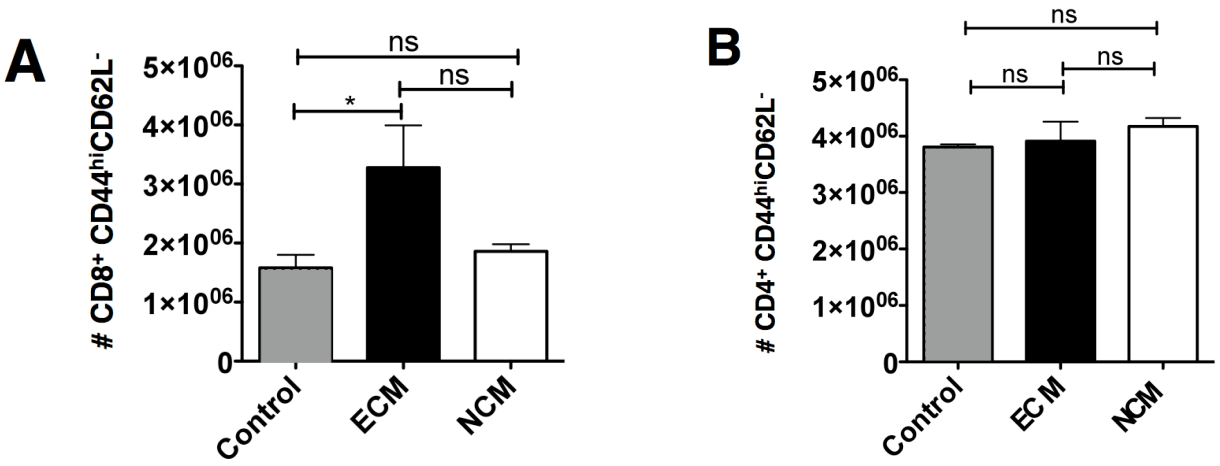

Figure 3.15. Animals subjected to chemical attenuation feature comparable numbers of splenic effector memory T cells at day 8 post-infection to infected controls. Animals (groups of 5) were assigned to ECM, NCM and control groups as described, NCM and ECM mice were infected with 10,000 *Pb*ANKA sporozoites and sacrificed at day 8 post-infection. Spleens were harvested and lymphocytes isolated and stained for CD8, CD4, CD44 and CD62L. Whole number splenic effector memory cells: A) $CD8^{+}CD44^{hi}CD62L^{-}$ and B) $CD4^{+}CD44^{hi}CD62L^{-}$ were calculated. Statistics calculated by one-way ANOVA with Bonferonni post-hoc adjustment. Asterisks signify degrees of significance where *** indicates $P < 0.001$, ** indicates $P = < 0.01$, * indicates $P < 0.05$ and "ns" indicates $P > 0.05$.

Furthermore, at day 8-9 post-infection, NCM mice show a decrease in expression of both CD69 and CD25 activation markers in splenic $CD8^{+}$ T cells and a decrease in CD69 expression on $CD4^{+}$ T cells compared to ECM control mice (fig 3.16).

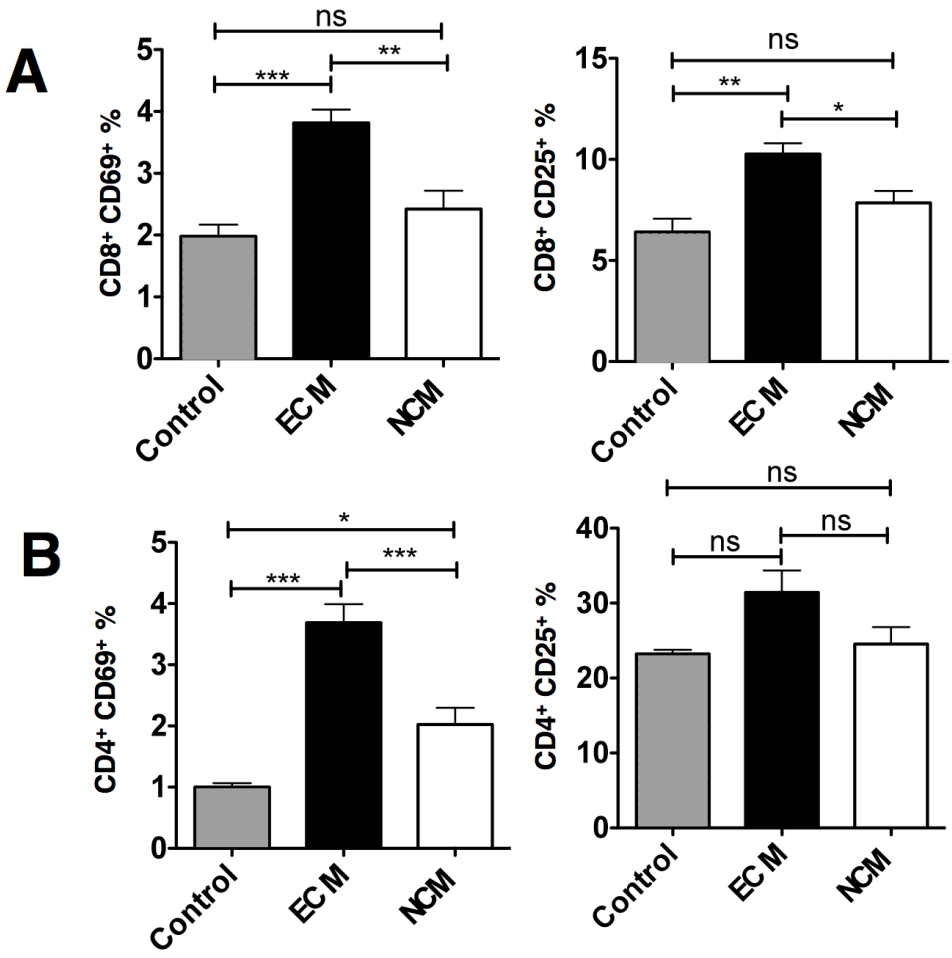

Figure 3.16. Animals subjected to chemical attenuation feature decreased expression of CD69 and CD25 on their splenic CD8+ T cells at day 8 post-infection. Animals (groups of 5) were assigned to ECM, NCM and control groups as described, NCM and ECM mice were infected with 10,000 *Pb*ANKA sporozoites and sacrificed at day 8 post-infection. Spleens were harvested and lymphocytes isolated and stained for CD8, CD4, CD69 and CD25. Expression of CD69 and CD25 markers by T lymphocytes expressed as percentage activation on A) $CD8^+$ T cells and B) $CD4^+$ T cells. Statistics calculated by one-way ANOVA with Bonferonni post-hoc adjustment. Asterisks signify degrees of significance where *** indicates $P < 0.001$, ** indicates $P = < 0.01$, * indicates $P < 0.05$ and "ns" indicates $P > 0.05$.

3.7 Flow cytometry analysis reveals a decrease in $CD11c^+$ DCs present at the liver and spleen in experimental animals subjected to chemical attenuation at day 8 post-infection

T cell activation in ECM occurs in response to a systemic Th1 environment and antigen presentation by $CD11c^+$ DCs [196, 211]. I observed a lower number of $CD11c^{high}CD8^+$ DCs in our NCM model in liver and a pronounced decrease in spleen at day 8 post-infection (fig 3.17).

This indicates a decreased capacity for APC-mediated T-cell priming in the NCM model, consistent with reduced T-cell activation and subsequent absence of cerebral pathology.

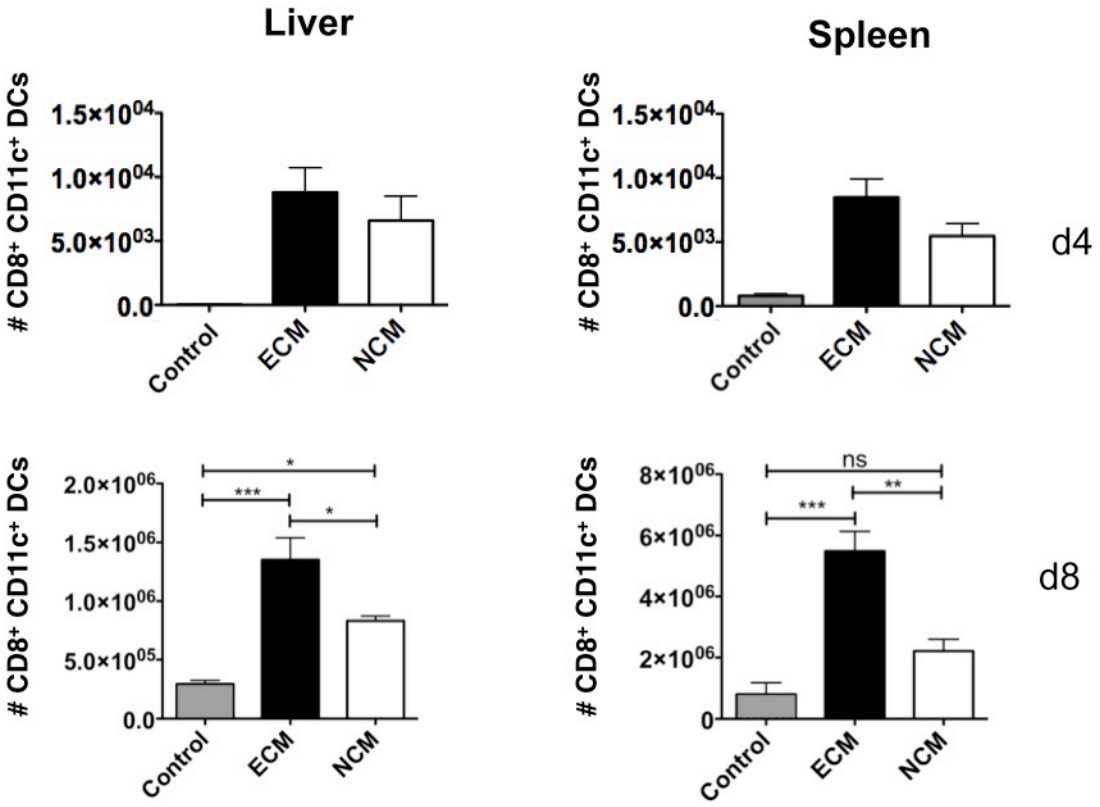

Figure 3.17. Animals subjected to chemical attenuation feature decreased numbers of $CD8^+CD11c^+$ DCs at the liver and spleen at day 8 post-infection. Animals (groups of 5) were assigned to ECM, NCM and control groups as described, and infected with 10,000 *Pb*ANKA sporozoites and sacrificed at day 4 and day 8 post infection. Liver (i) and spleen (ii) were harvested, lymphocytes isolated and stained for CD8 and CD11c to determine whole number of $CD8^+CD11c^+$ DC population. Statistics calculated by one-way ANOVA with Bonferonni post-hoc adjustment. Asterisks signify degrees of significance where *** indicates $P < 0.001$, ** indicates $P = < 0.01$, * indicates $P < 0.05$ and "ns" indicates $P > 0.05$.

3.8 Animals subjected to chemical attenuation feature a reduced cytokine cascade within the cerebral tissues

HCM is characterized by elevated pro-inflammatory cytokines in the serum of infected patients [190, 192]. Moreover, in ECM, depletion of pro-inflammatory cytokines including IFN-γ and TNF-α prevents cerebral pathology in mice [153, 182, 183, 200, 228, 229, 267, 268]. Furthermore, IFN-γR signalling regulates the sequestration of $CD8^+$ T cells in the brain [212].

Given that NCM is characterized by a reduction in sequestered lymphocytes in the cerebral tissues, I measured pro-inflammatory cytokine proteins present in the whole brains of animals by cytokine bead array analysis. It revealed an increase in IL-17 and a decrease in IL-10, IL-6, IL-4 and TNF-α at day 8 post-infection in the brains of mice subjected to chemical attenuation compared to control infected mice (fig 3.18).

3.9 Adoptive transfer of splenocytes from animals subjected to chemical attenuation leads to 70% protection against ECM and is ablated upon depletion of $CD8^+$ T cells

To investigate the transferability of the early cellular immune environment in NCM, I performed an adoptive transfer of 2 x 10^7 liver-derived lymphocytes at 48 h post-sporozoite inoculation into naïve animals, which were challenged with 10,000 *Pb*ANKA sporozoites 24 h later. This did not confer any protection to recipient animals that received lymphocytes from either chemically attenuated animals or ECM control animals. In contrast to this, adoptive transfer of 2 x 10^7 whole splenocytes from NCM donors to naïve mice caused approximately 70% protection against cerebral symptoms compared to 0 % protection in control animals that received splenocytes from ECM donor animals (fig 3.19). In order to determine the component of the transferred spleen lymphocyte subset responsible for protection, donor animals were depleted of their $CD8^+$ T cells. Strikingly, protection could not be conferred to recipient mice if donor NCM mice were depleted of $CD8^+$ T cells (fig 3.19). Protection could also not be conferred when splenocytes from uninfected animals were transferred. This indicates that NCM protection bears an essential requirement for $CD8^+$ T cells, as part of a systemic modulation of the early host immune response.

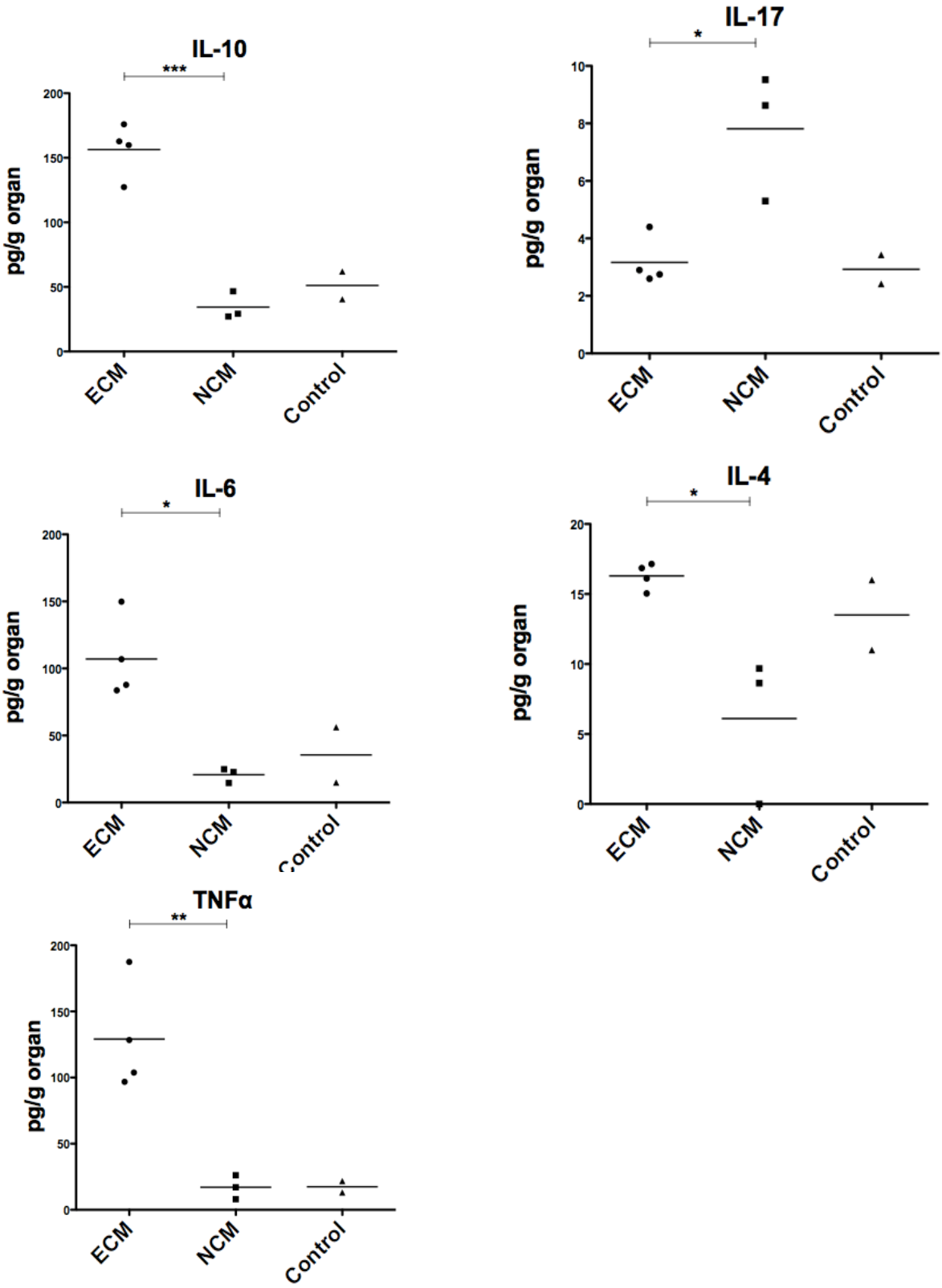

Figure 3.18. Mice subjected to chemical attenuation show decreased IFN-γ, IL-6, IL-4 and TNF-α and elevated IL-17 in *ex vivo* brain tissue at day 8 post-infection. Animals were subjected to chemical attenuation, sacrificed at day 8 post-infection and their brains were harvested assessed by cytokine bead array analysis. Statistics calculated by one-way ANOVA with Bonferonni post-hoc adjustment. Asterisks signify degrees of significance where *** indicates P < 0.001, ** indicates P = < 0.01, * indicates P < 0.05 and "ns" indicates P >0.05.

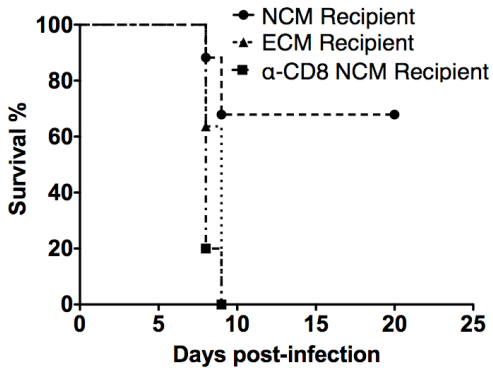

Figure 3.19. The NCM phenotype can be adoptively transferred to naïve recipient mice via splenocyte transfer, is abrogated upon depletion of CD8⁺ T cells. Animals (groups of 5) were assigned to ECM, NCM and control groups as described, NCM and ECM mice were infected either depleted or not for CD8⁺ T cells, infected with 10,000 *Pb* ANKA sporozoites and sacrificed at day 2 post-infection. Splenic lymphocytes from the depleted and undepleted donor groups were isolated, pooled and adoptively transferred into recipient mice (n=5).

Flow cytometric analysis of the adoptively transferred cells revealed that mice subjected to chemical attenuation have fewer $CD4^+$ and $CD8^+$ T cells present in the spleen at day 2 post-infection compared to uninfected mice. (fig 3.20).

3.10 Protection arising from chemical attenuation depends upon IL-10

Given the apparent downregulation of the Th1 response during fulminant infection in chemically-attenuated mice, I investigated the role of the anti-inflammatory cytokine IL-10. IL-10 is a master regulator of immunity to malaria and is important in ECM immunopathology, in which it is responsible for mitigating Th1 responses [269, 270]. Given the NCM paradigm, in which stronger pro-inflammatory responses occur at earlier timepoints, compared to ECM, and subsequently decrease at later infection, it seemed appropriate to investigate the role of IL-10 in the NCM model. IL-$10^{tm1Cgrn}$ knockout mice and WT mice treated with anti-IL-10 receptor antibody were subjected to to chemical attenuation and subsequently challenged with 10,000 *Pb*ANKA sporozoites. Both depleted and IL-$10^{-/-}$ animals developed ECM pathology and died at

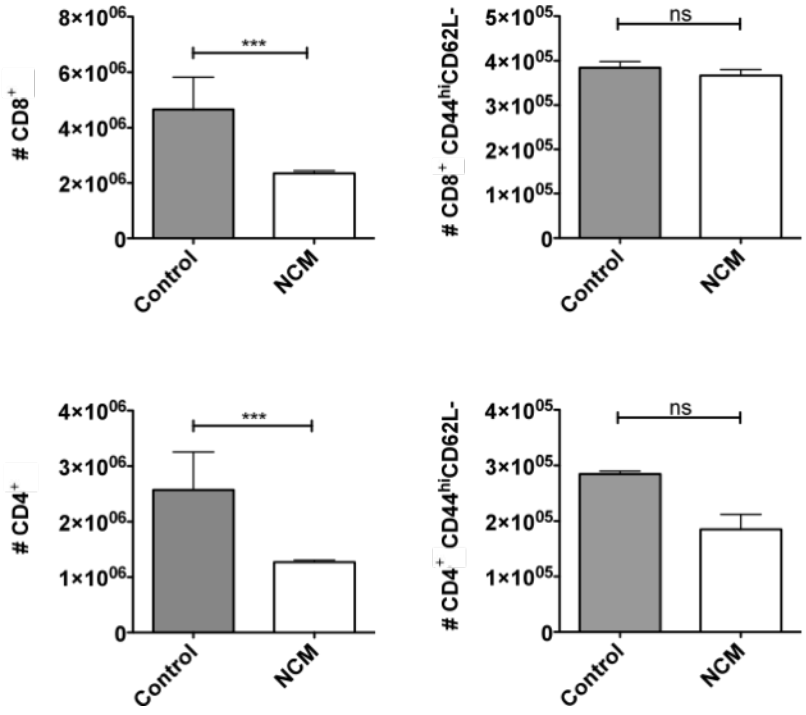

Figure 3.20. Constituent cell subsets in adoptive transfer of 2 x 10^7 splenocytes from NCM mice sacrificed at day 2 post-infection. Animals (groups of 5) were assigned to NCM and control groups as described, and infected with 10,000 *Pb*ANKA sporozoites and sacrificed at day 2 post infection. Spleens were harvested, lymphocytes isolated and stained for CD8, CD4, CD44 and CD62L. Numbers were normalized to the 2 x 10^7 shot. Statistics calculated by one-way ANOVA with Bonferonni post-hoc adjustment. Asterisks signify degrees of significance where *** indicates P < 0.001, ** indicates P = < 0.01, * indicates P < 0.05 and "ns" indicates P >0.05.

days 10-12, indicating the absolute requirement of IL-10 to the NCM phentotype (fig 3.21). I next injected mice subjected to chemical attnuation with IL-10-receptor antibody at day 5 post-infection, and protection was still abrogated, with all mice succumbing to ECM (fig 3.21). This suggests that the protective role of IL-10 in NCM is stage-specific and mediated from the later stages, not the pre-erythrocytic stage.

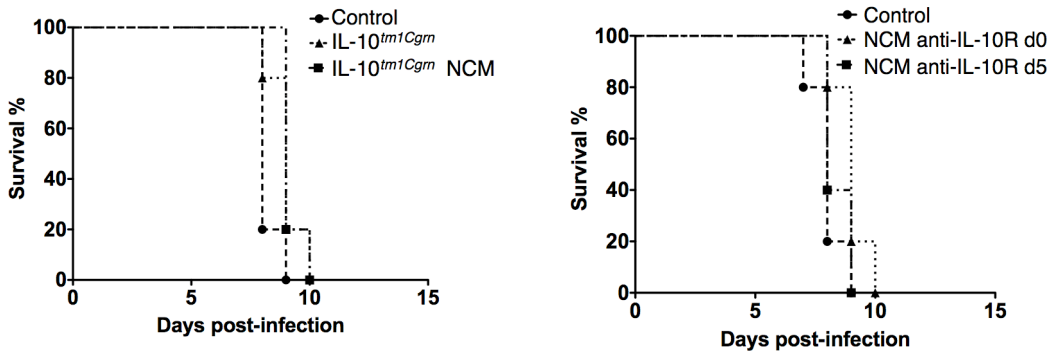

Figure 3.21. The NCM phenotype mediated by IL-10 at fulminant infection. First panel: Animals (groups of 5) were assigned to ECM, NCM and control groups as described. IL-10^{tm1Cgrn} knockout mice were subjected to NCM chemical attenuation, infected with 10,000 *Pb*ANKA sporozoites and survival tracked. Second panel: NCM mice were depleted of IL-10 via injection of anti-IL-10 receptor antibody intraperitoneally (i.p.) at either day 0 or day 5 post-infection and compared with control mice, infected with 10,000 *Pb*ANKA sporozoites and survival tracked.

3.11 Protection arising from chemical attenuation is independent of CD25

Since regulatory T cells are associated with the production of IL-10 and the limitation of inflammatory pathology [271] and have been associated with protection from ECM [242] I speculated that they may be responsible for the production of IL-10 or otherwise mediate T cell responses in the NCM model. However, depletion of CD25 had no effect on the protective phenotype (fig 3.22).

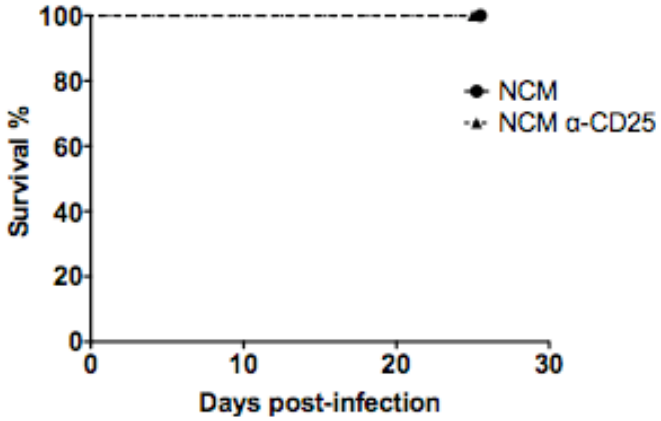

Figure 3.22. Depletion of CD25 in mice subjected to chemical attenuation does not alter the NCM phenotype. Mice subjected to chemical attenuation (n=4) were depleted of CD25 via injection of

anti-CD25 antibody i.p. 7 days before infection with 10,000 *Pb*ANKA sporozoites (NCM α-CD25) and survival tracked in comparison to undepleted mice subjected to chemically attenuation (NCM)

Chapter 4

Discussion

One of the primary complications and causes of mortality in malaria infection is cerebral malaria (HCM), causing up to 500,000 annual fatalities [128], mostly in older children who have already experienced previous malaria episodes [272]. HCM is also a significant risk factor to nonimmune travellers to malaria-endemic regions, who are at a very high risk of developing HCM and systemic shock upon first infection, possibly due to cross-reactivity of primed T cells [137]. Where applied, current antimalarial drug therapies are inadequately managing the cerebral malaria phenomenon, with a failure rate of 15-20% [130, 133]. This is not only due to the lack of medical infrastructure caused by the economic and social debilitation of sub-Saharan Africa, although this is an integral exacerbating factor [23]. Indeed, practical considerations apply, with the life cycle and immunopathogenesis of *Plasmodium* contributing to the death toll. DeSouza and colleagues identified two major causes of the high mortality and low success rate of interventions for HCM [133]:

1. The immunopathogenesis of HCM is poorly characterized.
2. The presentation of HCM symptoms, and hence diagnosis, occur a relatively short time before fatality.

The poor characterization of HCM is mostly due to ethical and practical restrictions posed by working with disease models in humans. Post-mortems are often not performed on patients who succumb to disease, or are otherwise resisted by the family of the deceased [273]. In the absence of post-mortem, failure rate in cerebral malaria diagnosis is very high [135] and atypical presentation of cerebral malaria in the absence of parasite sequestration is not uncommon [131].

Moreover, cerebral pathology causes a complicated series of events, both spatially and temporally, involving interaction between both parasite and host immune system. Dissecting the precise mechanisms that cause pathology on the molecular level would require a level of experimental intervention that is impossible in humans and, as a result, data within the literature is largely descriptive [133].

Thus, considering how cerebral immunopathogenesis has such a complicated and multifaceted causality it is impossible to replicate the syndrome via *in vitro* studies. Animal models are the only logical means by which the interrelated components of immunopathogensis can be elucidated. The advantage of using an inbred mouse model is that immune responses and disease pathologies are generally uniform. The C57BL/6 mouse strain has a distinct Th1 bias [226] which renders it susceptible to the inflammatory immunopathogeneis of experimental cerebral malaria (ECM) and replicates many of the features present in HCM. Nonetheless, the model is imperfect: parasite strain and dosage are critical factors in determining survival or death from ECM, let alone specific and subtle components such as activation of specific lymphocyte subsets, and death typically occurs in only approximately 80 % of infected animals [274].

In the classical description of ECM, the host undergoes a Th1 response involving the production of pro-inflammatory cytokines which commences upon infection of erythrocytes and their clearance in the spleen. This response involves the recruitment of innate immune cells such as monocytes and neutrophils and their chemotaxis to the brain microvasculature, effectively bypassing the liver [133, 199, 200, 275]. A diverse range of cytokines, especially the pro-inflammatory cytokine IFN-γ, increase expression of adhesion molecules such as ICAM-1 and lymphocyte function-associated antigen 1 (LFA-1) [182, 189]. Dendritic cells capture and present antigen during the rupture and clearance of parasitized erythrocytes in the spleen. This, along with the overriding Th1 environment and costimulatory signals provided by adhesion molecules

[276], causes T lymphocytes to become activated and migrate via chemotaxis to the brain microvasculature. It is this adaptive response associated with T cell activation that occurs in the late blood-stage of malaria infection that leads to blood-brain-barrier damage and pathology.

Numerous aspects of ECM immunopathogenesis during erythrocytic infection remain unknown. These include the antigen-specificity of lymphocytes that become activated within the spleen and migrate to the cerebral vessels [181], the nature of junctions that form at the parasite-endothelium interface, the role of systemic immune events as contrasted to those in the spleen or brain and the role mechanisms that lead to the activation of lymphocytes, monocytes and glial cells [133].

Two overlooked and undescribed components of cerebral immunopathogenesis are the pre-erythrocytic and early erythrocytic stages. Typically, schematic descriptions of the events that lead to both HCM and ECM commence at the rupture of infected erythrocytes, the release of *Plasmodium* moities into the circulation, the clearance of infected erythrocytes from the spleen and the resulting uptake and presentation of antigen by dendritic cells [133, 181, 277].

The liver stage is both clinically [264] and immunologically silent, but not entirely so. Immune responses are limited due to the unique and immune-privileged status of the liver, with lymphocyte responses specific to this organ characterized by reduced effector function, activation and increased apoptotic behaviours [66]. However, the *silence* that *Plasmodium* achieves during its invasion and expansion within the pre-erythrocytic stages are better described as an active process of stealth rather than a passive one in which the parasite simply does not do enough to cause attention to itself. This stealth is apparent in the parasite's interaction with two integral components of the innate immune response, MYD88 and NF-κB. MYD88 is a protein essential for TLR and cytokine signalling. It binds to TLRs via its toll-interleukin receptor (TIR)

domain and mediates the activation of numerous transcription factors, including NF-κB. It is important in innate immune responses, including pathogen recognition and the inducton of inflammation [278]. The transcription factor NF-κB regulates genes associated with both innate and adaptive immunity. It is activated via ligation of the B and T cell receptors and upregulates genes associated with lymphocyte proliferation and development [279]. MYD88 and NF-κB come into play upon invasion of the hepatocyte by the sporozoite. As the sporozoite invades and traverses host hepatocytes, cell rupture causes the release of cytosol from the hepatocyte - in a process that is not stealthly at all - triggering MYD88 to cause NF-κB activation of the nitric oxide synthase pathway in hepatocytes surrounding infected ones [280]. However, the parasite apparently masks its steps, as those cells it traverses do not undergo NF-κB activation *in vitro*. It has been hypothesized that this downregulation of the localized response is due to shed malarial CSP relocating to the cell nucleus and directly inhibiting the NF-κB pathway [33, 281]. Indeed, studies have shown that *Plasmodium* CSP shed by motile sporozoites inhibits the respiratory burst in kupffer cells by activating a suppressive signalling cascade [282], rendering them resistant to Th1-mediated activation, inducing their apoptosis [33, 283].

The lack of attention that the pre-erythrocytic stage has received in studies concerning cerebral malaria immunopathogenesis is most likely due to the clinical silence of this stage, which has, in the mind of many researchers, rendered it extraneous to most studies concerning cerebral malaria immunopathogenesis. However, the liver stage has proven to be of primary importance in anti-infective vaccine design and in studies generating and examining sterilizing immunity to malaria challenge in the form of attenuated parasite strains. Indeed, the pre-erythrocytic stage is considered a bottleneck in the life cycle at which point, if the parasite is successfully targeted by the immune system, the debilitating pathology associated with malaria disease can be avoided. Attenuation of the parasite by various means, such as γ-irradiation, gene-knockout of liver-stage

essential genes and the (prophylactic) administration of antimalarial compounds and antibiotics has created reproducible and sterilizing protective immune responses that are mostly cell-mediated, rather than humoral, involving $CD8^+$ T cells and IFN-γ. The refinement, description and characterization of these responses has made up a large part of the literature in the last fifty years and are a cornerstone in the field [284-286]. However, due to practical and safety concerns, the viability of directly transferring the whole-organism attenuated parasite approach to the field is open to question. In recent years, new forms of pre-erythrocytic attenuation have been published involving deletion of new essential genes in the parasite genome [287] the application of different antimalarial-acting compounds and antibiotics [117, 121]. Thus, the liver stage, although clinically silent, is of utmost pertinence in immunological studies and common thought within the field considers the liver stage to be of primary importance in understanding protective immune responses. This being so, why has it not been subject to much study in relation to ECM.

There is, in fact, some limited evidence that early responses can play an immunomodulatory role in ECM. However, the data in these studies are generally incidental, coming about in descriptive studies of protective models, rather a result of deliberate experimental intervention at the early stages. For example, a recent study reported that a transgenic parasite line lacking a *Plasmodium*-specific apicoplast protein resulted in impaired liver-stage development, attenuated merozoite formation, and reduced incidence of cerebral pathology [252]. Furthermore, two studies, one involving co-infection of *Pb*ANKA and *Pb*K173 [236] and another involving irradiated blood stage parasites [251] associated early pro-inflammatory cytokine responses with protection from ECM.

There appears to be a theme emerging: an early inflammatory response is shared between multiple studies concerning pre-erythrocytic immunity to malaria. This is logical, since IFN-γ is

an essential requirement for RAS immunity [98], GAP immunity [97] and CPS immunity [92, 96]. Furthermore, succesive immunizations with irradiated sporozoites has been shown to induce IL-12 and inflammation in kupffer cells within 24 hours, thought to augment APC activity in the acquisition of RAS immunity [288].

Thus the standard model for ECM immunopathogenesis, which commences at the point of erythrocyte rupture and lasts for some 5 to 10 days in a spiral of devastating immunological responses leading to death, is deserving of analysis at its pre-erythrocytic stages in a similar vein to RAS, GAP and CPS.

Taking that into consideration, this work aimed to modulate the course of parasite development by means of applying an antimalarial compound in a manner comparable to chloroquine chemoprophylaxis. The project addressed two primary questions: By attenuating the parasite during its liver stage development, is it possible to elicit immune responses broadly comparable to those that occur when the parasite is subjected to attenuation by other means? If it is possible to provoke an immune response that causes sterilizing immunity against subsequent parasite infection, is it possible to provoke a response that causes modulation of ECM immunopathogenesis? These questions were encompassed in the two primary aims of this study, to:

1. Attenuate *Plasmodium* at the pre-erythrocytic stage as a means of manipulating the host immune response to alter the clinical outcome of ECM via sub-therapeutic chemoprophylaxis
2. Functionally characterize any pre-erythrocytic immunological responses that are required for protection from ECM

To address the first point, it was necessary to select a suitable methodology to attenuate the liver stage. The aim of the study was to attenuate the parasite efficiently to induce a protective

response against cerebral pathology at its pre-erythrocytic stage, without killing the parasite entirely. This being so, the means of attenuation would have to target the parasite at the pre-erythrocytic stage, but nonetheless permit it to initate blood stage infection. Furthermore, it must have no further pharmacological influence once blood stage replication had commenced. Irradiation of sporozoites at levels lower than the level customary to induce sterilizing immunity was considered too imprecise and unlikely to induce appropriate immune responses [49]. Transgenic parasite lines lacking genes involved in liver-stage maturation was considered one option, and numerous clonal lines of such gene-knockouts have been generated that produce similar non-cerebral phenotypes [252] (S Lepper PhD Thesis, F Kohlhepp PhD Thesis, Y Maier PhD thesis, Fernandes *et al* unpublished). Unfortunately, the phenotype produced by these transgenic lines has proven to be unstable and typically result in 30-70% protection from ECM. It was therefore logical to utilize CPS in the attempt to generate a 100% reproducible phenotype that is relatively easy to administer by means of a compound that has a long description in the literature. Due to the aim of the study, the compound had to be active against the parasite's liver stage.

Antimalarial 8-aminoquinolines were synthesized in the 1940s and include pentaquine, isopentaquine and primaquine [289]. They have a proven gametocidal and liver-stage activity by means of their active metabolites which are structually similar to naphthaquinones [289]. Although not fully expounded, it is thought that they may disrupt *Plasmodium* metabolism by the presence of foreign redox reagents similar to naturally occurring ubiquinone [289, 290], binding to DNA and inhibiting DNA polymerase [289]. I tested a number of such 8-aminoquinolines at varying concentrations and by various administration routes and schemes (fig 3.1, table 3.1). The administration of isopentaquine at 60mg/kg by intraperitoneal injection proved to be cytotoxic whereas the administration of primaquine at any concentration either below 60mg/kg or by any means than intraperitoneal injection proved to be ineffective. The observed NCM phenotype,

delayed onset of blood stage parasitemia, absence of cerebral symptoms and death from hyperparasitemia-associated anaemia, occurred after administration of both primaquine and isopentaquine (fig 3.2 and 3.3). Although primaquine is the most efficacious 8-aminoquinoline, in terms of its success as a classical antimalarial therapy [289], the NCM phenotype that it caused was not as effective and required administration at a higher concentration than isopentaquine. Animals treated with primaquine died at parasitemias of approximately 60% at days 15-20 post-infection, whereas animals subjected to isopentaquine treatment reached parasitemias in excess of 80% and survived later than day 20 post-infection,. The phenotype produced by isopentaquine was deemed to be superior and was utilized for all subsequent experiments.

It is interesting to note that the NCM phenotype is by no means unique to isopentaquine. In a sense, this is pleasing, because it is further demonstration that NCM is not the result of a unique pharmacological interaction between drug and parasite. Indeed, in order to fulfil the criteria of Aim One, it was necessary to prove that the phenotype was the result of the host immune response rather than pharmacokinetic modulation of the parasite's kinetics or metabolism. This was achieved in part by the isolation and transfer of parasitized erythrocytes from animals subjected to chemical attenuation into naïve animals (fig 3.8). Animals succumbed to cerebral pathology indicating that a) the protective effect is the result of a host response, rather than a modification of the parasite itself and b) the origin of the modulating effect is most likely pre-erythrocytic. This latter point was further confirmed by the administration of parasitized erythrocytes to animals subjected to chemical attenuation, which were also susceptible to ECM (fig 3.8).

A potential critique of this experiment and the conclusion drawn from it may be that the phenotype is the result of reduced blood stage inocula, which have been shown to induce protective immunity in *P. falciparum* by the induction of a cellular immune response [123].

However, it has never been proved definitively that low parasitemia is correlated with absence of ECM, although one study demonstrated that older animals were less susceptible to ECM due to lower parasitemia [154]. Furthermore, the adoptive transfer experiment involved the harvesting of splenocytes at 48 hours post-infection, long before the onset of patent parasitemia (fig 3.19). Moreover, it could be argued that the question is somewhat redundant, given that, in nature, the pre-erythrocytic stage is never bypassed, rendering the question of whether the effect is due to attenuated liver stage development causing reduced blood stage inocula or attenuated liver stage development itself a moot point. Following the onset of parasitemia, the kinetics in mice subjected to chemical attenuation show no deviation from untreated controls, contrary to the low blood stage parasitemia that one would expect to see as the result of a low blood-stage inoculum.

Nonetheless, it is my judgement that the adoptive transfer and CD8 neutralization experiments definitively proves that $CD8^+$ T cells are responsible for the induction of protection, and hence the immune response is a pre-erythrocytic one, rather than erythrocytic (fig 3.19). Furthermore, these experiments demonstrate that the protective effect is immunological in origin.

The modulation in the immunopathogenesis of infection in NCM was addressed by harvesting the animals at two key timepoints post-infection. In our experience, normal wild type *Pb*ANKA infection does not cause patent parasitemia until day 4 post-sporozoite-infection and animals do not succumb to cerebral symptoms until days 8-9 post-sporozoite-infection. Chemically attenuated *Pb*ANKA infection, however, induces patent parasitemia at approximately day 6 post-sporozoite-infection and mice succumb to hyperparasitemia-associated anaemia at approximately day 25 post-sporozoite-infection. Thus three timepoints were envisaged for the immunological characterization of the NCM phenotype: days, 2, 4 and 8. Day 2 was chosen for the adoptive transfer experiments as a very early stage at which point liver stage parasites, even in untreated

infection, have not reached schizogony. This stage is firmly in the pre-erythrocytic phase during which one would expect innate immune responses and perhaps very early adaptive immune responses to malaria infection. Flow cytometric analysis of the adoptively transferred cells at day 2 post-infection revealed that mice subjected to chemical attenuation have fewer $CD4^+$ and $CD8^+$ T cells present in the spleen at day 2 post-infection compared to uninfected mice. It is possible that this is because there is a significant recruitment of cells from the spleen to the liver. However, there was no significant difference in numbers of splenic $CD8^+$ and $CD4^+$ T effector cells at day 2 post-infection between chemically attenuated and control animals (fig 3.20).

Day 4 represents the timepoint that in untreated infection represents the temporal interface between the liver stage and blood stage. In order to draw a fair comparison between ECM and NCM it was necessary to select a timepoint at which blood stage infection had not yet occurred. This is because blood stage infection is known to have a modulating influence on liver immune responses [291, 292]. Also, given that it is coincident with late liver stage development and schizogony in untreated animals, it was selected as the principle timepoint to analyse *early* responses in NCM immunopathogenesis. Day 8 was chosen on the basis that it is the timepoint when susceptible mice succumb to cerebral pathology.

Based on experiments at these timepoints, the data indicate that an altered early host immune response is indeed responsible for modulating cerebral malaria immunopathogenesis and causing the NCM phenotype. This early response is a pro-inflammatory, cell-mediated one with increased T-cell activation in liver and spleen, higher numbers of effector T cells, cytokine-secreting T cells and proliferating, multifunctional T cells producing pro-inflammatory cytokines (fig 3.9, 3.11, 3.12, 3.13). Dendritic cell numbers, T-cell activation and infiltration of $CD8^+$ T cells to the brain are decreased in later infection, mediated by the anti-inflammatory cytokine IL-10 (fig 3.5, 3.15, 3.17, 3.21). Strikingly, this protection can be transferred to naïve animals by adoptive transfer of lymphocytes from the spleen at very early infection (fig 3.19). This data

suggests that a subpopulation belonging to $CD8^+$ T cells as early as day 2 post infection are responsible for protection (fig 3.19).

Indeed, this study uncovers a relationship in both localization and timing of anti-parasitic T-cell responses involved in the immunopathogenesis of ECM and a previously undescribed role for the pre-erythrocytic stage in malaria. Chemical attenuation induces T cell activation and increased Th1 multifunctionality at an earlier timepoint than it occurs in a normal ECM infection, marked by increased Th1 cytokine production (fig 3.10, 3.11, 3.12). Inflammation is severe in the liver (fig 3.9), an organ that does not normally undergo significant inflammatory pathology in the first days post-sporozoite inoculation in C57BL/6 mice [293]. Indeed, ECM models with unnaturally early IFN-γ responses have been associated with protection from ECM [236, 251], where it diverges from its normal role of mediating splenic T-cell activation and the development of pathology during the fulminant stage of disease [133].

The protection in the NCM model may occur via similar dynamics to these studies, with attenuated pre-erythrocytic parasite development leading to increased early liver-stage T-cell activation associated with IFN-γ and increased Th1 responses. This unnaturally early peak leads to modulation of later inflammatory immunopathogenesis in the host, during the phase where splenic T cells would normally become activated and migrate to the brain at the crucial timepoint between day 8-10 post-infection (day 4-6 post-blood infection) [133]. NCM hosts display decreased $CD11cCD8^+$ DC numbers, downregulation of T-cell activation, no cerebral infiltration and a complete absence of cerebral pathology. This downregulation is mediated by IL-10 during the fulminant stage of disease. $CD8^+$ T cells, including the effector memory subset, are a constituent of the unnaturally early peak and I assume are largely responsible, as adoptive transfer of splenocytes from NCM hosts cannot confer protection to naïve animals in their absence.

Based on these data, I have assembled a new working hypothesis for the immunopathogenesis of *Pb*ANKA infection in mice subjected to chemical attenuation, leading to the NCM phenotype (graphical demonstration see fig 4.1) contrasted with key steps involved in ECM immunopathogenesis described above (section 1.8):

STEP ONE: Following sporozoite invasion, chemical attenuation of the parasite causes prolonged pre-erythrocytic development in the liver prior to the onset of blood stage infection.

Sporozoites invade hepatocytes in the same process as with untreated sporozoites. The presence of isopentaquine within the serum causes a cytotoxic effect against the developing parasite. This effect, like the activity of the majority of 4-aminoquinolines, is not well characterized. Parasite development is delayed and results in a stalling in the development of the parasite within the liver and the onset of blood stage infection. This prolonged development may be concurrent with hepatocyte apoptosis.

STEP TWO: Attenuated development at this early time point causes an increase in T effector cells at the liver, increased multifunctionality and proliferation of Th1-skewed cells and pro-inflammatory cytokine production.

Due to attenuated parasite growth concurrent with hepatocyte apoptosis, innate immune cells, T cells and dendritic cells are recruited to the liver and sample parasite antigen displayed on MHC-I. Phagocytosis of apoptotic hepatocytes and perforin-mediated cytotoxic lysis occurs by $CD8^+$ T cells, which in turn promotes the production of inflammatory cytokines and provokes a systemic Th1 response. Dendritic cells migrate to the draining lymph nodes that serve the liver, where they present antigen to T cells.

STEP THREE: Activated, Th1-skewed T cells migrate to the spleen where there is an associated increase in T effector cells, multi-functionality and Th1 responses prior to the release of merosomes and rupture of infected erythrocytes.

Up to blood stage infection, the inflammatory response is mediated by $CD8^+$ T cells activated from the liver, rather than dendritic cells.

STEP FOUR: At the point of blood-stage infection, the delicate balance required for ECM immunopathology is disrupted. Rupture of infected erythrocytes occurs as the early splenic pro-inflammatory response is in the process of being brought under control by emerging Th2 responses, mediated by IL-10.

Overriding systemic inflammation provokes the production of IL-10. This reduces the systemic Th1 response, dampens $CD8^+$ T cell activation and proliferation and downregulates the expression of adhesion molecules on the vascular endothelium. As blood stage parasites undergo schizogny and blood stage infection is established, clearance of parasitized erythrocytes in the spleen and the release of parasite moieties by ruptured erythrocytes causes the sampling of parasite antigen by dendritic cells. These present antigen but to reduced effect compared to control animals, since the host's Th1 response, concomitant with $CD8^+$ T cell activation and prodigious concentrations of pro-inflammatory cytokines, is already being brought under control.

STEP FIVE: Reduced numbers of $CD8^+CD11c^+$ dendritic cells in the spleen are associated with decreased phagocytosis of parasite moieties which in turn leads to decreased priming of lymphocytes.

The onset of fulminant infection does not provoke the Th1 response as occurs in control animals, and this is associated with a reduced number of splenic $CD8^+CD11c^+$ cells. Reduced

antigen presentation causes a signficant reduction in splenic T cell priming and numbers of $CD8^+$ T effector cells in the spleen at fulminant infection are reduced.

STEP SIX: Systemic inflammation is reduced at the fulminant stage of infection, mediated by IL-10, leading to reduced endothelial cell activation in the brain, reduced binding of infected erythrocytes to endothelial receptors and reduced migration of lymphocytes from the spleen to the brain microvasculature.

The critical and integral cause of ECM pathology is the migration of $CD8^+$ T cells, once activated, to the brain microvasculature by chemotaxis. Reduced systemic inflammation is associated with reduction in the production of chemokines, reduced priming and activation of $CD8^+$ T cells within the spleen causes a reduction in numbers of cells that migrate to the brain.

STEP SEVEN: This in turn reduces leukocyte and parasite sequestration and prevents damage to the blood-brain barrier and associated cerebral pathology.

The brain microvasculature in protected animals remains undamaged by histopathological analysis and levels of leukocyte sequestration remain comparable to naïve animals. Blood infection is still present and undiminished, and as a consequence animals become anaemic and die at parasitemias >80%.

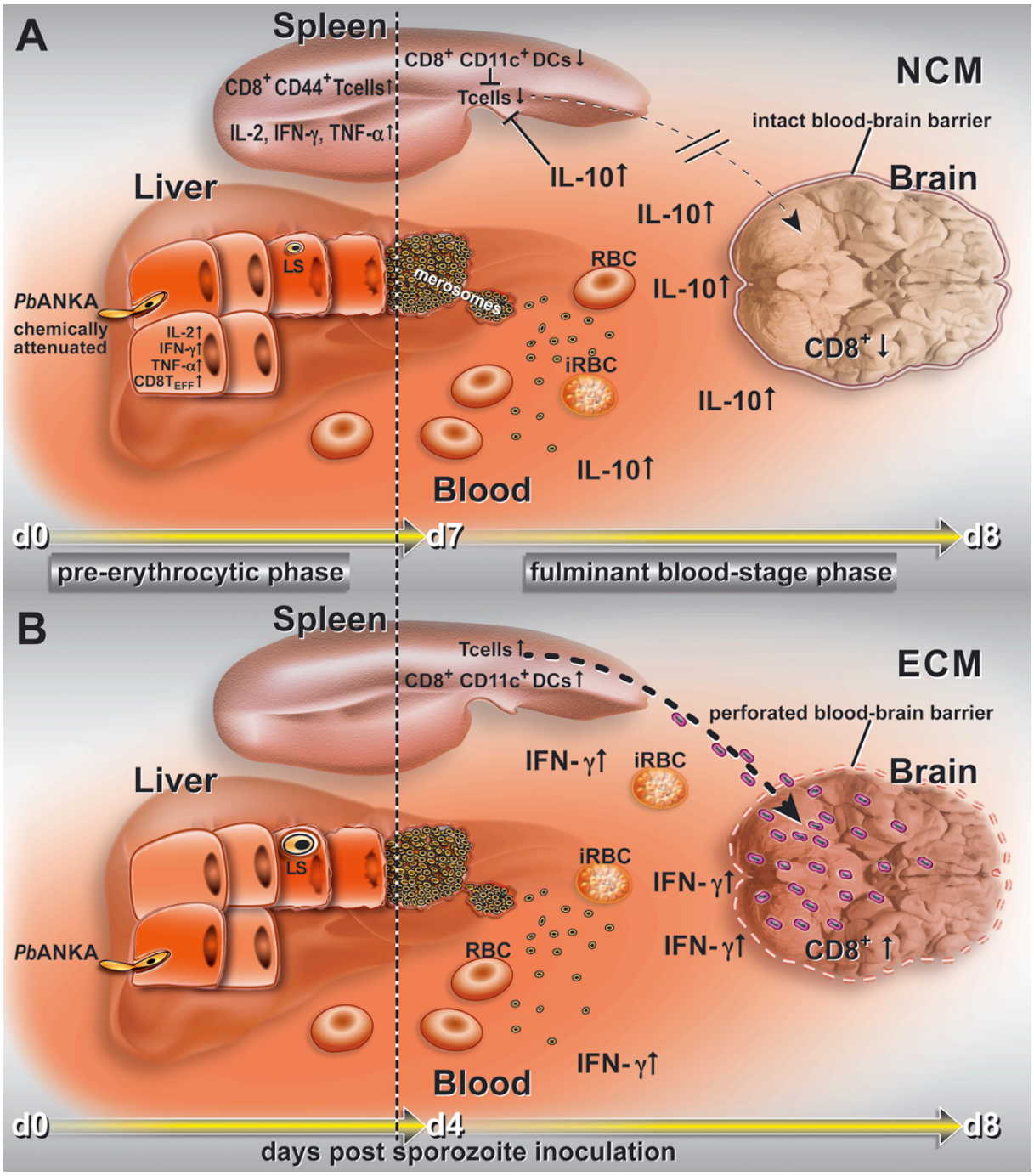

Figure 4.1. A hypothetical schema detailing how chemical attenuation affects immunopathogenesis of mice infected with *Pb*ANKA sporozoites (compiled from the data within this thesis and adaption of Renia et al 2006 and deSouza et al 2010 [181] [133]).
A) Chemical attenuation leads to NCM outcome. Following sporozoite invasion, chemical attenuation of the parasite causes prolonged pre-erythrocytic development in the liver prior to the onset of blood stage infection. Attenuated development at this early time point causes an increase in T effector cells at the liver, increased multifunctionality and proliferation of Th1-skewed cells and pro-inflammatory cytokine production. These activated, Th1-skewed T cells migrate to the spleen where there is an associated increase in T effector cells, multi-functionality and Th1 responses prior to the release of merosomes and rupture of infected erythrocytes. At the point of blood-stage infection, the delicate balance required for ECM immunopathology is disrupted. Rupture of infected erythrocytes occurs as the early splenic pro-inflammatory response is in the process of being brought under control by emerging Th2 responses,

mediated by IL-10. Reduced numbers of $CD8^+CD11c^+$ dendritic cells in the spleen are associated with decreased phagocytosis of parasite moieties which in turn leads to decreased priming of lymphocytes. Systemic inflammation is therefore reduced at the fulminant stage of infection, mediated by IL-10, leading to reduced endothelial cell activation in the brain, reduced binding of infected erythrocytes to endothelial receptors and reduced migration of lymphocytes from the spleen to the brain microvasculature. This in turn reduces leukocyte and parasite sequestration and prevents damage to the blood-brain barrier and associated cerebral pathology.
B) Absence of chemical attenuation leads to ECM outcome. Following sporozoite invasion, parasites undergo pre-erythrocytic development in the liver prior to the onset of blood stage infection. No significant protective pro-inflammatory response occurs at either liver or spleen at the pre-erythrocytic stage. At blood stage infection, increasing blood stage parasitemia and rupture of infected erythrocytes is associated with phagocytosis of parasite moieties by splenic $CD8^+CD11c^+$ dendritic cells, which exogenously process antigen via MHCI, prime and activate lymphocytes and cause systemic inflammation, associated with pro-inflammatory cytokines such as IFN-γ. Systemic inflammation increases endothelial activation in the brain, increased binding of infected erythrocytes to endothelial receptors and increased migration of lymphocytes from the spleen to the brain microvasculature in response to chemokines. This leukocyte and parasite sequestration damages the blood-brain barrier and leads to cerebral pathology, possibly through antigen-specific T cell cytotoxicity, via MHCI restricted presentation of parasite-derived antigen on endothelial cells; hemorrhaging, coma and death results.

Examination of the T cell activation markers at day 4 post-infection revealed an expression pattern that, on first examination, appears to be contradictory. Whereas mice subjected to chemical attenuation featured higher numbers of splenic $CD44^{hi}CD62L^-$ effector T cells relative to control ECM mice (fig 3.11), they featured decreased expression of splenic CD69 and CD25 activation markers (fig 3.14). However this is not unexpected, since both CD69 and CD25 are very early activation markers [251, 266]. I hypothesize that at day 4 post-infection in control ECM animals, blood stage infection has just commenced and DCs initiate the presentation of antigen to T cells, triggering their activation, and upregulation of CD69 and CD25 on the cell surface. This is in contrast to mice subjected to chemical attenuation, which become activated earlier due to prolonged antigen presentation at the liver and/or hepatocyte apoptosis, and whose T cells have become fully differentiated into the T effector subset by day 4 post-infection, concomitant with the increased Th1 response. It is unsurprising that there is no significant difference in the expression of CD25 and CD69 in the liver at day 4 post-infection between NCM animals and ECM controls, since the liver is unlikely to be a site of antigen presentation or T cell activation during normal *Pb*ANKA immunopathogenesis. In chemically attenuated animals, the liver already features an abundance of T effector cells by day 4 post-infection,

whose activation is complete, hence there is no significant difference between the number of CD69 and CD25 cells in the organ at this timepoint.

Some experimental ECM models with unnaturally early IFN-γ responses have been associated with protection from ECM [236, 251], where inflammatory responses may diverge from their normal role of mediating splenic T cell activation and the development of pathology during the fulminant stage of disease [133]. I hypothesize that chemical attenuation in the NCM model causes protection via similar dynamics (fig 4.1). Attenuated pre-erythrocytic parasite development induces T-cell activation, increased Th1 cytokine production and increased Th1 multifunctionality at an earlier timepoint than in a normal ECM infection. This early peak leads to modulation of later inflammatory immunopathogenesis in the host, during the phase where splenic T cells would normally become activated and migrate to the brain at the crucial timepoint between day 8-10 post-infection (day 4-6 post-blood infection) [133].

It is of interest that the data indicate the principle mediators of early protection from cerebral malaria in the NCM model to be IFN-γ producing $CD8^+$ T cells. These cells, although classically associated with the adaptive immune response, can produce nonclonally restricted IFN-γ under numerous conditions, such as bacterial infections [236, 248-250]. Lertmemongkolchai and colleagues suggest that rapid $CD8^+$ T cell activation in this manner may be a component of innate immunity to intracellular pathogens, possibly due to cytokine-mediated bystander events as opposed to engagement of the TCR [250]. An alternative explanation in the literature is that early IFN-γ may be produced by a minor population of $CD8^+$ T cells of nonclassical ontogeny expressing similar markers to $CD8^+$ T cells [236, 294, 295]. Our results are in accordance with the study by Mitchell *et al* which found the source of IFN-γ to be $CD8^+$ T cell derived, rather than NK derived as in previous models, which the authors attributed to "study differences or the occurrence of idiosyncratic processes *in vitro*" [236]. NK cells, innate cytotoxic lymphocytes,

bridge the gap between the innate and adaptive response [33] and play an important role in susceptibility. Indeed, NK cells are early producers of IFN-γ and this cytokine has been associated with spontaneously resolving infection in numerous *Plasmodium* species [80]. Conversely, lethal infection has been associated with the absence of NK-produced IFN-γ [80].

The question of the epitope specificity of these $CD8^+$ T cells is therefore an open one. The antigen-specificity of T cells that migrate to the brain in ECM is still unknown and little is known in general about antigen-specific T cells in malaria infection [296]. It is conceivable that $CD8^+$ T-cell mediated protection leading to NCM is not restricted to any one particular antigen. Indeed, it is possible that early T cell priming, regardless of antigen, causes a more generalized systemic downregulation of the Th1 response, antigen-presentation and T cell activation where and when it matters, at the onset of fulminant disease. Nonetheless, I hypothesize that protective T cells in NCM *are* specific to pre-erythrocytic parasite antigen and that a shared antigenic repertoire may exist between the parasitized hepatocyte and the infected erythrocyte and is displayed via MHCI on the cytokine-activated brain endothelial cell [181]. The induction of rapid parasite-specific T cell responses to malaria infection is not a novel concept, since it has been previously demonstrated that antigen-specific adaptive T cell responses occur rapidly in response to RAS immunization less than eight hours after infection [297]. Indeed, T cells from transgenic mice bearing CSP-specific TCRs are able to differentiate from naïve to effector function, including cytotoxic activity, parasite-killing capacity and the production of IFN-γ, within merely 24 hours of infection [298]. The development of T effector populations in NCM protection at the much later timepoint of 4 days post-infection protection is therefore unsurprising.

Rapid T cell activation obviously necessitates very fast DC activation and uptake of foreign antigen. Although no significant difference was observed between NCM and ECM groups at day

4 post-infection, this is consistent with DC migratory behaviour. The time between antigen phagocytosis and egress from the liver is only one hour [299]. Analysis of those DCs presenting in the liver-draining lymph nodes may provide further data regarding antigen presentation in the NCM model. Furthermore, it is possible that isopentaquine treatment enhances antigen uptake due to the induction of apoptosis in infected hepatocytes. RAS immunization has been shown to induce DC antigen uptake in a similar manner and may enhance the immune response [300].

However, my observation of a decreased number of DCs in animals subjected to chemical attenuation at day 8 post-infection is consistent with reduced T-cell activation at the fulminant stage of infection, a component of the overall downregulation in Th1 responses. The connection between $CD11c^{hi}CD8^{+}$ DCs and ECM is well established. Parasites associate with these DCs, which capture dying cells and exogenously process antigen for cross-presentation via MHCI [197]. They have been shown to prime naïve $CD8^{+}$ T-cell proliferation and cytotoxic T lymphocyte (CTL) effector functions [209] with the induction of specific $CD8^{+}$ T-cell responses abrogated in their absence [301]. Recent work indicates that it is the $CD11c^{high}CD8^{+}$ DCs that are responsible for ECM immunopathogenesis [196]. Chemically attenuated NCM hosts display decreased $CD11c^{hi}CD8^{+}$ DC numbers which in turn downregulates T-cell activation, resulting in the absence of cerebral infiltration and a complete absence of cerebral pathology.

This downregulation is mediated by the anti-inflammatory cytokine IL-10 during the fulminant stage of disease in a response that I hypothesize represents the host bringing its early pro-inflammatory response under control at the stage where T cell priming and/or chemotaxis to the brain would occur. IL-10 plays an essential role in ECM immunopathology that can both inhibit pathogen clearance and decrease immunopathology [269, 270]. Furthermore, it has been demonstrated that neutralization of IL-10 leads to ECM symptoms in otherwise resistant mice [184]. Since regulatory T cells are associated with the production of IL-10 and the limitation of

inflammatory pathology [271] and have been associated with protection from ECM [242] I speculated that they may be responsible for the production of IL-10 in the NCM model or otherwise mediate T cell responses. However, depletion of CD25 had no effect on the protective phenotype (fig 3.22). The source of IL-10 therefore remains unknown, though recent literature reports an IL-10 producing $CD4^{+}CD25^{-}Foxp3^{-}$ regulatory T cell subset associated with the modulation of pathology in *P. yoelli* [302, 303].

This work has larger implications in dissecting the immunological basis of HCM pathology, a complex sequence of inter-related events thought to begin with pRBC sequestration or rupture [133]. These data do indeed suggest a role for the early intrahepatic host immune responses that can alter the course of downstream systemic immunopathogenesis as outlined in the working hypothesis for NCM immunopathogenesis above.

Liver tolerance may explain why such potentially protective pre-erythrocytic responses do not naturally occur in HCM: The liver is served by the hepatic portal vein as its main blood source, and this vein delivers blood from the gut, consisting of various endotoxins, bacterial products and food antigens [66]. This continuous presence of non-self commensal antigens places restrictions on the activation and effector function of T cell responses in the liver, and for this reason, immune responses to infections such as malaria are controlled [39].

Children do not develop HCM on first infection and older children, who have suffered multiple infections before, are at a higher risk of succumbing [272]. This is likely due to a memory-cell triggered adaptive inflammatory immune response during the erythrocytic phase [133]. Artavanis-Tsakonas and colleagues hypothesize that first infection of an infant living in an endemic area induces the innate immune response to produce only low levels of both IFN-γ and

TNF-α because T cells have not been primed to parasite-specific antigen. The authors suggest that clinical symptoms are minimal due to maternal antibody, cytokine-mediated killing or due to physiological barriers, such as dietry deficiencies. However, the authors hypothesize that upon subsequent infection, primed T cells produce increased IFN-γ leading to HCM and systemic shock [137]. In light of the data contained within this project, I tentatively present an alternative hypothesis. It is possible that first infection of children induces an early inflammatory response in the liver that is, relative to the response induced at the erythrocytic stage, very high and comparable to that observed in NCM, either antigen-specific or due to bystander $CD8^+$ activation as described by Lertmemongkolchai *et al* [250]. This may lead to downregulation of the inflammatory response at fulminant infection. Upon subsequent infection, the early liver response retains its tolerance and is therefore much lower in comparison to the spleen-localized adaptive immune response at erythrocytic infection, which has now acquired the full force of a secondary immune response. This counteracts any downstream downregulation of fulminant inflammation due to early pre-erythrocytic inflammation.

These data may also provide a mechanistic basis for the decrease in severe pathology observed in the RTS,S malaria vaccination trials and other pre-erythrocytic malaria interventions. RTS,S does not cause sterilizing immunity but rather causes patent but non-severe malaria, with an absence of cerebral malaria, possibly due to attenuated liver stage development and impaired merozoite release [304-306]. This end result – *tolerated patency* - is comparable to the erythrocytic tolerance due to TLR-signalling refractoriness that occurs in individuals exposed to multiple infections who live in endemic areas [307]. Due to ethical and practical constraints, it would be difficult to demonstrate this in humans.

Nonetheless, within the animal model, the work contained within this project could be expanded

in various ways. Since it has been demonstrated that DCs can phagocytose antigen and egress from the liver within one hour [299] and T cells can differentiate within 24 hours post-infection [298] it would be of interest to elucidate DC and T cell migratory behaviour in the first 24 hours post-infection. Indeed, an ideal analysis would consist of a thorough determination of DC, T cell and systemic cytokine behaviours on a day-by-day basis throughout the course of infection from day 0 to 12 post-infection to determine T cell activation, differentiation and activity. It would be of interest to study the precise requirements and pathways for T cell activation in NCM by disrupting the signals mediated by key molecules such as CD45, ICOS and IL-12R by subjecting transgenic knockout mice lacking these molecules to chemical attenuation. Furthermore it would be of interest to disrupt key effector functions in cytotoxic T cells, such as perforin and granzymes.

An ambitious potential further experiment would be to determine the epitope specificity of the $CD8^+$ T cells involved in NCM phenotype and to establish whether this specificity is maintained from liver infection to fulminant infection and if it is shared between liver and spleen. I hypothesize that antigens specific to MSP-1 are a good candidate for conserved epitope specificity in NCM since MSP-1 is expressed in both the liver and blood stage [308]. This could be achieved by utilizing MSP-1 specific peptide-MHC-I tetramers using MSP-1 $CD8^+$ T cell epitopes identified by computational prediction tools with the capacity to bind MHC-I in C57BL/6 mice [309]. Antigen-specific T cells can be detected and characterized by flow cytometry of tetravalent complexes consisting of multimers of four biotinylated peptide/MHC complexes displayed on streptavidin. This technology could determine which antigen-specific T cells undergo priming, expansion and differentiation in NCM, which organs they are localized to and when they migrate there. T cell migration in NCM could be particularly interesting to research, to determine the relative contribution of the spleen and liver in the protective phenotype. Upon demonstration that NCM is caused by antigen-specific $CD8^+$ T cells, their

thresholds, kinetics and differentiation into memory phenotypes could be ascertained and contrasted to natural infection.

Finally, it would be of interest to study the contribution, if any, of other cell types of both the innate and adaptive immune system, such as $CD4^+$ T cells, NK cells or NKT cells, on the NCM phenotype. I am particularly interested in attributing responsibility for the production of IL-10, which is a crucial requirement for NCM protection. Since I have excluded $CD25^+$ cells, it is possible that IL-10 produced by Tr1 or adaptive regulatory T cells may moderate the immunopathogenesis of disease. Examination of CD25, Foxp3 and IL-10 mRNA within the $CD4^+$ T cells of animals subjected to chemical attenuation may give an indication as to the specific cell type producing IL-10. Due to the idiosyncratic expression pattern of such a cell type, it could be that this cell type cannot be neutralized via a neutralizing antibody. Therefore, upon identification of a likely candidate, this cell type could be separated by flow cytometry or magnetic cell sorting in animals subjected to chemical attenuation from both wild type and IL-10 knockout genetic backgrounds. At this point, the purified cells could be adoptively transferred into infected but non-chemically attenuated mice and chemically attenuated IL-10 knockout mice. If the cell type isolated from wild type mice, but not IL-10 knockout mice, is able to induce protection in both chemically attenuated IL-10 knockout animals and infected wild type animals, this would provide very strong evidence that this cell type is responsible for the protective IL-10 in NCM.

In conclusion, this work has larger implications in dissecting the complex sequence of inter-related events that form the immunological basis of HCM pathology and presents an insight into the potential role of the pre-erythrocytic response in tempering downstream cerebral immunopathogenesis. Artavanis-Tsakonas and colleagues wrote of the Th1 immune response to malaria:

"Th1 celllular responses are required for parasite clearance, but need to be induced in a controlled, site- or organ-specific manner in order to avoid systemic disease" [137].

The data described herein support this statement, with the added proviso that in addition to organ specificity, temporal specificity of the Th1 response is also of paramount importance. The incorporation of these principles into future malaria prevention strategies is an endeavour well worth pursuing. Immuno-modulatory therapies that are able to provoke a temporally and physically specific Th1 response may serve to be an effective adjunctive therapy to antimalarials and/or vaccines in the effective management of the malaria pandemic.

Chapter 5

Appendicies

Label Score Description	Score	Description
Coordination		
Gait	0–2	(none – ataxic – normal)
Balance	0–2	(no body extension – extends front feet on wall – entire body lift)
Exploratory Behavior		
Motor Performance	0–2	(none – 2–3 corners explored in 90 seconds – explores 4 corners in 15 seconds)
Strength and Tone		
Body Position	0–2	(on side – hunched – full extension)
Limb Strength	0–2	(hypotonic, no grasp – weak pull-back[front paw grasp only] – strong pull-back)
Reflexes and Self-Preservation		
Touch Escape	0–2	(none – unilateral – instant and bilateral; in 3 attempts)
Pinna Reflex	0–2	(none – unilateral – instant and bilateral; in 3 attempts)
Toe Pinch	0–2	(none – unilateral – instant and bilateral; in 3 attempts)
Aggression	0–2	(none – bite attempt with tail cut – bite attempt prior to tail cut, in 5 seconds
Hygiene-Related Behavior		
Grooming	0–2	(ruffled, with swaths of hair out of place – dusty/piloerection – normal with sheen)

Appendix 1: The Rapid Murine Coma and Behavior Scale (RMCBS) as outlined in Carrol et al 2010. The scale consists of 10 parameters, each scored from 0 to 2. 0 = lowest function, 2 = highest. An accumulative score of 0 to 20 is obtained per animal.

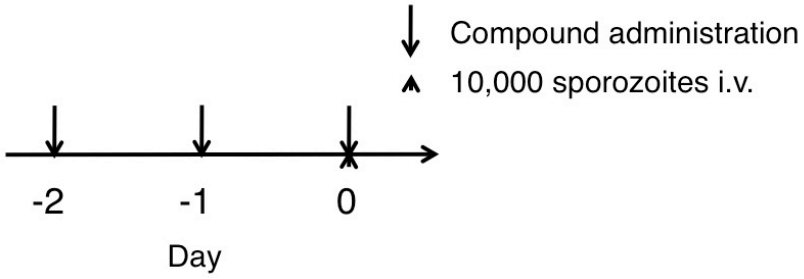

Appendix 2: Schema depicting the administration of isopentaquine and sporozoites that leads to NCM outcome. 30mg/kg isopentaquine was administered three times subcutaneous injection at 24 hour intervals. One hour after the third administration, 10,000 *Pb*ANKA salivary gland sporozoites were inoculated intravenously.

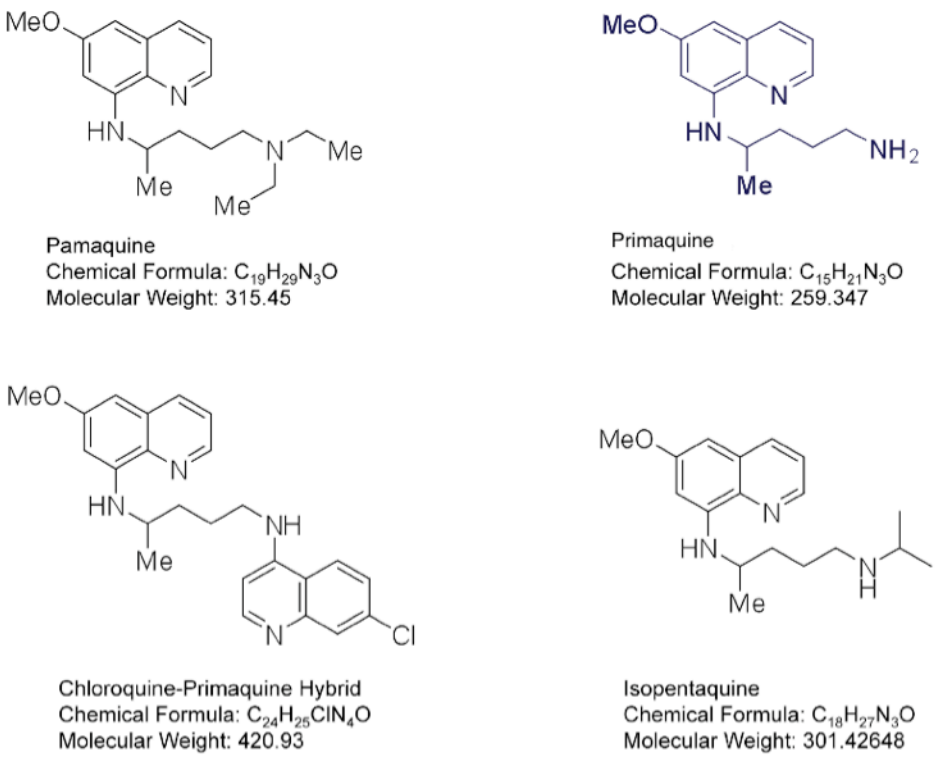

Appendix 3: Structural formulas of 8-aminoquinoline compounds used in this work. (Primaquine structure taken from Wikimedia Commons). Compounds synthesized by Melanie Diegel, University of Wuerzburg, and Eleonora Paulsen, University of Copenhagen.

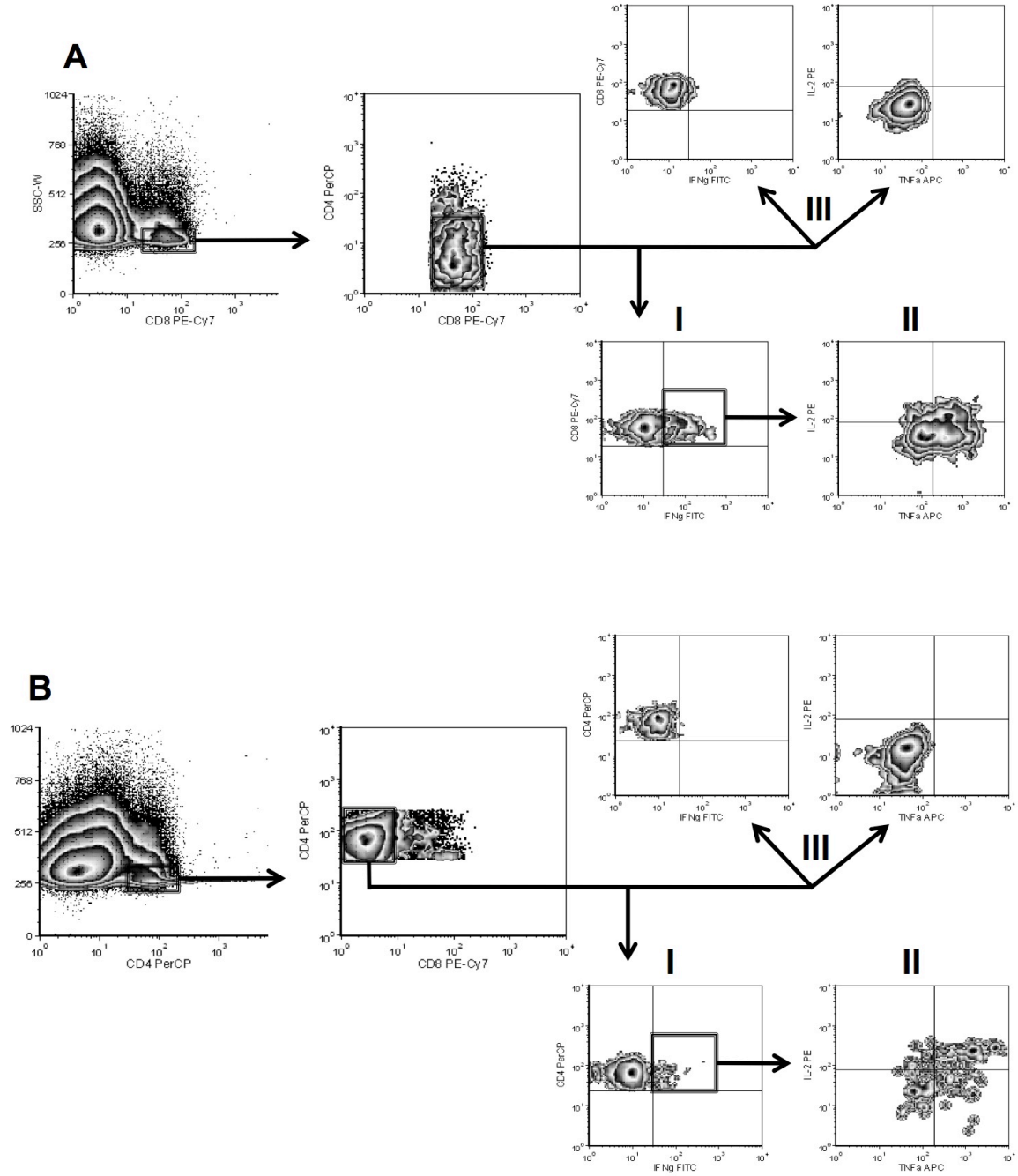

Appendix 4: Gating strategy for multifunctional T cells. Cells were stained for CD8, CD4, IFN-γ, TNF-α and IL-2. CD8 (A) or CD4 (B) versus width of SSC was used to exclude doublets. Additionally CD8 versus CD4 was used to determine an accurate CD8 (A) and CD4 (B) positive cell population, excluding autofluorescent cells. IFN-γ positive cells (I) were gated and assessed for their multifunctionality by co-expression of TNF-α and IL-2 (II), represented by percentage according to whether they express one (IFN-γ), two (IFN-γ and TNF-α or IL-2) or three (IFN-γ, TNF-α and IL-2) cytokines, visualized within a pie chart. Analysis performed by Jochen Behrends, Research Institute Borstel.

A

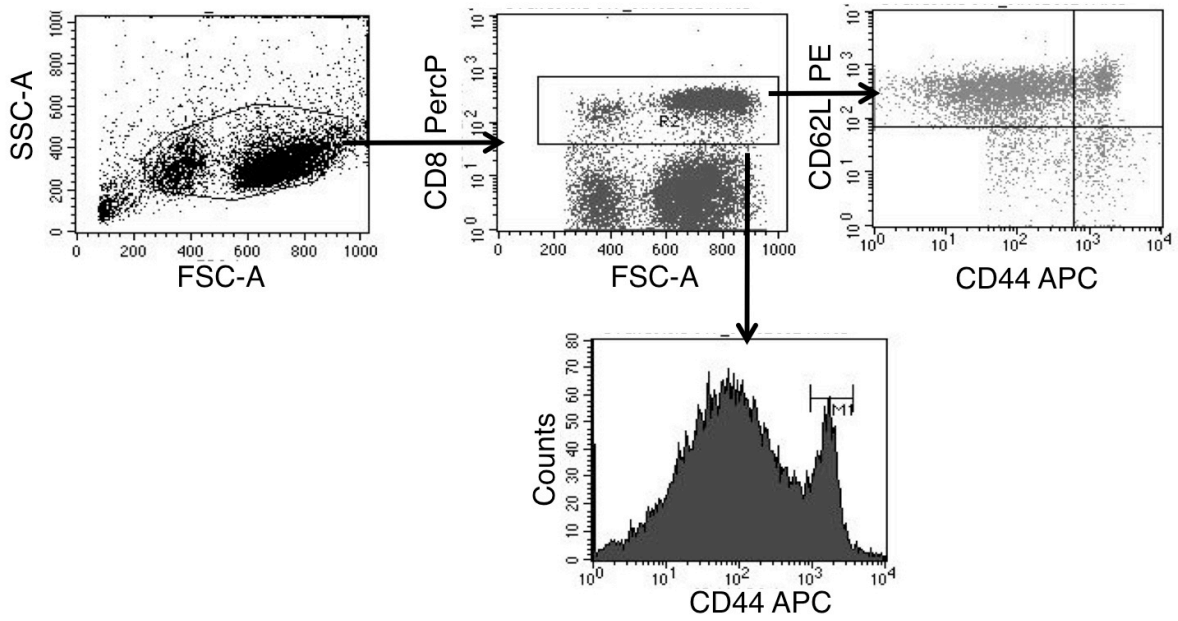

B

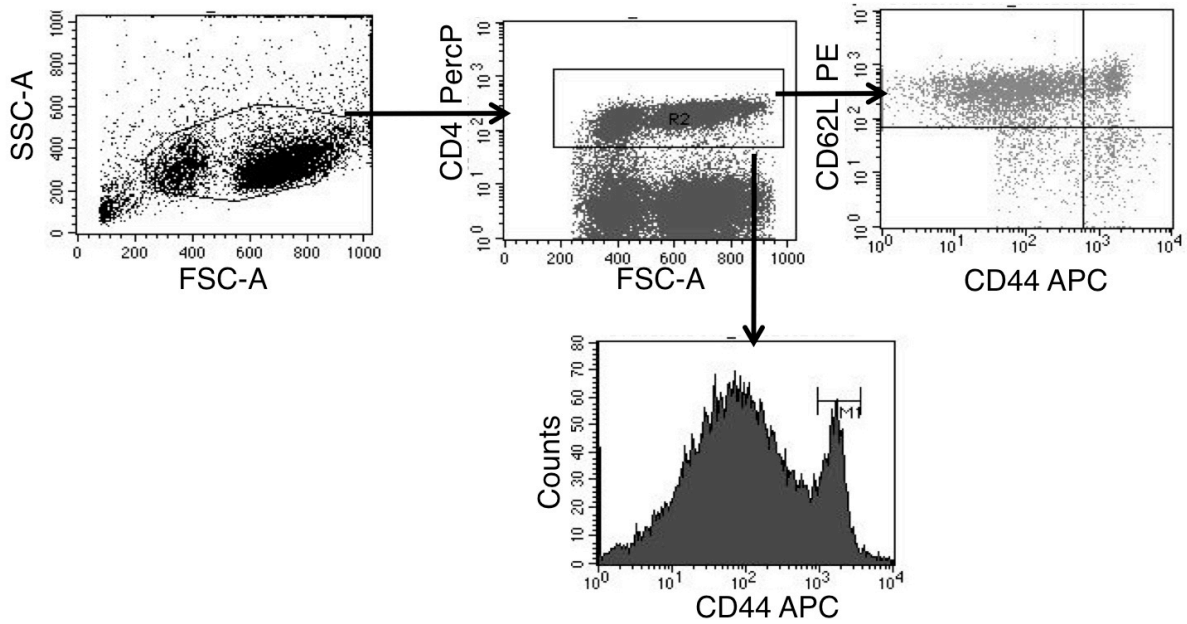

Appendix 5: Gating strategy for effector T cells. Cells were stained for CD8, CD4, CD44 and CD63L. Lymphocyte populations were gated in the FSC vs SSC scatter plot and FSC vs CD8 (A) or CD4 (B) was used to determine an accurate CD8 (A) and CD4 (B) positive cell populations. CD8 or CD4 cells were gated and single and co-expression of CD62L and CD44 was determined to distinguish between specific cell phenotypes, which were isolated by a quadrat in a CD44 vs CD62L scatter plot.

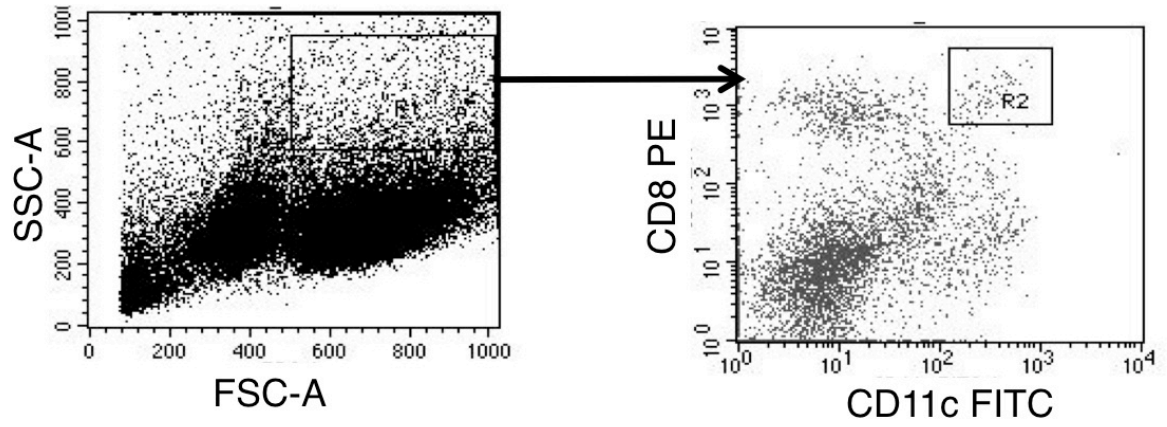

Appendix 6: Gating strategy for CD11c$^+$ dendritic cells [310]. Cells were stained for CD8 and CD11c. FSC-high and SSC-high cells were gated in the FSC vs. SSC scatter plot and used to determine an accurate CD8 and CD11c co-expressing cell populations. Example shown is an uninfected control.

A

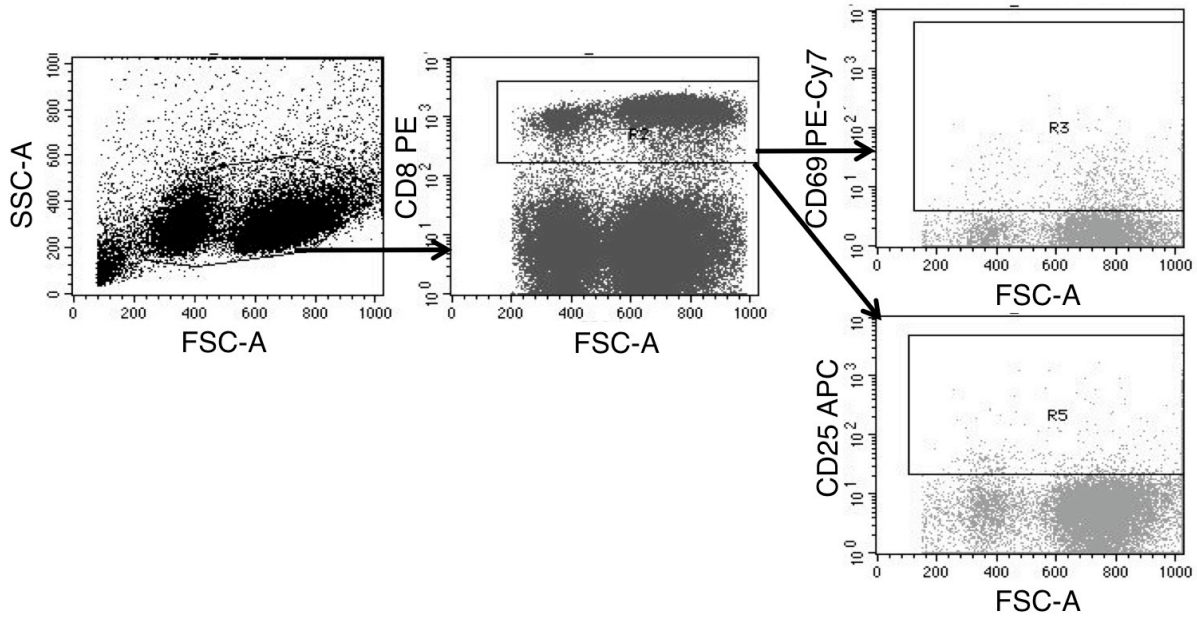

B

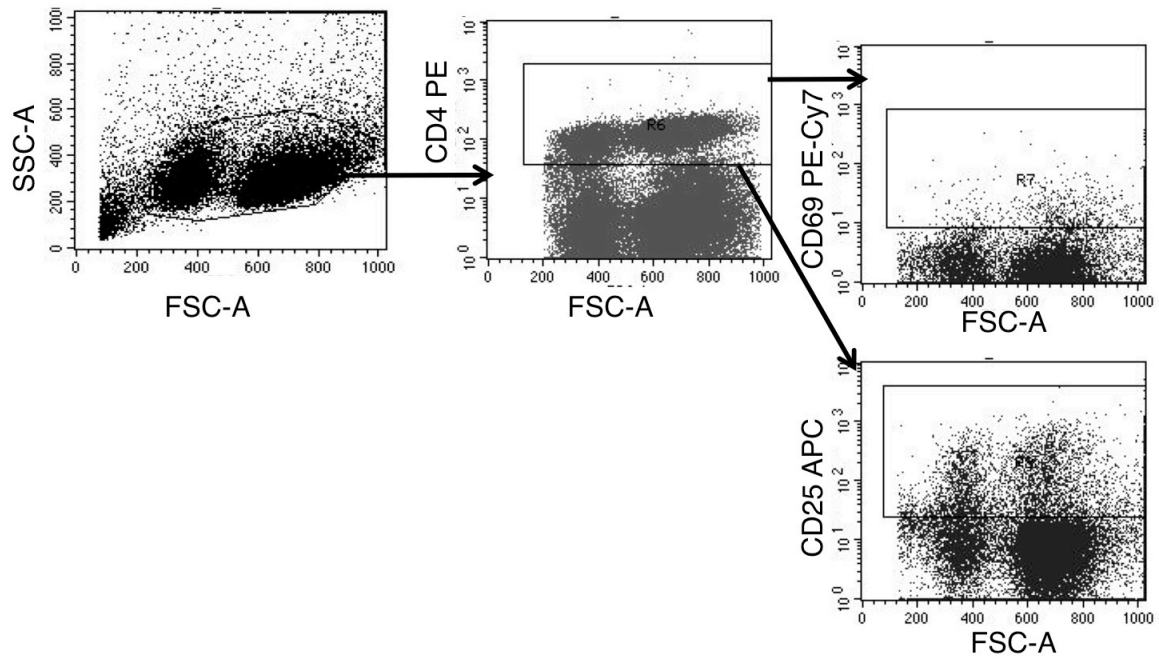

Appendix 7: Gating strategy for CD69$^+$ and CD25$^+$ CD4 and CD8 Lymphocytes Cells were stained for CD8 (A), CD4 (B), CD25 and CD69. Lymphocyte populations were gated in the FSC vs SSC scatter plot and FSC vs CD8 (A) or CD4 (B) was used to determine an accurate CD8 (A) and CD4 (B) positive cell populations. CD8 or CD4 cells were expression of CD25 or CD69 was determined, relative to a negative unstained control. Examples shown are uninfected controls.

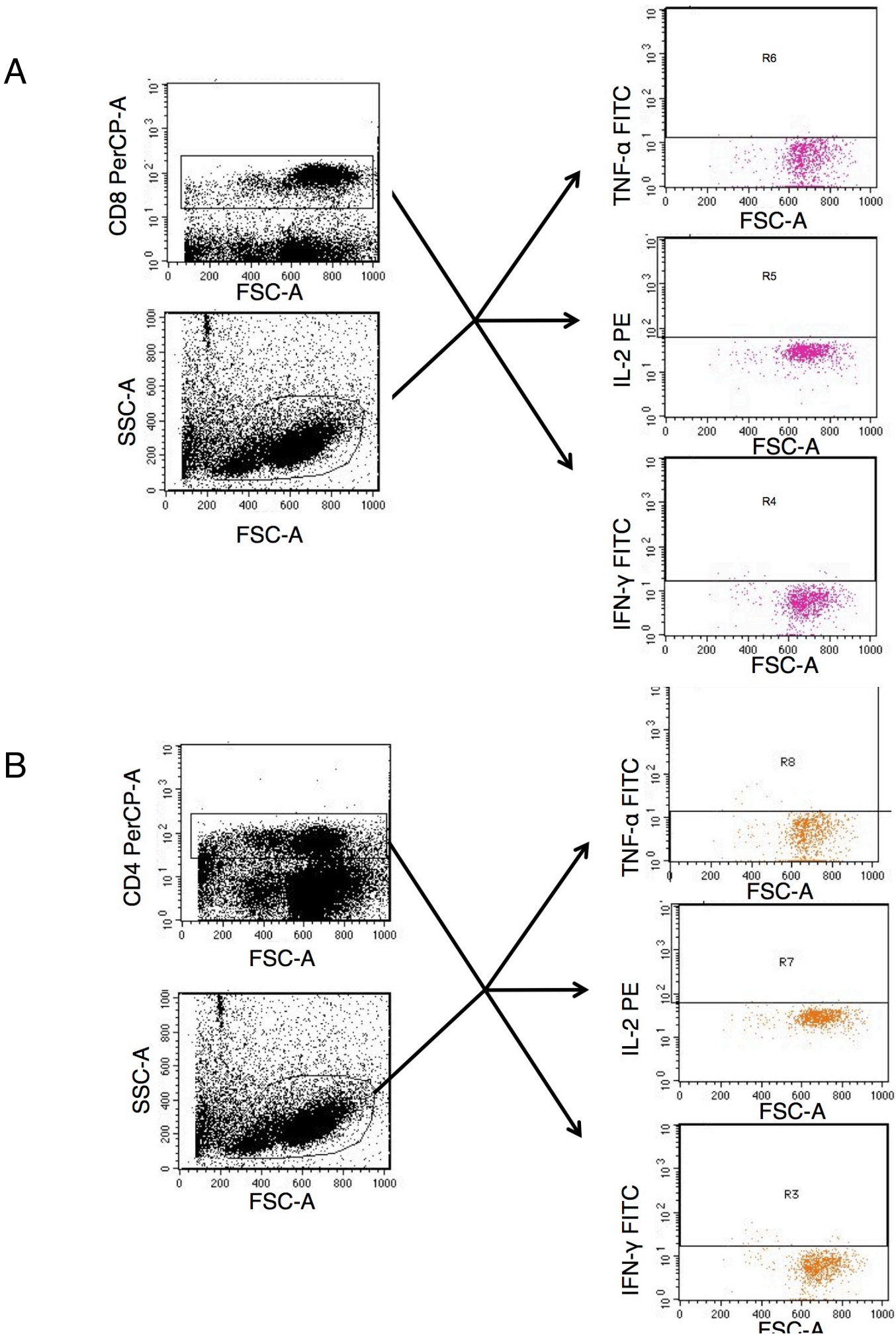
A
CD8 PerCP-A
FSC-A
SSC-A
FSC-A
TNF-α FITC
R6
FSC-A
IL-2 PE
R5
FSC-A
IFN-γ FITC
R4
FSC-A
B
CD4 PerCP-A
FSC-A
SSC-A
FSC-A
TNF-α FITC
R8
FSC-A
IL-2 PE
R7
FSC-A
IFN-γ FITC
R3
FSC-A

Appendix 8: Gating strategy for CD69+ and CD25+ CD4 and CD8 Lymphocytes Cells were stained for CD8 (A), CD4 (B), IL-2, IFN-γ and TNF-α. Lymphocyte populations were gated in the FSC vs SSC scatter plot and FSC vs CD8 (A) or CD4 (B) was used to to determine an accurate CD8 (A) and CD4 (B) positive cell populations. CD8 or CD4 cells were expression of IL-2, IFN-γ and TNF-α. was determined, relative to a negative unstained control. Examples shown are negative controls.

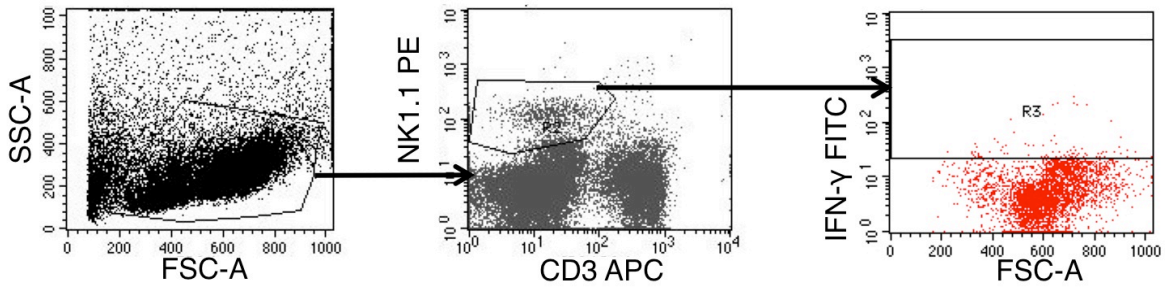

Appendix 9: Gating strategy for *ex vivo* NK and IFN-γ-producing NK cells. Cells were stained for NK1.1 and CD3. Lymphocyte populations were gated in the FSC vs. SSC scatter plot and CD3 vs NK1.1 was used to determine an accurate NK1.1 positive and CD3 negative cell population (NK cells, contrasted to NK1.1 positive and CD3 positive NKT cells). Gated cells were analysed for expression of IFN-γ relative to a negative unstained control. Example shown is from a negative control.

Chapter 6

References

1. Reiter, P., *From Shakespeare to Defoe: malaria in England in the Little Ice Age.* Emerg Infect Dis, 2000. **6**(1): p. 1-11.

2. Sallares, R., A. Bouwman, and C. Anderung, *The spread of malaria to Southern Europe in antiquity: new approaches to old problems.* Med Hist, 2004. **48**(3): p. 311-28.

3. Celsus, A.C., et al., *Aur. Corn. Celsi De medicina libri octo*, Amstelaedami,: Apud Joannem Wolters. [48], 574, [26] p.

4. Conway, D.J., et al., *Origin of Plasmodium falciparum malaria is traced by mitochondrial DNA.* Mol Biochem Parasitol, 2000. **111**(1): p. 163-71.

5. Harper, K. and G. Armelagos, *The changing disease-scape in the third epidemiological transition.* Int J Environ Res Public Health, 2010. **7**(2): p. 675-97.

6. Dobson, M.J., *Contours of death and disease in early modern England*1997, Cambridge: Cambridge University Press.

7. Hirayasu, K., et al., *Significant association of KIR2DL3-HLA-C1 combination with cerebral malaria and implications for co-evolution of KIR and HLA.* PLoS Pathog, 2012. **8**(3): p. e1002565.

8. Kwiatkowski, D.P., *How malaria has affected the human genome and what human genetics can teach us about malaria.* Am J Hum Genet, 2005. **77**(2): p. 171-92.

9. Laveran, A., *Nature parasitaire des accidents de l'impaludisme : description d'un nouveau parasite trouv©* dans le sang des malades atteints de fi© vre palustre*1881, Paris: J.-B. Bailli© re. 101 p., 2 leaves of plates.

10. Ross, R., *Observations on a Condition Necessary to the Transformation of the Malaria Crescent.* Br Med J, 1897. **1**(1883): p. 251-5.

11. Willcox, M.L. and G. Bodeker, *Traditional herbal medicines for malaria.* BMJ, 2004. **329**(7475): p. 1156-9.

12. Nerlich, A.G., et al., *Plasmodium falciparum in ancient Egypt.* Emerg Infect Dis, 2008. **14**(8): p. 1317-9.

13. Sherman, I.W., *Malaria : parasite biology, pathogenesis, and protection*1998, Washington, D.C.: ASM Press.

14. Rosenthal, P.J., *Antimalarial chemotherapy : mechanisms of action, resistance, and new directions in drug discovery*2001, Totowa, N.Y.: Humana Press.

15. Achan, J., et al., *Quinine, an old anti-malarial drug in a modern world: role in the treatment of malaria.* Malar J, 2011. **10**: p. 144.

16. Sinclair, D., S. Donegan, and D.G. Lalloo, *Artesunate versus quinine for treating severe malaria.* Cochrane Database Syst Rev, 2011(3): p. CD005967.

17. Boyd, M.F., *Malariology : a comprehensive survey of all aspects of this group of diseases from a global standpoint*1949, Philadelphia ; London: W.B. Saunders Co.

18. Wongsrichanalai, C., et al., *Epidemiology of drug-resistant malaria.* Lancet Infect Dis, 2002. **2**(4): p. 209-18.

19. Walther, B. and M. Walther, *What does it take to control malaria?* Ann Trop Med Parasitol, 2007. **101**(8): p. 657-72.

20. Murray, C.J., et al., *Global malaria mortality between 1980 and 2010: a systematic analysis.* Lancet, 2012. **379**(9814): p. 413-31.

21. Carter, R. and K.N. Mendis, *Evolutionary and historical aspects of the burden of malaria.* Clin Microbiol Rev, 2002. **15**(4): p. 564-94.

22. Breman, J.G., M.S. Alilio, and A. Mills, *Conquering the intolerable burden of malaria: what's new, what's needed: a summary.* Am J Trop Med Hyg, 2004. **71**(2 Suppl): p. 1-15.

23. Lewis, M., *Malaria: connecting reality with research.* Eur J Immunol, 2011. **41**(4): p. 882-4.

24. Mendis, K., et al., *From malaria control to eradication: The WHO perspective.* Trop Med Int Health, 2009. **14**(7): p. 802-9.

25. Greenwood, B.M., et al., *Malaria.* Lancet, 2005. **365**(9469): p. 1487-98.

26. Lin, J.T., J.J. Juliano, and C. Wongsrichanalai, *Drug-Resistant Malaria: The Era of ACT.* Curr Infect Dis Rep, 2010. **12**(3): p. 165-73.

27. Brown, A.W., *The insecticide-resistance problem: a review of developments in 1956 and 1957.* Bull World Health Organ, 1958. **18**(3): p. 309-21.

28. Hamon, J., et al., *[Presence in the southwestern part of Upper Volta of a population of Anopheles gambiae "A" resistant to DDT].* Med Trop (Mars), 1968. **28**(4): p. 521-8.

29. Enayati, A. and J. Hemingway, *Malaria management: past, present, and future.* Annu Rev Entomol, 2010. **55**: p. 569-91.

30. Beare, N.A., et al., *Malarial retinopathy: a newly established diagnostic sign in severe malaria.* Am J Trop Med Hyg, 2006. **75**(5): p. 790-7.

31. Trampuz, A., et al., *Clinical review: Severe malaria.* Crit Care, 2003. **7**(4): p. 315-23.

32. Amino, R., et al., *Host cell traversal is important for progression of the malaria parasite through the dermis to the liver.* Cell Host Microbe, 2008. **3**(2): p. 88-96.

33. Hafalla, J.C., O. Silvie, and K. Matuschewski, *Cell biology and immunology of malaria.* Immunol Rev, 2011. **240**(1): p. 297-316.

34. Frevert, U., et al., *Nomadic or sessile: can Kupffer cells function as portals for malaria sporozoites to the liver?* Cell Microbiol, 2006. **8**(10): p. 1537-46.

35. Frevert, U., et al., *Plasmodium sporozoite passage across the sinusoidal cell layer.* Subcell Biochem, 2008. **47**: p. 182-97.

36. Pradel, G. and U. Frevert, *Malaria sporozoites actively enter and pass through rat Kupffer cells prior to hepatocyte invasion.* Hepatology, 2001. **33**(5): p. 1154-65.

37. Baer, K., et al., *Kupffer cells are obligatory for Plasmodium yoelii sporozoite infection of the liver.* Cell Microbiol, 2007. **9**(2): p. 397-412.

38. Mota, M.M., et al., *Migration of Plasmodium sporozoites through cells before infection.* Science, 2001. **291**(5501): p. 141-4.

39. Frevert, U., et al., *Intravital observation of Plasmodium berghei sporozoite infection of the liver.* PLoS Biol, 2005. **3**(6): p. e192.

40. Frevert, U. and E. Nardin, *Cellular effector mechanisms against Plasmodium liver stages.* Cell Microbiol, 2008. **10**(10): p. 1956-67.

41. Bano, N., et al., *Cellular interactions of Plasmodium liver stage with its host mammalian cell.* Int J Parasitol, 2007. **37**(12): p. 1329-41.

42. Gething, P.W., et al., *A new world malaria map: Plasmodium falciparum endemicity in 2010.* Malar J, 2011. **10**: p. 378.

43. Silvie, O., et al., *Hepatocyte CD81 is required for Plasmodium falciparum and Plasmodium yoelii sporozoite infectivity.* Nat Med, 2003. **9**(1): p. 93-6.

44. Silvie, O., et al., *Alternative invasion pathways for Plasmodium berghei sporozoites.* Int J Parasitol, 2007. **37**(2): p. 173-82.

45. Rodrigues, C.D., et al., *Host scavenger receptor SR-BI plays a dual role in the establishment of malaria parasite liver infection.* Cell Host Microbe, 2008. **4**(3): p. 271-82.

46. Yalaoui, S., et al., *Scavenger receptor BI boosts hepatocyte permissiveness to Plasmodium infection.* Cell Host Microbe, 2008. **4**(3): p. 283-92.

47. Sultan, A.A., et al., *TRAP is necessary for gliding motility and infectivity of plasmodium sporozoites.* Cell, 1997. **90**(3): p. 511-22.

48. Kappe, S., et al., *Conservation of a gliding motility and cell invasion machinery in Apicomplexan parasites.* J Cell Biol, 1999. **147**(5): p. 937-44.

49. Silvie, O., et al., *Interactions of the malaria parasite and its mammalian host.* Curr Opin Microbiol, 2008. **11**(4): p. 352-9.

50. Sturm, A., et al., *Manipulation of host hepatocytes by the malaria parasite for delivery into liver sinusoids.* Science, 2006. **313**(5791): p. 1287-90.

51. Tarun, A.S., et al., *Quantitative isolation and in vivo imaging of malaria parasite liver stages.* Int J Parasitol, 2006. **36**(12): p. 1283-93.

52. Baer, K., et al., *Release of hepatic Plasmodium yoelii merozoites into the pulmonary microvasculature.* PLoS Pathog, 2007. **3**(11): p. e171.

53. Miller, L.H., et al., *Evidence for differences in erythrocyte surface receptors for the malarial parasites, Plasmodium falciparum and Plasmodium knowlesi.* J Exp Med, 1977. **146**(1): p. 277-81.

54. Deas, J.E. and L.T. Lee, *Competitive inhibition by soluble erythrocyte glycoproteins of penetration by Plasmodium falciparum.* Am J Trop Med Hyg, 1981. **30**(6): p. 1164-7.

55. Perkins, M., *Inhibitory effects of erythrocyte membrane proteins on the in vitro invasion of the human malarial parasite (Plasmodium falciparum) into its host cell.* J Cell Biol, 1981. **90**(3): p. 563-7.

56. Pasvol, G., et al., *Glycophorin as a possible receptor for Plasmodium falciparum.* Lancet, 1982. **2**(8305): p. 947-50.

57. Iyer, J., et al., *Invasion of host cells by malaria parasites: a tale of two protein families.* Mol Microbiol, 2007. **65**(2): p. 231-49.

58. Deharo, E., et al., *The erythrocytic schizogony of two synchronized strains of plasmodium berghei, NK65 and ANKA, in normocytes and reticulocytes.* Parasitol Res, 1996. **82**(2): p. 178-82.

59. Holder, A.A. and R.R. Freeman, *Biosynthesis and processing of a Plasmodium falciparum schizont antigen recognized by immune serum and a monoclonal antibody.* J Exp Med, 1982. **156**(5): p. 1528-38.

60. Mitchell, G.H., et al., *Apical membrane antigen 1, a major malaria vaccine candidate, mediates the close attachment of invasive merozoites to host red blood cells.* Infect Immun, 2004. **72**(1): p. 154-8.

61. Lingelbach, K. and K.A. Joiner, *The parasitophorous vacuole membrane surrounding Plasmodium and Toxoplasma: an unusual compartment in infected cells.* J Cell Sci, 1998. **111 (Pt 11)**: p. 1467-75.

62. Lal, A.A., et al., *Anti-mosquito midgut antibodies block development of Plasmodium falciparum and Plasmodium vivax in multiple species of Anopheles mosquitoes and reduce vector fecundity and survivorship.* Proc Natl Acad Sci U S A, 2001. **98**(9): p. 5228-33.

63. Klein, I. and I.N. Crispe, *Complete differentiation of CD8+ T cells activated locally within the transplanted liver.* J Exp Med, 2006. **203**(2): p. 437-47.

64. Winau, F., et al., *Ito cells are liver-resident antigen-presenting cells for activating T cell responses.* Immunity, 2007. **26**(1): p. 117-29.

65. Knolle, P.A. and G. Gerken, *Local control of the immune response in the liver.* Immunol Rev, 2000. **174**: p. 21-34.

66. Crispe, I.N., *Hepatic T cells and liver tolerance.* Nat Rev Immunol, 2003. **3**(1): p. 51-62.

67. Hugel, F.U., G. Pradel, and U. Frevert, *Release of malaria circumsporozoite protein into the host cell cytoplasm and interaction with ribosomes.* Mol Biochem Parasitol, 1996. **81**(2): p. 151-70.

68. Atkinson, C.T., et al., *Expression of Plasmodium berghei circumsporozoite antigen on the surface of exoerythrocytic schizonts and merozoites.* Am J Trop Med Hyg, 1989. **41**(1): p. 9-17.

69. Plebanski, M., et al., *Direct processing and presentation of antigen from malaria sporozoites by professional antigen-presenting cells in the induction of CD8 T-cell responses.* Immunol Cell Biol, 2005. **83**(3): p. 307-12.

70. Fauve, R.M., H. Jusforgues, and B. Hevin, *Maintenance of granuloma macrophages in serum-free medium.* J Immunol Methods, 1983. **64**(3): p. 345-51.

71. Marsh, K. and S. Kinyanjui, *Immune effector mechanisms in malaria.* Parasite Immunol, 2006. **28**(1-2): p. 51-60.

72. Crompton, P.D., et al., *A prospective analysis of the Ab response to Plasmodium falciparum before and after a malaria season by protein microarray*. Proc Natl Acad Sci U S A, 2010. **107**(15): p. 6958-63.

73. Bate, C.A., J. Taverne, and J.H. Playfair, *Malarial parasites induce TNF production by macrophages*. Immunology, 1988. **64**(2): p. 227-31.

74. Miller, L.H., M.F. Good, and G. Milon, *Malaria pathogenesis*. Science, 1994. **264**(5167): p. 1878-83.

75. Medzhitov, R. and C.A. Janeway, Jr., *Innate immunity: the virtues of a nonclonal system of recognition*. Cell, 1997. **91**(3): p. 295-8.

76. Pichyangkul, S., et al., *Malaria blood stage parasites activate human plasmacytoid dendritic cells and murine dendritic cells through a Toll-like receptor 9-dependent pathway*. J Immunol, 2004. **172**(8): p. 4926-33.

77. Krishnegowda, G., et al., *Induction of proinflammatory responses in macrophages by the glycosylphosphatidylinositols of Plasmodium falciparum: cell signaling receptors, glycosylphosphatidylinositol (GPI) structural requirement, and regulation of GPI activity*. J Biol Chem, 2005. **280**(9): p. 8606-16.

78. Coban, C., et al., *Toll-like receptor 9 mediates innate immune activation by the malaria pigment hemozoin*. J Exp Med, 2005. **201**(1): p. 19-25.

79. Artavanis-Tsakonas, K. and E.M. Riley, *Innate immune response to malaria: rapid induction of IFN-gamma from human NK cells by live Plasmodium falciparum-infected erythrocytes*. J Immunol, 2002. **169**(6): p. 2956-63.

80. Stevenson, M.M. and E.M. Riley, *Innate immunity to malaria*. Nat Rev Immunol, 2004. **4**(3): p. 169-80.

81. Riley, E.M., et al., *Regulating immunity to malaria.* Parasite Immunol, 2006. **28**(1-2): p. 35-49.

82. Walther, M., et al., *Upregulation of TGF-beta, FOXP3, and CD4+CD25+ regulatory T cells correlates with more rapid parasite growth in human malaria infection.* Immunity, 2005. **23**(3): p. 287-96.

83. Walther, M., et al., *Distinct roles for FOXP3 and FOXP3 CD4 T cells in regulating cellular immunity to uncomplicated and severe Plasmodium falciparum malaria.* PLoS Pathog, 2009. **5**(4): p. e1000364.

84. Wipasa, J., et al., *Long-lived antibody and B Cell memory responses to the human malaria parasites, Plasmodium falciparum and Plasmodium vivax.* PLoS Pathog, 2010. **6**(2): p. e1000770.

85. Doolan, D.L., et al., *Identification of Plasmodium falciparum antigens by antigenic analysis of genomic and proteomic data.* Proc Natl Acad Sci U S A, 2003. **100**(17): p. 9952-7.

86. Bouharoun-Tayoun, H. and P. Druilhe, *Antibodies in falciparum malaria: what matters most, quantity or quality?* Mem Inst Oswaldo Cruz, 1992. **87 Suppl 3**: p. 229-34.

87. Bouharoun-Tayoun, H. and P. Druilhe, *Plasmodium falciparum malaria: evidence for an isotype imbalance which may be responsible for delayed acquisition of protective immunity.* Infect Immun, 1992. **60**(4): p. 1473-81.

88. Oeuvray, C., et al., *Cytophilic immunoglobulin responses to Plasmodium falciparum glutamate-rich protein are correlated with protection against clinical malaria in Dielmo, Senegal.* Infect Immun, 2000. **68**(5): p. 2617-20.

89. Drakeley, C.J., et al., *Estimating medium- and long-term trends in malaria transmission by using serological markers of malaria exposure.* Proc Natl Acad Sci U S A, 2005. **102**(14): p. 5108-13.

90. Weiss, G.E., et al., *Atypical memory B cells are greatly expanded in individuals living in a malaria-endemic area.* J Immunol, 2009. **183**(3): p. 2176-82.

91. Asito, A.S., et al., *Alterations on peripheral B cell subsets following an acute uncomplicated clinical malaria infection in children.* Malar J, 2008. **7**: p. 238.

92. Belnoue, E., et al., *Protective T cell immunity against malaria liver stage after vaccination with live sporozoites under chloroquine treatment.* J Immunol, 2004. **172**(4): p. 2487-95.

93. Mueller, A.K., et al., *Genetically modified Plasmodium parasites as a protective experimental malaria vaccine.* Nature, 2005. **433**(7022): p. 164-7.

94. Nussenzweig, R.S., et al., *Protective immunity produced by the injection of x-irradiated sporozoites of plasmodium berghei.* Nature, 1967. **216**(5111): p. 160-2.

95. Hoffman, S.L., et al., *Protection of humans against malaria by immunization with radiation-attenuated Plasmodium falciparum sporozoites.* J Infect Dis, 2002. **185**(8): p. 1155-64.

96. Nganou-Makamdop, K., et al., *Long term protection after immunization with P. berghei sporozoites correlates with sustained IFNgamma responses of hepatic CD8+ memory T cells.* PLoS One, 2012. **7**(5): p. e36508.

97. Mueller, A.K., et al., *Genetically attenuated Plasmodium berghei liver stages persist and elicit sterile protection primarily via CD8 T cells.* Am J Pathol, 2007. **171**(1): p. 107-15.

98. Schofield, L., et al., *Gamma interferon, CD8+ T cells and antibodies required for immunity to malaria sporozoites.* Nature, 1987. **330**(6149): p. 664-6.

99. Weiss, W.R., et al., *CD8+ T cells (cytotoxic/suppressors) are required for protection in mice immunized with malaria sporozoites.* Proc Natl Acad Sci U S A, 1988. **85**(2): p. 573-6.

100. Hafalla, J.C., I.A. Cockburn, and F. Zavala, *Protective and pathogenic roles of CD8+ T cells during malaria infection.* Parasite Immunol, 2006. **28**(1-2): p. 15-24.

101. Ferreira, A., et al., *Inhibition of development of exoerythrocytic forms of malaria parasites by gamma-interferon.* Science, 1986. **232**(4752): p. 881-4.

102. Nardin, E., et al., *Pre-erythrocytic malaria vaccine: mechanisms of protective immunity and human vaccine trials.* Parassitologia, 1999. **41**(1-3): p. 397-402.

103. Tsuji, M. and F. Zavala, *T cells as mediators of protective immunity against liver stages of Plasmodium.* Trends Parasitol, 2003. **19**(2): p. 88-93.

104. Oliveira, G.A., et al., *Class II-restricted protective immunity induced by malaria sporozoites.* Infect Immun, 2008. **76**(3): p. 1200-6.

105. Yazdani, S.S., et al., *Immune responses to asexual blood-stages of malaria parasites.* Curr Mol Med, 2006. **6**(2): p. 187-203.

106. Doolan, D.L. and S.L. Hoffman, *The complexity of protective immunity against liver-stage malaria.* J Immunol, 2000. **165**(3): p. 1453-62.

107. Doolan, D.L. and S.L. Hoffman, *IL-12 and NK cells are required for antigen-specific adaptive immunity against malaria initiated by CD8+ T cells in the Plasmodium yoelii model.* J Immunol, 1999. **163**(2): p. 884-92.

108. Mueller, A.K., et al., *Plasmodium liver stage developmental arrest by depletion of a protein at the parasite-host interface.* Proc Natl Acad Sci U S A, 2005. **102**(8): p. 3022-7.

109. van Dijk, M.R., et al., *Genetically attenuated, P36p-deficient malarial sporozoites induce protective immunity and apoptosis of infected liver cells.* Proc Natl Acad Sci U S A, 2005. **102**(34): p. 12194-9.

110. Jobe, O., et al., *Genetically attenuated Plasmodium berghei liver stages induce sterile protracted protection that is mediated by major histocompatibility complex Class I-dependent interferon-gamma-producing CD8+ T cells.* J Infect Dis, 2007. **196**(4): p. 599-607.

111. Tarun, A.S., et al., *Protracted sterile protection with Plasmodium yoelii pre-erythrocytic genetically attenuated parasite malaria vaccines is independent of significant liver-stage persistence and is mediated by CD8+ T cells.* J Infect Dis, 2007. **196**(4): p. 608-16.

112. Labaied, M., et al., *Plasmodium yoelii sporozoites with simultaneous deletion of P52 and P36 are completely attenuated and confer sterile immunity against infection.* Infect Immun, 2007. **75**(8): p. 3758-68.

113. Kumar, K.A., et al., *Conserved protective mechanisms in radiation and genetically attenuated uis3(-) and uis4(-) Plasmodium sporozoites.* PLoS One, 2009. **4**(2): p. e4480.

114. van Schaijk, B.C., et al., *Gene disruption of Plasmodium falciparum p52 results in attenuation of malaria liver stage development in cultured primary human hepatocytes.* PLoS One, 2008. **3**(10): p. e3549.

115. VanBuskirk, K.M., et al., *Preerythrocytic, live-attenuated Plasmodium falciparum vaccine candidates by design.* Proc Natl Acad Sci U S A, 2009. **106**(31): p. 13004-9.

116. Yayon, A., Z.I. Cabantchik, and H. Ginsburg, *Susceptibility of human malaria parasites to chloroquine is pH dependent.* Proc Natl Acad Sci U S A, 1985. **82**(9): p. 2784-8.

117. Putrianti, E.D., et al., *Vaccine-like immunity against malaria by repeated causal-prophylactic treatment of liver-stage Plasmodium parasites.* J Infect Dis, 2009. **199**(6): p. 899-903.

118. Roestenberg, M., et al., *Protection against a malaria challenge by sporozoite inoculation.* N Engl J Med, 2009. **361**(5): p. 468-77.

119. Bijker, E.M., et al., *Protection against malaria after immunization by chloroquine prophylaxis and sporozoites is mediated by preerythrocytic immunity.* Proceedings of the National Academy of Sciences of the United States of America, 2013. **110**(19): p. 7862-7.

120. Mikolajczak, S.A., et al., *A genetically attenuated parasite vaccine does not require liver stage persistence to elicit sterile protective immunity against sporozoite-induced malaria in mice.* J Infect Dis, 2010. **201**(8): p. 1270-1; author reply 1271-2.

121. Friesen, J., et al., *Natural immunization against malaria: causal prophylaxis with antibiotics.* Sci Transl Med, 2010. **2**(40): p. 40ra49.

122. Genton, B., et al., *A recombinant blood-stage malaria vaccine reduces Plasmodium falciparum density and exerts selective pressure on parasite populations in a phase 1-2b trial in Papua New Guinea.* J Infect Dis, 2002. **185**(6): p. 820-7.

123. Pombo, D.J., et al., *Immunity to malaria after administration of ultra-low doses of red cells infected with Plasmodium falciparum.* Lancet, 2002. **360**(9333): p. 610-7.

124. Quelhas, D., et al., *Impact of intermittent preventive treatment with sulfadoxine-pyrimethamine on antibody responses to erythrocytic-stage Plasmodium falciparum antigens in infants in Mozambique.* Clin Vaccine Immunol, 2008. **15**(8): p. 1282-91.

125. Sutherland, C.J., C.J. Drakeley, and D. Schellenberg, *How is childhood development of immunity to Plasmodium falciparum enhanced by certain antimalarial interventions?* Malar J, 2007. **6**: p. 161.

126. Bignami, A., J. Mannaberg, and E. Marchiafava, *Two monographs on malaria and the parasites of malarial fevers. I. Marchiafava and Bignami. II. Mannaberg.* New Sydenham Society (Series)1894, London,. xxvi, 428 p.

127. Carter, J.A., et al., *Developmental impairments following severe falciparum malaria in children.* Trop Med Int Health, 2005. **10**(1): p. 3-10.

128. Idro, R., N.E. Jenkins, and C.R. Newton, *Pathogenesis, clinical features, and neurological outcome of cerebral malaria.* Lancet Neurol, 2005. **4**(12): p. 827-40.

129. Boivin, M.J., et al., *Cognitive impairment after cerebral malaria in children: a prospective study.* Pediatrics, 2007. **119**(2): p. e360-6.

130. Dondorp, A., et al., *Artesunate versus quinine for treatment of severe falciparum malaria: a randomised trial.* Lancet, 2005. **366**(9487): p. 717-25.

131. Haldar, K., et al., *Malaria: mechanisms of erythrocytic infection and pathological correlates of severe disease.* Annu Rev Pathol, 2007. **2**: p. 217-49.

132. Patnaik, J.K., et al., *Vascular clogging, mononuclear cell margination, and enhanced vascular permeability in the pathogenesis of human cerebral malaria.* Am J Trop Med Hyg, 1994. **51**(5): p. 642-7.

133. de Souza, J.B., et al., *Cerebral malaria: why experimental murine models are required to understand the pathogenesis of disease.* Parasitology, 2010. **137**(5): p. 755-72.

134. Clark, I.A., et al., *Tissue distribution of migration inhibitory factor and inducible nitric oxide synthase in falciparum malaria and sepsis in African children.* Malar J, 2003. **2**: p. 6.

135. Taylor, T.E., et al., *Differentiating the pathologies of cerebral malaria by postmortem parasite counts.* Nat Med, 2004. **10**(2): p. 143-5.

136. Mishra, S.K. and L. Wiese, *Advances in the management of cerebral malaria in adults.* Curr Opin Neurol, 2009. **22**(3): p. 302-7.

137. Artavanis-Tsakonas, K., J.E. Tongren, and E.M. Riley, *The war between the malaria parasite and the immune system: immunity, immunoregulation and immunopathology.* Clin Exp Immunol, 2003. **133**(2): p. 145-52.

138. Kampfl, A.W., et al., *Isolated pontine lesion in algid cerebral malaria: clinical features, management, and magnetic resonance imaging findings.* Am J Trop Med Hyg, 1993. **48**(6): p. 818-22.

139. Crawley, J., et al., *Seizures and status epilepticus in childhood cerebral malaria.* QJM, 1996. **89**(8): p. 591-7.

140. Patankar, T.F., et al., *Adult cerebral malaria: prognostic importance of imaging findings and correlation with postmortem findings.* Radiology, 2002. **224**(3): p. 811-6.

141. Penet, M.F., et al., *Imaging experimental cerebral malaria in vivo: significant role of ischemic brain edema.* J Neurosci, 2005. **25**(32): p. 7352-8.

142. Penet, M.F., et al., *Magnetic resonance spectroscopy reveals an impaired brain metabolic profile in mice resistant to cerebral malaria infected with Plasmodium berghei ANKA.* J Biol Chem, 2007. **282**(19): p. 14505-14.

143. Gysin, J., et al., *Experimental Plasmodium falciparum cerebral malaria in the squirrel monkey Saimiri sciureus.* Exp Parasitol, 1992. **75**(4): p. 390-8.

144. Aikawa, M., et al., *A primate model for human cerebral malaria: Plasmodium coatneyi-infected rhesus monkeys.* Am J Trop Med Hyg, 1992. **46**(4): p. 391-7.

145. Ibiwoye, M.O., et al., *Cerebral malaria in the rhesus monkey (Macaca mulatta): observations on host pathology.* J Comp Pathol, 1993. **108**(3): p. 303-10.

146. Yoeli, M. and B.J. Hargreaves, *Brain capillary blockage produced by a virulent strain of rodent malaria.* Science, 1974. **184**(4136): p. 572-3.

147. Rest, J.R., *Cerebral malaria in inbred mice. I. A new model and its pathology.* Trans R Soc Trop Med Hyg, 1982. **76**(3): p. 410-5.

148. Curfs, J.H., et al., *Plasmodium berghei: recombinant interferon-gamma and the development of parasitemia and cerebral lesions in malaria-infected mice.* Exp Parasitol, 1993. **77**(2): p. 212-23.

149. de Souza, J.B. and E.M. Riley, *Cerebral malaria: the contribution of studies in animal models to our understanding of immunopathogenesis.* Microbes Infect, 2002. **4**(3): p. 291-300.

150. Carroll, R.W., et al., *A rapid murine coma and behavior scale for quantitative assessment of murine cerebral malaria.* PLoS One, 2010. **5**(10).

151. Lackner, P., et al., *Behavioural and histopathological alterations in mice with cerebral malaria.* Neuropathol Appl Neurobiol, 2006. **32**(2): p. 177-88.

152. Clark, C.J., et al., *Differences in the neurochemical characteristics of the cortex and striatum of mice with cerebral malaria.* Parasitology, 2005. **130**(Pt 1): p. 23-9.

153. Engwerda, C.R., et al., *Locally up-regulated lymphotoxin alpha, not systemic tumor necrosis factor alpha, is the principle mediator of murine cerebral malaria.* J Exp Med, 2002. **195**(10): p. 1371-7.

154. Hearn, J., et al., *Immunopathology of cerebral malaria: morphological evidence of parasite sequestration in murine brain microvasculature.* Infect Immun, 2000. **68**(9): p. 5364-76.

155. Wassmer, S.C., V. Combes, and G.E. Grau, *Pathophysiology of cerebral malaria: role of host cells in the modulation of cytoadhesion.* Ann N Y Acad Sci, 2003. **992**: p. 30-8.

156. von Zur Muhlen, C., et al., *A contrast agent recognizing activated platelets reveals murine cerebral malaria pathology undetectable by conventional MRI.* J Clin Invest, 2008. **118**(3): p. 1198-207.

157. Wassmer, S.C., et al., *TGF-beta1 released from activated platelets can induce TNF-stimulated human brain endothelium apoptosis: a new mechanism for microvascular lesion during cerebral malaria.* J Immunol, 2006. **176**(2): p. 1180-4.

158. Desruisseaux, M.S., et al., *Cognitive dysfunction in mice infected with Plasmodium berghei strain ANKA.* J Infect Dis, 2008. **197**(11): p. 1621-7.

159. Nacer, A., et al., *Neuroimmunological blood brain barrier opening in experimental cerebral malaria.* PLoS Pathog, 2012. **8**(10): p. e1002982.

160. Bagot, S., et al., *Identification of two cerebral malaria resistance loci using an inbred wild-derived mouse strain.* Proc Natl Acad Sci U S A, 2002. **99**(15): p. 9919-23.

161. Nagayasu, E., et al., *Association of a determinant on mouse chromosome 18 with experimental severe Plasmodium berghei malaria.* Infect Immun, 2002. **70**(2): p. 512-6.

162. Ohno, T. and M. Nishimura, *Detection of a new cerebral malaria susceptibility locus, using CBA mice.* Immunogenetics, 2004. **56**(9): p. 675-8.

163. Campino, S., et al., *Genetic control of parasite clearance leads to resistance to Plasmodium berghei ANKA infection and confers immunity.* Genes Immun, 2005. **6**(5): p. 416-21.

164. Delahaye, N.F., et al., *Gene expression analysis reveals early changes in several molecular pathways in cerebral malaria-susceptible mice versus cerebral malaria-resistant mice.* BMC Genomics, 2007. **8**: p. 452.

165. Lovegrove, F.E., et al., *Expression microarray analysis implicates apoptosis and interferon-responsive mechanisms in susceptibility to experimental cerebral malaria.* Am J Pathol, 2007. **171**(6): p. 1894-903.

166. El-Assaad, F., et al., *Differential microRNA expression in experimental cerebral and noncerebral malaria.* Infect Immun, 2011. **79**(6): p. 2379-84.

167. Craig, A.G., et al., *The role of animal models for research on severe malaria.* PLoS Pathog, 2012. **8**(2): p. e1002401.

168. White, N.J., et al., *The murine cerebral malaria phenomenon.* Trends Parasitol, 2010. **26**(1): p. 11-5.

169. Carvalho, L.J., *Murine cerebral malaria: how far from human cerebral malaria?* Trends Parasitol, 2010. **26**(6): p. 271-2.

170. Berendt, A.R., G.D. Tumer, and C.I. Newbold, *Cerebral malaria: the sequestration hypothesis.* Parasitol Today, 1994. **10**(10): p. 412-4.

171. Franke-Fayard, B., et al., *Murine malaria parasite sequestration: CD36 is the major receptor, but cerebral pathology is unlinked to sequestration.* Proc Natl Acad Sci U S A, 2005. **102**(32): p. 11468-73.

172. Baptista, F.G., et al., *Accumulation of Plasmodium berghei-infected red blood cells in the brain is crucial for the development of cerebral malaria in mice.* Infect Immun, 2010. **78**(9): p. 4033-9.

173. Jennings, V.M., A.A. Lal, and R.L. Hunter, *Evidence for multiple pathologic and protective mechanisms of murine cerebral malaria.* Infect Immun, 1998. **66**(12): p. 5972-9.

174. Randall, L.M., et al., *Common strategies to prevent and modulate experimental cerebral malaria in mouse strains with different susceptibilities.* Infect Immun, 2008. **76**(7): p. 3312-20.

175. Nie, C.Q., et al., *IP-10-mediated T cell homing promotes cerebral inflammation over splenic immunity to malaria infection.* PLoS Pathog, 2009. **5**(4): p. e1000369.

176. Clark, I.A., et al., *Possible roles of tumor necrosis factor in the pathology of malaria.* Am J Pathol, 1987. **129**(1): p. 192-9.

177. Thumwood, C.M., et al., *Breakdown of the blood-brain barrier in murine cerebral malaria.* Parasitology, 1988. **96 (Pt 3)**: p. 579-89.

178. Grau, G.E., et al., *TNF-induced microvascular pathology: active role for platelets and importance of the LFA-1/ICAM-1 interaction.* Eur Cytokine Netw, 1993. **4**(6): p. 415-9.

179. Lou, J., R. Lucas, and G.E. Grau, *Pathogenesis of cerebral malaria: recent experimental data and possible applications for humans.* Clin Microbiol Rev, 2001. **14**(4): p. 810-20, table of contents.

180. Combes, V., et al., *Pathogenic role of P-selectin in experimental cerebral malaria: importance of the endothelial compartment.* Am J Pathol, 2004. **164**(3): p. 781-6.

181. Renia, L., et al., *Pathogenic T cells in cerebral malaria.* Int J Parasitol, 2006. **36**(5): p. 547-54.

182. Amani, V., et al., *Involvement of IFN-gamma receptor-medicated signaling in pathology and anti-malarial immunity induced by Plasmodium berghei infection.* Eur J Immunol, 2000. **30**(6): p. 1646-55.

183. Togbe, D., et al., *Both functional LTbeta receptor and TNF receptor 2 are required for the development of experimental cerebral malaria.* PLoS One, 2008. **3**(7): p. e2608.

184. Kossodo, S., et al., *Interleukin-10 modulates susceptibility in experimental cerebral malaria.* Immunology, 1997. **91**(4): p. 536-40.

185. Amante, F.H., et al., *A role for natural regulatory T cells in the pathogenesis of experimental cerebral malaria.* Am J Pathol, 2007. **171**(2): p. 548-59.

186. Nie, C.Q., et al., *CD4+ CD25+ regulatory T cells suppress CD4+ T-cell function and inhibit the development of Plasmodium berghei-specific TH1 responses involved in cerebral malaria pathogenesis.* Infect Immun, 2007. **75**(5): p. 2275-82.

187. Saeftel, M., et al., *Mice deficient in interleukin-4 (IL-4) or IL-4 receptor alpha have higher resistance to sporozoite infection with Plasmodium berghei (ANKA) than do naive wild-type mice.* Infect Immun, 2004. **72**(1): p. 322-31.

188. Beeson, J.G., et al., *Parasite adhesion and immune evasion in placental malaria.* Trends Parasitol, 2001. **17**(7): p. 331-7.

189. Bauer, P.R., et al., *Regulation of endothelial cell adhesion molecule expression in an experimental model of cerebral malaria.* Microcirculation, 2002. **9**(6): p. 463-70.

190. Good, M.F., et al., *Development and regulation of cell-mediated immune responses to the blood stages of malaria: implications for vaccine research.* Annu Rev Immunol, 2005. **23**: p. 69-99.

191. Weiser, S., et al., *Interferon-gamma synergises with tumour necrosis factor and lymphotoxin-alpha to enhance the mRNA and protein expression of adhesion molecules in mouse brain endothelial cells.* Cytokine, 2007. **37**(1): p. 84-91.

192. Schofield, L. and G.E. Grau, *Immunological processes in malaria pathogenesis.* Nat Rev Immunol, 2005. **5**(9): p. 722-35.

193. Hanum, P.S., M. Hayano, and S. Kojima, *Cytokine and chemokine responses in a cerebral malaria-susceptible or -resistant strain of mice to Plasmodium berghei ANKA infection: early chemokine expression in the brain.* Int Immunol, 2003. **15**(5): p. 633-40.

194. Engwerda, C.R., L. Beattie, and F.H. Amante, *The importance of the spleen in malaria.* Trends Parasitol, 2005. **21**(2): p. 75-80.

195. Mebius, R.E. and G. Kraal, *Structure and function of the spleen.* Nat Rev Immunol, 2005. **5**(8): p. 606-16.

196. Piva, L., et al., *Cutting edge: Clec9A+ dendritic cells mediate the development of experimental cerebral malaria.* J Immunol, 2012. **189**(3): p. 1128-32.

197. den Haan, J.M., S.M. Lehar, and M.J. Bevan, *CD8(+) but not CD8(-) dendritic cells cross-prime cytotoxic T cells in vivo.* J Exp Med, 2000. **192**(12): p. 1685-96.

198. Medana, I.M., N.H. Hunt, and T. Chan-Ling, *Early activation of microglia in the pathogenesis of fatal murine cerebral malaria.* Glia, 1997. **19**(2): p. 91-103.

199. Pais, T.F. and S. Chatterjee, *Brain macrophage activation in murine cerebral malaria precedes accumulation of leukocytes and CD8+ T cell proliferation.* J Neuroimmunol, 2005. **163**(1-2): p. 73-83.

200. Grau, G.E., et al., *Tumor necrosis factor (cachectin) as an essential mediator in murine cerebral malaria.* Science, 1987. **237**(4819): p. 1210-2.

201. Belnoue, E., et al., *Chemokine receptor CCR2 is not essential for the development of experimental cerebral malaria.* Infect Immun, 2003. **71**(6): p. 3648-51.

202. Belnoue, E., et al., *CCR5 deficiency decreases susceptibility to experimental cerebral malaria.* Blood, 2003. **101**(11): p. 4253-9.

203. Nitcheu, J., et al., *Perforin-dependent brain-infiltrating cytotoxic CD8+ T lymphocytes mediate experimental cerebral malaria pathogenesis.* J Immunol, 2003. **170**(4): p. 2221-8.

204. Toro, G. and G. Roman, *Cerebral malaria. A disseminated vasculomyelinopathy.* Arch Neurol, 1978. **35**(5): p. 271-5.

205. Sedgwick, J.D., et al., *Tumor necrosis factor: a master-regulator of leukocyte movement.* Immunol Today, 2000. **21**(3): p. 110-3.

206. Favre, N., et al., *Role of ICAM-1 (CD54) in the development of murine cerebral malaria.* Microbes Infect, 1999. **1**(12): p. 961-8.

207. Bachmann, M.F., et al., *Cutting edge: distinct roles for T help and CD40/CD40 ligand in regulating differentiation of proliferation-competent memory CD8+ T cells.* J Immunol, 2004. **173**(4): p. 2217-21.

208. Hansen, D.S., et al., *NK cells stimulate recruitment of CXCR3+ T cells to the brain during Plasmodium berghei-mediated cerebral malaria.* J Immunol, 2007. **178**(9): p. 5779-88.

209. Lundie, R.J., et al., *Blood-stage Plasmodium infection induces CD8+ T lymphocytes to parasite-expressed antigens, largely regulated by CD8alpha+ dendritic cells.* Proc Natl Acad Sci U S A, 2008. **105**(38): p. 14509-14.

210. Miyakoda, M., et al., *Malaria-specific and nonspecific activation of CD8+ T cells during blood stage of Plasmodium berghei infection.* J Immunol, 2008. **181**(2): p. 1420-8.

211. deWalick, S., et al., *Cutting edge: conventional dendritic cells are the critical APC required for the induction of experimental cerebral malaria.* J Immunol, 2007. **178**(10): p. 6033-7.

212. Belnoue, E., et al., *Control of pathogenic CD8+ T cell migration to the brain by IFN-gamma during experimental cerebral malaria.* Parasite Immunol, 2008. **30**(10): p. 544-53.

213. Bagot, S., et al., *Comparative study of brain CD8+ T cells induced by sporozoites and those induced by blood-stage Plasmodium berghei ANKA involved in the development of cerebral malaria.* Infect Immun, 2004. **72**(5): p. 2817-26.

214. Pober, J. and R.S. Cotran, *What can be learned from the expression of endothelial adhesion molecules in tissues?* Lab Invest, 1991. **64**(3): p. 301-5.

215. Monso-Hinard, C., et al., *Expression of major histocompatibility complex antigens on mouse brain microvascular endothelial cells in relation to susceptibility to cerebral malaria.* Immunology, 1997. **92**(1): p. 53-9.

216. Potter, S., et al., *Fas and perforin contribute to the pathogenesis of murine cerebral malaria.* Redox Rep, 1999. **4**(6): p. 333-5.

217. Belnoue, E., et al., *On the pathogenic role of brain-sequestered alphabeta CD8+ T cells in experimental cerebral malaria.* J Immunol, 2002. **169**(11): p. 6369-75.

218. Yanez, D.M., et al., *Participation of lymphocyte subpopulations in the pathogenesis of experimental murine cerebral malaria.* J Immunol, 1996. **157**(4): p. 1620-4.

219. Hermsen, C., et al., *Depletion of CD4+ or CD8+ T-cells prevents Plasmodium berghei induced cerebral malaria in end-stage disease.* Parasitology, 1997. **114 (Pt 1)**: p. 7-12.

220. Polder, T.W., et al., *Ultrastructural changes in the blood-brain barrier of mice infected with Plasmodium berghei.* Acta Leiden, 1992. **60**(2): p. 31-46.

221. Finley, R.W., L.J. Mackey, and P.H. Lambert, *Virulent P. berghei malaria: prolonged survival and decreased cerebral pathology in cell-dependent nude mice.* J Immunol, 1982. **129**(5): p. 2213-8.

222. Grau, G.E., et al., *L3T4+ T lymphocytes play a major role in the pathogenesis of murine cerebral malaria.* J Immunol, 1986. **137**(7): p. 2348-54.

223. Boubou, M.I., et al., *T cell response in malaria pathogenesis: selective increase in T cells carrying the TCR V(beta)8 during experimental cerebral malaria.* Int Immunol, 1999. **11**(9): p. 1553-62.

224. Grau, G.E., et al., *Late administration of monoclonal antibody to leukocyte function-antigen 1 abrogates incipient murine cerebral malaria.* Eur J Immunol, 1991. **21**(9): p. 2265-7.

225. Yanez, D.M., et al., *Gamma delta T-cell function in pathogenesis of cerebral malaria in mice infected with Plasmodium berghei ANKA.* Infect Immun, 1999. **67**(1): p. 446-8.

226. Locksley, R.M., et al., *Murine cutaneous leishmaniasis: susceptibility correlates with differential expansion of helper T-cell subsets.* Ann Inst Pasteur Immunol, 1987. **138**(5): p. 744-9.

227. Ouma, C., et al., *Haplotypes of IL-10 promoter variants are associated with susceptibility to severe malarial anemia and functional changes in IL-10 production.* Hum Genet, 2008. **124**(5): p. 515-24.

228. Grau, G.E., et al., *Monoclonal antibody against interferon gamma can prevent experimental cerebral malaria and its associated overproduction of tumor necrosis factor.* Proc Natl Acad Sci U S A, 1989. **86**(14): p. 5572-4.

229. Curfs, J.H., et al., *Tumour necrosis factor-alpha and macrophages in Plasmodium berghei-induced cerebral malaria.* Parasitology, 1993. **107 (Pt 2)**: p. 125-34.

230. Rudin, W., et al., *Resistance to cerebral malaria in tumor necrosis factor-alpha/beta-deficient mice is associated with a reduction of intercellular adhesion molecule-1 up-regulation and T helper type 1 response.* Am J Pathol, 1997. **150**(1): p. 257-66.

231. Sanni, L.A., et al., *Cerebral edema and cerebral hemorrhages in interleukin-10-deficient mice infected with Plasmodium chabaudi.* Infect Immun, 2004. **72**(5): p. 3054-8.

232. Neill, A.L. and N.H. Hunt, *Effects of endotoxin and dexamethasone on cerebral malaria in mice.* Parasitology, 1995. **111 (Pt 4)**: p. 443-54.

233. Hafalla, J.C., et al., *The CTLA-4 and PD-1/PD-L1 inhibitory pathways independently regulate host resistance to Plasmodium-induced acute immune pathology.* PLoS Pathog, 2012. **8**(2): p. e1002504.

234. Schmidt, K.E., et al., *Induction of pro-inflammatory mediators in Plasmodium berghei infected BALB/c mice breaks blood-brain-barrier and leads to cerebral malaria in an IL-12 dependent manner.* Microbes Infect, 2011. **13**(10): p. 828-36.

235. Pamplona, A., et al., *Heme oxygenase-1 and carbon monoxide suppress the pathogenesis of experimental cerebral malaria.* Nat Med, 2007. **13**(6): p. 703-10.

236. Mitchell, A.J., et al., *Early cytokine production is associated with protection from murine cerebral malaria.* Infect Immun, 2005. **73**(9): p. 5645-53.

237. Niikura, M., S. Inoue, and F. Kobayashi, *Role of interleukin-10 in malaria: focusing on coinfection with lethal and nonlethal murine malaria parasites.* J Biomed Biotechnol, 2011. **2011**: p. 383962.

238. Eckwalanga, M., et al., *Murine AIDS protects mice against experimental cerebral malaria: down-regulation by interleukin 10 of a T-helper type 1 CD4+ cell-mediated pathology.* Proc Natl Acad Sci U S A, 1994. **91**(17): p. 8097-101.

239. Specht, S., et al., *Filaria-induced IL-10 suppresses murine cerebral malaria.* Microbes Infect, 2010. **12**(8-9): p. 635-42.

240. Niikura, M., et al., *IL-10 plays a crucial role for the protection of experimental cerebral malaria by co-infection with non-lethal malaria parasites.* Int J Parasitol, 2010. **40**(1): p. 101-8.

241. Voza, T., et al., *Species-specific inhibition of cerebral malaria in mice coinfected with Plasmodium spp.* Infect Immun, 2005. **73**(8): p. 4777-86.

242. Haque, A., et al., *CD4+ natural regulatory T cells prevent experimental cerebral malaria via CTLA-4 when expanded in vivo.* PLoS Pathog, 2010. **6**(12): p. e1001221.

243. Kellum, J.A. and R. Venkataraman, *Blood purification in sepsis: an idea whose time has come?* Crit Care Med, 2002. **30**(6): p. 1387-8.

244. de Souza, J.B., et al., *Oral activated charcoal prevents experimental cerebral malaria in mice and in a randomized controlled clinical trial in man did not interfere with the pharmacokinetics of parenteral artesunate.* PLoS One, 2010. **5**(4): p. e9867.

245. Jacobine, A.M., et al., *Malaria-infected mice live until at least day 30 after a new artemisinin-derived thioacetal thiocarbonate combined with mefloquine are administered together in a single, low, oral dose.* J Med Chem, 2012. **55**(17): p. 7892-9.

246. Zijlstra, M., et al., *Beta 2-microglobulin deficient mice lack CD4-8+ cytolytic T cells.* Nature, 1990. **344**(6268): p. 742-6.

247. Kambayashi, T., et al., *Memory CD8+ T cells provide an early source of IFN-gamma.* J Immunol, 2003. **170**(5): p. 2399-408.

248. Berg, R.E., C.J. Cordes, and J. Forman, *Contribution of CD8+ T cells to innate immunity: IFN-gamma secretion induced by IL-12 and IL-18*. Eur J Immunol, 2002. **32**(10): p. 2807-16.

249. Berg, R.E., et al., *Memory CD8+ T cells provide innate immune protection against Listeria monocytogenes in the absence of cognate antigen*. J Exp Med, 2003. **198**(10): p. 1583-93.

250. Lertmemongkolchai, G., et al., *Bystander activation of CD8+ T cells contributes to the rapid production of IFN-gamma in response to bacterial pathogens*. J Immunol, 2001. **166**(2): p. 1097-105.

251. Gerald, N.J., et al., *Protection from experimental cerebral malaria with a single dose of radiation-attenuated, blood-stage Plasmodium berghei parasites*. PLoS One, 2011. **6**(9): p. e24398.

252. Haussig, J.M., K. Matuschewski, and T.W. Kooij, *Inactivation of a Plasmodium apicoplast protein attenuates formation of liver merozoites*. Mol Microbiol, 2011. **81**(6): p. 1511-25.

253. Tsuji, M., et al., *Demonstration of heat-shock protein 70 in the sporozoite stage of malaria parasites*. Parasitol Res, 1994. **80**(1): p. 16-21.

254. Hall, N. and J. Carlton, *Comparative genomics of malaria parasites*. Curr Opin Genet Dev, 2005. **15**(6): p. 609-13.

255. Nakabayashi, H., et al., *Growth of human hepatoma cells lines with differentiated functions in chemically defined medium*. Cancer Res, 1982. **42**(9): p. 3858-63.

256. Kuhn, R., et al., *Interleukin-10-deficient mice develop chronic enterocolitis*. Cell, 1993. **75**(2): p. 263-74.

257. Hall, N., et al., *A comprehensive survey of the Plasmodium life cycle by genomic, transcriptomic, and proteomic analyses*. Science, 2005. **307**(5706): p. 82-6.

258. Lackner, P., et al., *Behavioural and histopathological alterations in mice with cerebral malaria.* Neuropathology and applied neurobiology, 2006. **32**(2): p. 177-88.

259. Hollingdale, M.R., P. Leland, and A.L. Schwartz, *In vitro cultivation of the exoerythrocytic stage of Plasmodium berghei in a hepatoma cell line.* Am J Trop Med Hyg, 1983. **32**(4): p. 682-4.

260. Bruna-Romero, O., et al., *Detection of malaria liver-stages in mice infected through the bite of a single Anopheles mosquito using a highly sensitive real-time PCR.* Int J Parasitol, 2001. **31**(13): p. 1499-502.

261. Takahashi, T., et al., *Immunologic self-tolerance maintained by CD25(+)CD4(+) regulatory T cells constitutively expressing cytotoxic T lymphocyte-associated antigen 4.* J Exp Med, 2000. **192**(2): p. 303-10.

262. Pasare, C. and R. Medzhitov, *Toll-dependent control mechanisms of CD4 T cell activation.* Immunity, 2004. **21**(5): p. 733-41.

263. Neill, A.L. and N.H. Hunt, *Pathology of fatal and resolving Plasmodium berghei cerebral malaria in mice.* Parasitology, 1992. **105 (Pt 2)**: p. 165-75.

264. Prudencio, M., A. Rodriguez, and M.M. Mota, *The silent path to thousands of merozoites: the Plasmodium liver stage.* Nat Rev Microbiol, 2006. **4**(11): p. 849-56.

265. Qiu, Z., et al., *Multifunctional CD4 T cell responses in patients with active tuberculosis.* Sci Rep, 2012. **2**: p. 216.

266. Chao, K.H., et al., *Expression of the interleukin-2 receptor alpha (CD25) is selectively decreased on decidual CD4+ and CD8+ T lymphocytes in normal pregnancies.* Mol Hum Reprod, 2002. **8**(7): p. 667-73.

267. Rudin, W., et al., *Interferon-gamma is essential for the development of cerebral malaria.* Eur J Immunol, 1997. **27**(4): p. 810-5.

268. Randall, L.M., et al., *Cutting edge: selective blockade of LIGHT-lymphotoxin beta receptor signaling protects mice from experimental cerebral malaria caused by Plasmodium berghei ANKA.* J Immunol, 2008. **181**(11): p. 7458-62.

269. Couper, K.N., D.G. Blount, and E.M. Riley, *IL-10: the master regulator of immunity to infection.* J Immunol, 2008. **180**(9): p. 5771-7.

270. Langhorne, J., et al., *Dendritic cells, pro-inflammatory responses, and antigen presentation in a rodent malaria infection.* Immunol Rev, 2004. **201**: p. 35-47.

271. Rubtsov, Y.P., et al., *Regulatory T cell-derived interleukin-10 limits inflammation at environmental interfaces.* Immunity, 2008. **28**(4): p. 546-58.

272. Marsh, K. and R.W. Snow, *Malaria transmission and morbidity.* Parassitologia, 1999. **41**(1-3): p. 241-6.

273. Milner, D.A., Jr., et al., *Supraorbital postmortem brain sampling for definitive quantitative confirmation of cerebral sequestration of Plasmodium falciparum parasites.* J Infect Dis, 2012. **205**(10): p. 1601-6.

274. Amani, V., et al., *Cloned lines of Plasmodium berghei ANKA differ in their abilities to induce experimental cerebral malaria.* Infect Immun, 1998. **66**(9): p. 4093-9.

275. Medana, I.M., N.H. Hunt, and G. Chaudhri, *Tumor necrosis factor-alpha expression in the brain during fatal murine cerebral malaria: evidence for production by microglia and astrocytes.* Am J Pathol, 1997. **150**(4): p. 1473-86.

276. Sharpe, A.H., *Analysis of lymphocyte costimulation in vivo using transgenic and 'knockout' mice.* Curr Opin Immunol, 1995. **7**(3): p. 389-95.

277. Renia, L., et al., *Cerebral malaria: mysteries at the blood-brain barrier.* Virulence, 2012. **3**(2): p. 193-201.

278. von Bernuth, H., et al., *Experimental and natural infections in MyD88- and IRAK-4-deficient mice and humans.* Eur J Immunol, 2012. **42**(12): p. 3126-35.

279. Livolsi, A., et al., *Tyrosine phosphorylation-dependent activation of NF-kappa B. Requirement for p56 LCK and ZAP-70 protein tyrosine kinases.* Eur J Biochem, 2001. **268**(5): p. 1508-15.

280. Torgler, R., et al., *Sporozoite-mediated hepatocyte wounding limits Plasmodium parasite development via MyD88-mediated NF-kappa B activation and inducible NO synthase expression.* J Immunol, 2008. **180**(6): p. 3990-9.

281. Singh, A.P., et al., *Plasmodium circumsporozoite protein promotes the development of the liver stages of the parasite.* Cell, 2007. **131**(3): p. 492-504.

282. Usynin, I., C. Klotz, and U. Frevert, *Malaria circumsporozoite protein inhibits the respiratory burst in Kupffer cells.* Cell Microbiol, 2007. **9**(11): p. 2610-28.

283. Klotz, C. and U. Frevert, *Plasmodium yoelii sporozoites modulate cytokine profile and induce apoptosis in murine Kupffer cells.* Int J Parasitol, 2008. **38**(14): p. 1639-50.

284. Borrmann, S. and K. Matuschewski, *Targeting Plasmodium liver stages: better late than never.* Trends Mol Med, 2011. **17**(9): p. 527-36.

285. Borrmann, S. and K. Matuschewski, *Protective immunity against malaria by 'natural immunization': a question of dose, parasite diversity, or both?* Curr Opin Immunol, 2011. **23**(4): p. 500-8.

286. Matuschewski, K., et al., *Arrested Plasmodium liver stages as experimental anti-malaria vaccines.* Hum Vaccin, 2011. **7 Suppl**: p. 16-21.

287. Butler, N.S., et al., *Superior antimalarial immunity after vaccination with late liver stage-arresting genetically attenuated parasites.* Cell Host Microbe, 2011. **9**(6): p. 451-62.

288. Steers, N., et al., *The immune status of Kupffer cells profoundly influences their responses to infectious Plasmodium berghei sporozoites.* Eur J Immunol, 2005. **35**(8): p. 2335-46.

289. Grewal, R.S., *Pharmacology of 8-aminoquinolines.* Bull World Health Organ, 1981. **59**(3): p. 397-406.

290. Gutteridge, W.E. and G.H. Coombs, *Biochemistry ofparasitic protozoa*1977, [S.l.]: Univ. Park Press.

291. Ocana-Morgner, C., M.M. Mota, and A. Rodriguez, *Malaria blood stage suppression of liver stage immunity by dendritic cells.* J Exp Med, 2003. **197**(2): p. 143-51.

292. Orjih, A.U., *Acute malaria prolongs susceptibility of mice to Plasmodium berghei sporozoite infection.* Clin Exp Immunol, 1985. **61**(1): p. 67-71.

293. Scheller, L.F., R.A. Wirtz, and A.F. Azad, *Susceptibility of different strains of mice to hepatic infection with Plasmodium berghei.* Infect Immun, 1994. **62**(11): p. 4844-7.

294. Das, G., S. Sheridan, and C.A. Janeway, Jr., *The source of early IFN-gamma that plays a role in Th1 priming.* J Immunol, 2001. **167**(4): p. 2004-10.

295. Takayama, E., et al., *Mouse CD8+ CD122+ T cells with intermediate TCR increasing with age provide a source of early IFN-gamma production.* J Immunol, 2000. **164**(11): p. 5652-8.

296. Lamb, T.J., et al., *Insights into the immunopathogenesis of malaria using mouse models.* Expert Rev Mol Med, 2006. **8**(6): p. 1-22.

297. Hafalla, J.C., et al., *Short-term antigen presentation and single clonal burst limit the magnitude of the CD8(+) T cell responses to malaria liver stages.* Proc Natl Acad Sci U S A, 2002. **99**(18): p. 11819-24.

298. Sano, G., et al., *Swift development of protective effector functions in naive CD8(+) T cells against malaria liver stages.* J Exp Med, 2001. **194**(2): p. 173-80.

299. Sallusto, F. and A. Lanzavecchia, *Understanding dendritic cell and T-lymphocyte traffic through the analysis of chemokine receptor expression.* Immunol Rev, 2000. **177**: p. 134-40.

300. Leiriao, P., M.M. Mota, and A. Rodriguez, *Apoptotic Plasmodium-infected hepatocytes provide antigens to liver dendritic cells.* J Infect Dis, 2005. **191**(10): p. 1576-81.

301. Jung, S., et al., *In vivo depletion of CD11c+ dendritic cells abrogates priming of CD8+ T cells by exogenous cell-associated antigens.* Immunity, 2002. **17**(2): p. 211-20.

302. Couper, K.N., et al., *IL-10 from CD4CD25Foxp3CD127 adaptive regulatory T cells modulates parasite clearance and pathology during malaria infection.* PLoS Pathog, 2008. **4**(2): p. e1000004.

303. Abel, S., et al., *Strong impact of CD4+ Foxp3+ regulatory T cells and limited effect of T cell-derived IL-10 on pathogen clearance during Plasmodium yoelii infection.* J Immunol, 2012. **188**(11): p. 5467-77.

304. Agnandji, S.T., et al., *A phase 3 trial of RTS,S/AS01 malaria vaccine in African infants.* N Engl J Med, 2012. **367**(24): p. 2284-95.

305. Alonso, P.L., et al., *Efficacy of the RTS,S/AS02A vaccine against Plasmodium falciparum infection and disease in young African children: randomised controlled trial.* Lancet, 2004. **364**(9443): p. 1411-20.

306. Bejon, P., et al., *Calculation of liver-to-blood inocula, parasite growth rates, and preerythrocytic vaccine efficacy, from serial quantitative polymerase chain reaction studies of volunteers challenged with malaria sporozoites.* J Infect Dis, 2005. **191**(4): p. 619-26.

307. Boutlis, C.S., T.W. Yeo, and N.M. Anstey, *Malaria tolerance--for whom the cell tolls?* Trends Parasitol, 2006. **22**(8): p. 371-7.

308. Kawabata, Y., et al., *Merozoite surface protein 1-specific immune response is protective against exoerythrocytic forms of Plasmodium yoelii.* Infect Immun, 2002. **70**(11): p. 6075-82.

309. Altman, J.D., et al., *Phenotypic analysis of antigen-specific T lymphocytes.* Science, 1996. **274**(5284): p. 94-6.

310. Baker, K., et al., *Neonatal Fc receptor for IgG (FcRn) regulates cross-presentation of IgG immune complexes by CD8-CD11b+ dendritic cells.* Proceedings of the National Academy of Sciences of the United States of America, 2011. **108**(24): p. 9927-32.

Theses Cited:

A Joschko MSc Thesis, *Immunopathological characterization of Plasmodium berghei NK65 infection and the protective role of IL-10* 2012

F Kohlhepp PhD Thesis, *EHD proteins in Apicomplexan parasites*, 2012

S Lepper PhD Thesis, *Characterization of Plasmodium berghei actin and coronin*, 2011

Y Maier PhD Thesis, 2013

Chapter 7

Acknowledgements

First and foremost, I am deeply grateful to my supervisor, Ann-Kristin Mueller, for her support and guidance throughout my time in her group.

I would also like to extend my gratitude to all those who contributed to the success of my projects: Aina Martin Valls, Asa Hidmark, Beatrix Schumak, Eleonora Paulsen, Felix Lasitschka, Florian Kohlhepp, Freddy Frischknecht, Gerhard Bringmann, Jessica Kehrer, Jochen Behrends, Johannes Pfeil, Kirsten Heiss, Martin Dittmer, Melanie Diegel, Michael Lanzer, Miriam Griesheimer, Roland Frank and Yvonne Maier.

Many thanks to those colleagues who supported my work through discussion and advice: Britta Nyboer, Christiane Hammerschmidt-Kamper, Christian Epp, Eva Morath, Jennifer Schahn, Julia Sattler, Priyanka Fernandes and Sirikamol "Nick" Srismith.

Special thanks to Sarah Calne for inspiring my interest in biology.

This thesis is dedicated to my parents.